UC San Diego

UC San Diego Electronic Theses and Dissertations

Title

A tale of two drug metabolizing enzymes : the CYP1A1-GFP transgenic mouse and the promiscuous nature of UGTs

Permalink

https://escholarship.org/uc/item/0qx6p2s7

Author

Operaña, Theresa Necesito

Publication Date

2008

Peer reviewed|Thesis/dissertation

eScholarship.org Powered by the California Digital Library
University of California

UNIVERSITY OF CALIFORNIA, SAN DIEGO

A Tale of Two Drug Metabolizing Enzymes:

The CYP1A1-GFP Transgenic Mouse and the Promiscuous Nature of UGTs

A Dissertation submitted in partial satisfaction of the requirement for the degree

Doctor of Philosophy

in

Biomedical Sciences

by

Theresa Necesito Operaña

Committee in charge:

Professor Robert H. Tukey, Chair
Professor Mark H. Ellisman
Professor Eric F. Johnson
Professor Mark A. Lawson
Professor Alexandra C. Newton
Professor Palmer W. Taylor

2008

Copyright

Theresa Necesito Operaña, 2008

All rights reserved.

The Dissertation of Theresa Necesito Operaña is approved, and it is acceptable in quality and form for publication on microfilm:

_____

_____

_____

_____

_____

_____
Chair

University of California, San Diego

2008

DEDICATION

To Peter and Cecilia Operaña

and my grandmother Lucia F. Bender

TABLE OF CONTENTS

SIGNATURE PAGE…… iii

DEDICATION..…….…… iv

TABLE OF CONTENTS……..... v

LIST OF ABBREVIATIONS…….……..... viii

LIST OF FIGURES……..... xi

LIST OF TABLES…..…….. xiii

ACKNOWLEDGEMENTS……..... xiv

VITA……..... xvi

ABSTRACT……..... xx

CHAPTER 1 Introduction to Drug Metabolism…… 1

Evolutionary Perspective on Drug Metabolizing Enzymes…… 2
The Role of Drug Metabolizing Enzymes…….. 3
Cytochrome P450s…….. 3
Bioactivation of PAHs by Cytochrome P450s…… 7
Environmental Contamination and TCDD…….. 9
Characterization of CYP1A1 Induction…….. 10
AhR Mediates CYP1A1 Induction…….. 13
Molecular Mechanism of CYP1A1 Induction……. 15
CYP1A1 Induction is a Biomarker for Exposure to Environmental Contaminants……... 19
Phase II Metabolism and the Process of Glucuronidation……... 22
Purification and Characterization of UGTs……...……. 23
Implications in Disease and Toxicity Due to Glucuronidation Deficiency. 33
Proposed Structure of UGTs…… 37
Potential Protein-Protein Interaction Among the UGTs…….. 38
Objectives of the Dissertation…….. 39
References……... 42

CHAPTER 2 Human CYP1A1^{GFP} Expression in Transgenic Mice Serves as a Biomarker for Environmental Toxicant Exposure…….. 68

Introduction……. 69
Materials and Methods…… 71
Results……. 77
Characterization of CYP1A1^{GFP} Tissue Expression in Tg-*CYP1A1^{GFP}* Mice…….. 77
Fluorescence Analysis of Tissue Sections of Liver and Lung……... 83
CYP1A1^{GFP} Expression in Primary Hepatocytes……... 85
Induction and Function of CYP1A1^{GFP} Following Oral Administration of Benzo[a]pyrene…….. 88
Discussion……... 94
Acknowledgements……. 97
References……... 98

CHAPTER 3 Oligomerization of UDP-Glucuronosyltransferase 1A Proteins: Homo- and Heterodimerization Analysis by Fluorescence Resonance Energy Transfer (FRET) and Co-immunoprecipitation……... 101

Introduction…….. 102
Materials and Methods……. 105
Results…….. 112
Determination of FRET Analysis with Expressed UGT1A^{CFP} and UGT1A^{YFP} ……... 112
Co-immunoprecipitation Confirms the Existence of Homo- and Heterodimerization of the UGT1A Proteins……... 120
Functional Analysis of Oligomeric UGT Isoforms..……... 126
Discussion…… 129
Acknowledgements…….. 134
References…… 136

CHAPTER 4 Dimerization Domains of UGTs……... 141

Introduction…….. 142
Materials and Methods……. 142
Results…….. 148
Determination of UGT1A1 Dimerization Domains Using Truncated Proteins……..... 149
Effects of Dimerization on UGT1A1 Function…… 154
Homology Modeling of UGT1A1……. 156
Discussion……..... 161
Acknowledgements…….. 166
References……..... 167

CHAPTER 5 Conclusions…….. 171

Generation and Characterization of the Human CYP1A1^{GFP} Transgenic Mouse Model……... 172
Elucidation of UGT Protein-Protein Interactions…… 175
Structural Domains Involved in UGT Dimerization……... 178
Homology Modeling of UGT1A1……... 183
References……... 187

LIST OF ABBREVIATIONS

AHH	aryl hydrocarbon hydroxylase
AhR	aryl hydrocarbon receptor
ARNT	aryl hydrocarbon nuclear translocator
BaP	benzo[a]pyrene
bHLH	basic helix loop helix
CALUX	chemically activated luciferase expression
CAT	chloramphenicol acetyltransferase
CBP/p300	creb binding protein/ binding protein p300
CFP	cyan fluorescent protein
CN-1,2	Crigler-Najjar Syndrome Type 1 or Type 2
CYP	cytochrome P450
DME	drug metabolizing enzymes
DMSO	dimethyl sulfoxide
ED_{50}	median effective dose
ER	endoplasmic reticulum
EROD	ethoxyresorufin-O-deethylase
EGFP	enhanced green fluorescent protein
FRET	fluorescence resonance energy transfer
GI	gastrointestinal tract
GFP	green fluorescent protein
HLM	human liver microsomes

Hsp	heat shock protein
^{3}[H]TCDD	tritiated 2,3,7,8-tetrachlorodibenzo-*p*-dioxin
i.p.	intraperitoneal
kD	kilo dalton
LI	large intestine
3-MC	3-methylcholanthrene
2-Nap	2-napthol
ß-NF	ß-napthoflavone
NCoA	nuclear receptor coactivator
O-gal	octygallate
PAH	polycyclic aromatic hydrocarbon
PAS	Per-Arnt-Sim
p/CIP	p160 coactivator
PCR	polymerase chain reaction
Per	period protein
p.o.	oral
p23	co-chaperone protein 23
RIP140	receptor-interacting protein 140
SI	small intestine
Sim	single minded protein
TEQ	toxic equivalent
Tg	transgenic
TLC	thin layer chromatography

TCDD	2,3,7,8-tetrachlorodibenzo-*p*-dioxin
UDPGA	uridine diphosphate glucuronic acid
UGT	udp-glucuronosyltransferase
XAP2	hepatitis B virus X-associated protein 2
XRE	xenobiotic response element
YFP	yellow fluorescent protein

LIST OF FIGURES

Figure 1-1.	Mechanism of CYP1A1 induction……..	18
Figure 1-2.	Genomic organization of the human UGT1A locus……	27
Figure 2-1.	Representation of the CYP1A1-GFP gene construct used to generate the transgenic *CYP1A1*^{GFP} mice……..	78
Figure 2-2.	Expression of CYP1A1^{GFP} in mouse and human hepatoma cells following stable transfection of the *CYP1A1-GFP* gene construct..	79
Figure 2-3.	Analysis of GFP fluorescence in tissues…….	81
Figure 2-4.	Induction of CYP1A1^{GFP} in transgenic mice following treatment with TCDD……..	82
Figure 2-5.	Confocal microscopy analysis of tissue- and cell-type specific expression of CYP1A1-GFP……	84
Figure 2-6.	Time-dependent increase of CYP1A1-GFP expression in primary hepatocytes after TCDD treatment……..	86
Figure 2-7.	Dose dependent induction of CYP1A1-GFP in primary hepatocytes using various Ah Receptor ligands……..	77
Figure 2-8.	Differential expression pattern of mCYP1A1 and CYP1A1^{GFP} in transgenic mice after oral vs. i.p. treatment with BaP…….	89
Figure 2-9.	Induction of UGTs in the liver after oral BaP treatment of Tg-*UGT1* mice…….	93
Figure 3-1.	Detection of fluorescence following pUGT1A1-CFP and pUGT1A1-YFP transfection into COS cells……...	113
Figure 3-2A.	Detection of FRET in COS cells co-transfected with pUGT1A1-CFP and pUGT1A1-YFP……..	114
Figure 3-2B.	Detection of FRET in COS cells co-transfected with pUGT1A1-CFP and pUGT1A1-YFP……..	155

Figure 3-3. Homodimerization analysis of UGT1A proteins by FRET Analysis…….. 118

Figure 3-4. Heterodimerization analysis of UGT1A1 with other UGT1A proteins by FRET analysis…….. 119

Figure 3-5. Co-immunoprecipitation analysis of UGT1A1 homodimerization.. 133

Figure 3-6. The anti-HA beads immunoprecipitate UGT1A^{HA} expressed proteins.……..... 123

Figure 3-7. Oligomerization of UGT1A Proteins..……. 125

Figure 3-8A. Functional analysis of chimeric and oligomeric UGT1A proteins.. 127

Figure 3-8B. Functional analysis of chimeric and oligomeric UGT1A proteins.. 128

Figure 3-8C. Functional analysis of chimeric and oligomeric UGT1A proteins.. 128

Figure 4-1. Schematic of UGT1A1 and the C-terminal UGT1A1 truncation constructs…… 151

Figure 4-2. Co-expression of UGT1A1 with truncated constructs……... 153

Figure 4-3. Co-expression of UGT1A1 with truncated constructs……... 155

Figure 4-4. Effects of Dimerization on UGT1A1 function……... 156

Figure 4-5. Homology model of UGT1A1…… 158

Figure 4-6. Potential dimerization domains and dimer orientation of UGT1A1……. 160

LIST OF TABLES

Table 2-1.	EROD activity in the liver……...	91
Table 3-1.	Plasmid constructs used in FRET analysis and co-immunoprecipitation studies……..	135

ACKNOWLEDGEMENTS

I would like to thank my parents, my four brothers (Oliver, Walter, Richard, and John), grandma Lucia, Mamang, and Lolo Paul, for shaping me into the person I am today and encouraging me to define my own path in life. Thanks to all of my beautiful nieces and nephews who have inspired me to be a good role model.

I would like to thank my thesis advisor, Dr. Robert H. Tukey, for being a wonderful mentor and having the patience to put up with me all of these years. Thank you for your guidance and support, but most of all for the confidence you instilled in me by giving me the freedom to pursue my own scientific interests outside of the lab's realm. The Tukey lab members have been like a second family to me, thank you all for your support during the trials and tribulations of graduate school and my personal life. I am grateful to Nghia Nguyen for training me in the art of cloning, Deirdre La Placa for teaching me how to handle unruly mice, Dr. Shujuan Chen and Dr. Mei-Fei Yueh for sharing their technical expertise and the engaging late night scientific discussions to figure out why my experiments weren't working. I must also thank the past and present graduate students of the lab who have endured the graduate school vortex with me: Daniel Machemer for inspiring me to overcome any scientific adversity, Jessica Bonzo for being a great graduate student role model, Erin Brace-Sinnokrak, Kathy Senekeo-Effenberger, and Camille Konoponicki for their friendship and fun-filled nature which made me look forward to coming in to work every day.

The Biomedical Sciences Graduate Program has been an amazing environment filled with supportive faculty members and extremely talented students. I would like to thank my thesis committee members: Dr. Mark Ellisman, Dr. Eric Johnson, Dr. Mark

Lawson, Dr. Alexandra Newton, and Dr. Palmer Taylor for their guidance, helpful suggestions, and opening their doors so I could obtain technical assistance and reagents from their laboratories. I am grateful to Dr. Laurence Brunton for his wonderful mentorship during my undergraduate career and setting me on the path to pursue my graduate degree at UCSD. I would like to thank Dr. Stefaan Sansen, Dr. Mei Hsu, and Keith Griffin for their collaborative assistance with my UGT project. To my BMS classmates who have contributed to making this journey an unforgettable adventure, I will surely miss the Mexico surfing trips and of course, nothing will ever compare to the Mexico Thanksgiving feasts. Thanks to Minh-Ha Do for being a wonderful friend and confidante, Marc Mendillo for being my best friend during graduate school, inspiring me to work hard, and being supportive to the end, and Andrew Miller for keeping me sane while writing my dissertation.

Chapter 2, in full, is a reprint of the material as it appears in Operaña TN, Nguyen N, Chen S, Beaton D, Tukey RH. "Human CYP1A1GFP expression in transgenic mice serves as a biomarker for environmental toxicant exposure" *Journal of Toxicological Sciences* (2007) Jan;95(1):98-107. I was the primary investigator and author of this article. Chapter 3, in full, is a reprint of the material as it appears in Operaña TN, and Tukey RH. "Oligomerization of the UDP-glucuronosyltransferase 1A proteins: homo- and heterodimerization analysis by fluorescence resonance energy transfer and co-immunoprecipitation" *Journal of Biological Chemistry* (2007) Feb 16;282(7):4821-9. I was the primary investigator and author of this article.

VITA

EDUCATION

2002-2008 Ph.D - Doctor of Philosophy (Biomedical Sciences Graduate Program), University of California San Diego, La Jolla, California

1998-2002 B.S. - Bachelor of Science (Pharmacological Chemistry), University of California San Diego, La Jolla, California (Cum Laude)

PROFESSIONAL EXPERIENCE

Sep 2002- Jun 2008 **PhD. Student**: "Regulation and Function of Human Drug Metabolizing Enzymes: Characterization of the CYP1A1-GFP Transgenic Mouse and Investigation of UDP-glucuronosyltransferase Oligomerization by Fluorescence Resonance Energy Transfer", supervised by Robert Tukey, PhD, Professor, Departments of Pharmacology and Chemistry& Biochemistry, University of California San Diego, La Jolla, CA.

Jun 2002-Sep 2002 **Summer Research Intern**: "ERK kinase inhibition stabilizes the aryl hydrocarbon receptor: implications for transcriptional activation and protein degradation", supervised by Robert Tukey, PhD, Professor, Departments of Pharmacology and Chemistry/Biochemistry, University of California San Diego, La Jolla, CA.

Jun 2001-Sep 2001 **Summer Research Intern**: "Cloning and Characterization of GFP-tagged UDP-glucuronosyltransferases UGT1A8*1, UGT1A8*2 and UGT1A4", supervised by Robert Tukey, PhD, Professor, Departments of Pharmacology and Chemistry/Biochemistry, University of California San Diego, La Jolla, CA.

Sep 2001-Jun 2002 **Undergraduate Research Intern**: "Novel Nicotine Cessation Therapeutics", supervised by John Cashman, PhD, Director of The Human Biomolecular Research Institute, San Diego, CA.

HONORS AND AWARDS:

2007 Graduate Student Travel Award to the ISSX annual meeting in Sendai, Japan
2007 First Place Graduate Student Best Abstract Award in the Drug Metabolism Division at the 2007 ASPET annual meeting in Washington DC.
2006 Third Place Graduate Student Best Abstract Award in the Toxicology Division at the 2006 ASPET annual meeting in San Francisco, California.
2006 Graduate Student Travel Award to the ASPET annual meeting at Experimental Biology 2006 Meeting in San Francisco, California.
2006 Graduate Student Travel Award to the 15th IUPHAR World Congress of Pharmacology 2006 in Beijing, China
2005 Best Abstract Award at the 2005 Superfund Basic Research Program Annual Meeting in New York City, New York.
2002 Summer Undergraduate Research Fellowship (Pharmacology Department, University of California San Diego)
2001 Summer Undergraduate Research Fellowship (Pharmacology Department, University of California San Diego)

TEACHING EXPERIENCE

Mar 2004-Jun 2004 **Teaching Assistant** in undergraduate Pharmacology and Toxicology. Department of Pharmacology, University of California, San Diego, La Jolla, CA.

Sep 2002-Jun 2004 **Chemistry & Biology Tutor** at the University of California San Diego, La Jolla, CA.

Sep 2001-Mar 2002 **Teaching Assistant** in General Chemistry. Department of Chemistry & Biochemistry, University of California San Diego, La Jolla, CA.

PUBLICATIONS

1. **Operaña TN**, Tukey RH. Oligomerization of UDP-Glucuronosyltransferase 1A Proteins. Homo- and Heterodimerization Analysis by Fluorescence Resonance Energy Transfer (FRET) and Co-Immunoprecipitation. *J Biol Chem.* 2007 Feb 16;282(7):4821-9.

2. **Operaña TN**, Nguyen N, Chen S, Beaton D, Tukey RH. Human CYP1A1-GFP Expression in Transgenic Mice Serves as a Biomarker for Environmental Toxicant Exposure. *Toxicol Sci.* 2007 Jan;95(1):98-107.

3. Chen S, **Operaña T**, Bonzo J, Nguyen N, Tukey RH. Erk kinase inhibition leads to induction of cellular Ah receptor levels. Implications for transcriptional activation and protein degradation. *J Biol Chem*. 2005 Feb 11;280(6):4350-9.

ABSTRACTS AND PRESENTATIONS

1. Invited Speaker: "Promiscuous Nature of UGTs" at the Superfund Basic Research Program Annual Meeting in Raleigh Durham, North Carolina, December 2007.

2. "Oligomerization of UDP-Glucuronosyltransferases Visualized by Fluorescence Resonance Energy Transfer (FRET) in Living Cells" at the American Society of Pharmacology and Experimental Therapeutics in Washington D.C, May 2007.

3. "Protein-Protein Interactions of UDP-Glucuronosyltransferases: Implications on Function and Substrate Specificity" at the Superfund Basic Research Program Annual Meeting in La Jolla, CA, December 2006.

4. "In Vivo Analysis of hUGT1A1 Homodimerization Using Fluorescence Resonance Energy Transfer (FRET)" at the International Union of Basic and Clinical Pharmacology in Beijing, China, July 2006.

5. "CYP1A1 regulation by oral exposure to benzo[α]pyrene using a *CYP1A1*^{GFP} transgenic mouse model" at the American Society of Pharmacology and Experimental Therapeutics in San Francisco, California, April 2006.

6. "h-CYP1A1-GFP Transgenic Mouse Model: Fluorescent Biomarker for Toxicant Exposure" at the Society of Toxicology Meeting in San Diego, California, March 2006.

7. Invited Speaker: "h-CYP1A1-GFP Transgenic Mouse Model: Fluorescent Biomarker for Toxicant Exposure" at the Superfund Basic Research Program Annual Meeting in New York City, NY, January 2006.

8. "The Role of Glucuronidation in N-OH-PhIP and B[a]P 7,8-diol Induced Apoptosis" at the International Workshop on Glucuronidation in Dundee, Scotland, UK, September 2004.

EXTRACURRICULAR ACTIVITIES

- Graduate Student member of the Biomedical Sciences Seminar Committee (2005-present)
- Mentor for University of California San Diego Trio Outreach Program for high school students (2004- present)

PROFESSIONAL AFFILIATIONS

American Society for Pharmacology and Experimental Therapeutics (2005-present)

International Society for the Study of Xenobiotics (2007-present)

ABSTRACT OF THE DISSERTATION

A Tale of Two Drug Metabolizing Enzymes:

The CYP1A1-GFP Transgenic Mouse and the Promiscuous Nature of UGTs

by

Theresa Necesito Operaña

Doctor of Philosophy in Biomedical Sciences

University of California, San Diego, 2008

Professor Robert H. Tukey, Chair

Drug metabolism can be divided into Phase I and Phase II reactions, which catalyze the conversion of a lipophilic compound into a more water soluble metabolite that can be readily eliminated from the body. Cytochrome P450s classically represent the Phase I enzymes and detoxify a myriad of substrates. The human *CYP1A1* gene is regulated by the aryl hydrocarbon receptor (AhR) and induction of CYP1A1 is known to play an important role in xenobiotic metabolism. Exposure to prevalent environmental

contaminants result in the induction of cytochrome P450 1A1 (CYP1A1), and this response is widely used as a biomarker for toxicant exposure. To examine the regulation of human CYP1A1 in vivo, we created a transgenic mouse strain (Tg-*CYP1A1*^{GFP}) expressing a chimeric gene consisting of the entire human *CYP1A1* gene (15 kb) fused with a *GFP* reporter gene. The treatment of Tg-*CYP1A1*^{GFP} mice with TCDD led to induction of CYP1A1^{GFP} in both the liver and lung as determined by fluorescence and Western blot analysis. The ability to identify fluorescently labeled CYP1A1 in vivo provides a sensitive measurement of gene response, and links exposure to potential environmental toxicants and activation of the AhR.

The process of glucuronidation is catalyzed by UDP-glucuronosyltransferases (UGTs), and is the most important Phase II reaction for the detoxification of xenobiotic compounds. Recent biochemical evidence indicates that the UGT proteins may oligomerize within the ER. To investigate the potential homo/heterodimerization capacity of UGT1A proteins, fluorescence resonance energy transfer was utilized to study dimerization in live cells, in conjunction with co-immunoprecipitation experiments. These complementary techniques demonstrated that all of the UGT1A proteins homodimerize and heterodimerize with UGT1A1. These studies suggest that the UGT1A family of proteins form oligomerized complexes in the membrane, a property that may influence function and substrate selectivity. The regions facilitating protein interactions among UGTs was also explored using truncation analysis and co-immunoprecipitation experiments, which revealed that multiple dimerization domains may exist. A homology model of UGT1A1 was constructed which gave insight into the potential orientation of the dimers, as well as the pertinent regions that could be involved in dimerization.

CHAPTER 1

Introduction to Drug Metabolism

Evolutionary Perspective on Drug Metabolizing Enzymes

Drug metabolizing enzyme (DME) genes have existed on this planet for more than 2.5 billion years and first evolved for critical life functions in prokaryotes (Loomis, 1988). It is postulated that the earliest P450-mediated reactions may have been reductase and isomerase functions because of the highly anaerobic environment of the earth but later evolved to encompass oxidation functions when the atmospheric oxygen levels increased dramatically (Nebert and Feyereisen, 1994). The ability to detoxify oxygen became an increasingly important defense mechanism to protect against oxidative stress and was crucial for survival (Schlezinger *et al.,* 1999). DMEs also likely played key roles in life processes such as cell growth and division, development, electrolyte balance, and the metabolism of endogenous substrates (Danielson, 2002).

During the past 1,000 million years, DME genes in animals have expanded to include the role of detoxification of dietary products, evolving plant metabolites, and more recently, pharmaceutical drugs (Nebert and Dieter, 2000). It is believed that the evolution of DME genes in animals occurred because of the necessary interactions between animals and plants. When animals first came on to land about 400 million years ago and began devouring terrestrial plants, it set the stage for the co-evolution of animal-plant warfare resulting in the explosion of animal DME gene duplication events that began to take place presumably to adapt to the new dietary constituents. As a means of defense, plants retaliated by evolving new genes and thus new metabolites called phytoalexins to make themselves less palatable and more toxic to animals (Gonzalez and Nebert, 1990). In response to the increased toxic metabolites in plants, animals evolved

new DME genes in order to adapt to the constantly changing milieu of ingested toxicants. The development of the defense mechanism to detoxify plant metabolites by animal DMEs undoubtedly evolved into the existing metabolic bioactivation and detoxification of environmental pollutants, carcinogens, and drugs that is now found in humans.

The Role of Drug Metabolizing Enzymes

DMEs play central roles in the metabolism, detoxification, and elimination of endogenous substrates, as well as drugs and xenobiotics that are introduced into the human body. The clearance of lipophilic xenobiotic compounds from the body can be divided into Phase I and Phase II reactions (Williams, 1949). During Phase I metabolism a substrate can undergo oxidation, reduction, and hydrolysis reactions which converts the compound into a more water soluble form. Phase I oxidative metabolism by cytochrome P450 enzymes is the primary method of drug metabolism and commonly introduces a functional group, such as a hydroxyl group, that enables conjugative Phase II reactions to occur. Phase II enzymes utilize a functional group to covalently link large polar moieties such as glucuronic acid, sulfate, glutathione, glucose, and cysteine to further increase the metabolite's water solubility and facilitate excretion into the urine or the bile (Williams, 1971).

Cytochrome P450s

The P450 gene superfamily is composed of highly diversified and extremely abundant set of heme containing proteins that classically represent Phase I metabolism (Nebert and Gonzalez, 1987). The cytochrome P450 proteins were first discovered in

1958 due to their unique reduced carbon monoxide spectrum that has an absorbance at 450 nm, thus called pigment at 450 or P450 (Klingenberg, 1958; Garfinkel, 1958). Cytochrome P450s are sometimes called mixed function oxidases or monooxygenases referring to their ability to incorporate one oxygen atom to the substrate. In addition to hydroxylation reactions, cytochrome P450s can also catalyze a broad range of other chemical reactions including deaminations, desulfurations, dehalogenations, epoxidations, dealkylations, N-oxidations, peroxidations, and sulfoxidations (Isin and Guengerich, 2007). However, the hydroxylation reaction is the prominent reaction and facilitates the biotransformation of compounds that otherwise lack functional groups and introduces hydroxyl groups into unreactive hydrocarbon chains and aromatic rings. The cytochrome P450s are the only mammalian enzyme system with the oxidative power to efficiently functionalize primary carbons using molecular oxygen, requiring an enormous amount of oxidation-reduction potential of about $E_{1/2}$~ 1.8 V (Macdonald *et al.,* 1989). This complex catalytic process requires the donation of two electrons sequentially from the electron donor, such as the NADPH cytochrome P450 reductase. The substrate binding to the cytochrome P450 triggers the transfer of the single electron that reduces the ferric iron to its ferrous form. The cytochrome P450/ substrate complex then binds and reacts with molecular oxygen producing an unstable ferrous dioxygen-bound complex that accepts the transfer of a second electron and finally results in an oxygenated substrate and release of water (Guengerich and Macdonald, 1990; Urlacher and Schmid, 2002).

The broad array of Cytochrome P450 enzymes play a key role in catalyzing reactions for endogenous compounds such as steroid hormones, arachidonic acid and

prostaglandins, activation of vitamins A and D, and secondary metabolites in plants and insects (Nebert and Gonzalez, 1987). The function of cytochrome P450s was originally identified for being pertinent for oxidation of steroids (Estabrook *et al.,* 1963, Cooper *et al.,* 1963). The major cytochrome P450s involved in endogenous chemical synthesis include CYP4A11 for fatty acids (Hsu *et al.,* 2007), CYP1B1, CYP11Bs, and CYP21A2 for sterols (Norlin and Wikvall, 2007), the CYP4Fs for eicosanoids (Kalsotra and Strobel, 2006), and CYP26A and CYP2Bs for vitamins (Prosser and Jones, 2004; Haque and Anreola, 1998). However, the importance for endogenous function has been overshadowed by their role in the metabolism of pharmaceutical compounds. Meanwhile, detoxification of xenobiotic compounds by the cytochrome P450s is probably the minor function of these versatile enzymes and most likely an extension of their ability to metabolize endogenous substrates. For example, CYP2C family is perceived to function exclusively as hepatic metabolizers of pharmaceutical compounds (Goldstein and de Morais, 1994). However, studies indicate that the CYP2C family is involved in the synthesis of 11, 12 expoxyeicosatrienoic acid (Fisslthaler *et al.,* 1999). Similarly, CYP2D6 is highly associated with the clearance of a plethora of drugs, however, it is constitutively expressed at high levels in the brain suggesting an alternative and native function (Niznik *et al.,* 1990; Dorado *et al.,* 2007). In addition, cytochrome P450s also seem to play an important role in the metabolism of endogenous substrates during early development (Ryner and Swain, 1995).

The cytochrome P450 enzymes are best known for their role in the detoxification of pharmaceutical drugs and their function contributes to the clearance of over 70% of drugs that we ingest (Johnson, 2008). Of the 57 cytochrome P450 proteins encoded in the

human genome, 15 are involved in clearance of drugs and xenobiotic compounds. However, only 5 cytochrome P450 enzymes are primarily responsible for the oxidative metabolism of most drugs. CYP3A4 is by far the most important drug metabolizing enzyme accounting for approximately 46 % of all drug oxidative metabolism, CYP2C9 accounts for 16 %, CYP2C19 and CYP2D6 each account for about 12 %, while CYP1A1/CYP1A2 about 14% (Rendic, 2002; Williams *et al.,* 2004). Although cytochrome P450s are ubiquitously expressed throughout most tissues, the liver contains the greatest concentration of the enzymes and is therefore the primary organ for detoxification of drugs and xenobiotic compounds. Varied response of individual patients to administered drugs is of significant interest, as it is well known that some people metabolize drugs quite rapidly, while others metabolize the same drug at a much slower rate. In many cases, this phenomenon can be attributed to the varying amount of cytochrome P450 expression levels in the liver and small intestines due to genetic polymorphisms (Danielson, 2002).

Numerous external factors have also been found to influence the expression and functionality of cytochrome P450s including diet, exposure to other drugs, tobacco and alcohol consumption, and environmental contaminants. An example of a widely known interaction with CYP3A4 occurs with the dietary consumption of grapefruit juice. The effects of grapefruit juice were first observed with felodipine, a calcium channel antagonist, where it led to the elevation of serum concentrations of the drug (Bailey *et al.,* 1989; Bailey *et al.,* 1991). Since then numerous studies have shown that grapefruit juice inhibits the CYP3A4 enzyme, thereby decreasing the pre-systematic metabolism, resulting in increased bioavailability of the compound (Lundahl *et al.,* 1997; Kiani and

Imam, 2007). This increase in bioavailability of the drug has been associated with high frequency of dose dependent adverse effects. This action is similar to the drug-drug interaction caused by cytochrome P450 inhibiting drugs such as itraconazole, ketoconazole, and erythromycin (Kivisto *et al.,* 1997; Kivisto *et al.,* 1998, Floren *et al.,* 1997).

Bioactivation of PAHs by Cytochrome P450s

Metabolism by cytochrome P450s is generally regarded as a detoxification pathway, however, these reactions can also lead to the bioactivation of compounds. This bioactivation process converts compounds to more reactive species that can covalently link to cellular components, such as DNA, resulting in the initiation and promotion of tumorigenesis (Danielson, 2002; Guengerich, 2006; Guengerich, 1988; Shimada *et al.,* 1987; Yamazaki *et al.,* 1991). This also holds true for chemical carcinogens that we are exposed to through environmental exposure, such as polycyclic aromatic hydrocarbons (PAHs) (Weisburger, 1980). Humans are exposed to PAHs from a wide range of sources such as tobacco smoke, automobile exhaust, smoked and cooked foods, and industrial processes. In the early 1900s, studies correlated high incidence of cancer in workers exposed to soot, coal tar, and pitch (Norris, 1914; Hoffman, 1915; Yamagiwa and Ichikawa, 1977). It was then clearly demonstrated by Yamagiwa and Ichikawa that direct application of coal tar on the ears of rabbits led to the development of carcinomas (Yamagiwa and Ichikawa, 1977). Numerous carcinogenic PAH compounds were isolated from coal tar, and the major carcinogenic component was identified as benzo[a]pyrene (BaP) (Cook *et al.,* 1933). In the 1970s metabolic activation of polycyclic aromatic

hydrocarbons, such as BaP, were being elucidated and the ultimate carcinogen identified by detecting reactive metabolites and DNA adduct formation (Conney 1982). Borgen *et al.* reported BaP incubated with microsomes resulted in binding of various trans dihydrodiol metabolites of BaP to DNA with 10 fold greater affinity than BaP itself (Borgen *et al.,* 1973). Based on these reports, Sims and colleagues determined that the BaP 7,8-dihydrodiol metabolite was further metabolized into an epoxide which was identified to be the most potent BaP DNA alkylating metabolite (Sims *et al.,* 1974). It was also observed that BaP induced synthesis of its own hydroxylase, termed benzopyrene hydroxylase and known today as CYP1A1 (Conney *et al.,* 1957).

Exposure to PAHs have been causatively linked to higher incidence of cancer in various populations including cigarette smokers (Proctor, 2001). Thus, the metabolic activation of PAHs by cytochrome P450s is a critical step in the formation of cancer (Ma and Lu, 2007). Multiple forms of human cytochrome P450s play significant roles in the metabolic activation of environmental carcinogens, however, it has been suggested that CYP1A1 is mainly responsible for the activation of most PAHs (Conney, 1982). CYP1A1 is expressed primarily in extrahepatic tissues, including lung and mammary glands, and it could potentially contribute to the incidence of cancers in these organs upon exposure to procarcinogens (Shimada *et al.,* 2004). CYP1A1 is not basally expressed and is highly substrate inducible. In many cases, chemical inducers are substrates of CYP1A1, such as PAHs (Conney, 1982). Thus, exposure to PAHs induces CYP1A1 and leads to the metabolism of PAHs into a more reactive species. This feedback loop of a compound inducing its own metabolism by increasing CYP1A1 activity and its own carcinogenic potential seems paradoxical. However, the formation of

reactive metabolites can be countered by Phase II conjugation reactions that aid in the elimination and excretion of the carcinogenic metabolites. In a negative feedback loop, as PAHs are metabolized the expression levels of CYP1A1 diminish and the generation of carcinogenic metabolites also decrease, enabling the return to a homeostatic state (Nebert and Dalton, 2006). This delicate balance of bioactivation and detoxification can be tipped resulting in the promotion of cancer when the amount of procarcinogen exposure is overwhelming, as in the case of cigarette smoking. In addition, xenobiotic compounds which are potent inducers of CYP1A1, such as chlorinated dibenzo-*p*-dioxins, may escape the negative feedback loop mechanism and result in the generation of excessive reactive metabolites due to the inability of the CYP1A1 enzyme to efficiently metabolize the compound.

Environmental Contamination and TCDD

Chlorinated dibenzo-*p*-dioxins are extremely toxic and teratogenic compounds that have been inadvertently dispersed in the environment. They are generated as by-products of industrial processes including incineration, chlorine bleaching of paper and pulp, and manufacturing of some pesticides, herbicides, and fungicides (Schecter *et al.,* 2005). The toxic effects of dioxins were initially observed in the 1954 when several chloracne outbreaks were reported among employees of a chemical plant manufacturing the herbicide 2,4,5- tichlorophenoxyacetic acid (2,4,5-T Agent Orange) (Kimmig and Schulz 1957; Schulz, 1957). Agent Orange was found to be contaminated with trace amounts of numerous chlorinated dibenzo-*p*-dioxins and dibenzofurans. 2,3,7,8-tetrachlorodibenzo-*p*-dioxin (TCDD) is the prototype of dioxins, and it is an extremely

toxic and persistent pollutant in the environment. It is a known contaminant in the Agent Orange herbicide that was used during the Vietnam War (IOM, 2005) and the causative agent in chloracne outbreaks (Bleiberg *et al.,* 1964). TCDD is a nearly planar tricyclic aromatic molecule that is very lipophilic and is sequestered in the fat and liver. It is highly stable and has no known mechanism of metabolic detoxification and remains in the body with an estimated half-life of 7.5 years (Geyer *et al.,* 2002). In addition to its persistent/stable nature, it also has remarkable teratogenic potency and lethal potency (Schwetz *et al.,* 1973). In certain animals tested in the laboratory, TCDD caused death following very small doses and has been designated as one of the most toxic man-made chemicals. In 2004, TCDD was used to poison President Viktor Yushchenko of Ukraine during a dinner party (Chivers, 2004). His symptoms included back pain, acute pancreatitis, nerve paralysis, and bloating of the face with disfiguring chloracne (BBC, 2004). TCDD is also the most potent known inducer of CYP1A1 (Schecter *et al.,* 2005).

Characterization of CYP1A1 Induction

The molecular mechanism of CYP1A1 induction was established by the pioneering work of Nebert and co-workers when they observed that certain classes of compounds, such as PAHs, had the potential to induce aryl hydrocarbon hydroxylase activity (AHH) in cell culture (Nebert and Gelboin 1968a; Nebert and Gelboin 1968b). Upon treatment with actinomycin D, an inhibitor of RNA synthesis, and cycloheximide, an inhibitor protein synthesis, it was determined that induction of AHH activity involved both RNA synthesis and protein synthesis (Nebert and Gielen, 1971). In addition to the induction of AHH activity, mice treated with various aromatic hydrocarbons displayed

increases in other aromatic hydrocarbon inducible monooxygenase activities (Nebert *et al.,* 1973a). The genetic region responsible for the other monooxygenase activity was found to be associated at or near the same genetic locus as the aryl hydrocarbon (Ah) locus. The induced AHH activity was fractionated and isolated from mouse liver containing cytochromes P_{450} and P_{448}, later identified as CYP1A1 and CYP1A2 respectively, suggesting that the AHH activity was due to the function of the cytochromes present (Nebert *et al.,* 1973b). In 1979 conclusive evidence was obtained to determine that CYP1A1 was responsible for the AHH activity observed upon treatment with PAHs and TCDD (Negishi and Nebert, 1979). Two inducible forms of cytochrome P450 were purified from mice treated with 3-MC, and an antibody was developed for each form (anti-CYP1A1 and anti-CYP1A2). The inhibitory affects of the specific antibodies on the enzymatic activity of each purified protein was assessed. The anti-CYP1A1 antibody greatly decreased the 3-MC inducible AHH activity but did not affect the 3-MC inducible acetanilide 4-hydroxylase activity. While the anti-CYP1A2 antibody was found to inhibit 3-MC inducible acetanilide 4-hydroxylase activity with no affect on 3-MC inducible AHH activity. This study provided direct biochemical evidence that the Ah locus represents distinct forms of cytochrome P450s and that the induction of the AHH activity observed was due to the induction of CYP1A1 expression.

Characterization of the CYP1A1 gene led to the cloning and understanding of the transcriptional regulation of the Ah locus. Isolation of total cellular RNA from control and 3-MC treated mouse livers followed by in vitro translation of the isolated mRNA using the reticulocyte lysate system and immunoprecipitation using anti-CYP1A1 antibody revealed that there was 10 times more mRNA from 3-MC treated livers than

control livers (Negishi and Nebert, 1981). The cDNA of CYP1A1 was then isolated and further characterized after the reverse transcription of the mRNA (Negishi *et al.,* 1981). The mechanism of CYP1A1 induction by PAHs and TCDD was evaluated and found to be governed principally through an increase in specific gene transcription and not through decreased rate of mRNA degradation or increased rate of translation (Tukey *et al.,* 1981; Gonzalez *et al.,* 1984). The cloning of the mouse CYP1A1 gene from genomic DNA was achieved in 1983 (Nakamura *et al.,* 1983), and both mouse CYP1A1 and CYP1A2 genes were localized to mouse chromosome 9 (Tukey *et al.,* 1984). The human CYP1A1 gene was cloned from human breast cancer cells (Jaiswal *et al.,* 1985) and localized to chromosome 15 (Hildebrand *et al.,* 1985).

The induction of CYP1A1 is mediated through the aryl hydrocarbon receptor (AhR). The concept that a receptor was responsible for the regulation of the CYP1A1 gene stemmed from the studies that compared two strains of mice that had varying CYP1A1 activity responsiveness to chemical treatment. The mouse strain C57B1/6 was known to be responsive to PAH treatment and resulted in the induction of CYP1A1 activity, while the DBA/2 mouse strain lacked this same response (Nebert and Felton, 1975). Studies by Poland and Glover illustrated that TCDD and 3-methylcholanthrene (3-MC) induced CYP1A1 activity to the same maximal level. However, TCDD was found to be 30,000 times more potent (Poland and Glover, 1974). It was hypothesized that the failure of certain inbred strains of mice to respond to polycyclic hydrocarbon induction of CYP1A1 was most likely due to a mutation in a receptor resulting in a defect of binding to the inducing compound. Upon realizing that TCDD was much more potent than the PAHs, investigators began to treat the PAH nonresponsive strain DBA/2 with high doses

of TCDD until maximal AHH activity was reached and comparable to the PAH responsive strain C57B1/6 (Poland *et al.,* 1974). These studies illustrated that the DBA/2 mouse strain expressed the genetic and regulatory elements pertinent for CYP1A1 induction but had a diminished capacity to bind to the inducer. Defects in ligand binding to a putative receptor seemingly accounted for the differences in the murine strains, which could be overcome by using much higher concentrations of TCDD. The mediator of the induction of the CYP1A1 activity was termed the aryl hydrocarbon receptor (AhR).

AhR Mediates CYP1A1 Induction

The existence of the AhR was initially identified when the PAH responsive strain of mice was found to express a receptor that bound TCDD with greater affinity when compared to PAH nonresponsive mice (Poland and Glover, 1975). The presence of the AhR was firmly established through in vitro experiments on binding of [^{3}H]TCDD to hepatic cytosols from PAH responsive mice, which revealed a small pool of high-affinity binding sites that stereospecifically and reversibly bind TCDD (Poland *et al.,* 1976). In addition, the binding affinities of 23 halogenated dibenzo-p-dioxins and dibenzofurans for this receptor were tested and the Kds closely correlated with the potencies of these compounds as inducers of CYP1A1. Moreover, the PAHs that induce CYP1A1 were competitive inhibitors of [^{3}H]TCDD. Similar studies were conducted to determine the ED_{50} of TCDD in various mouse cell lines that were either responsive or nonresponsive to PAH treatment. The ED_{50} of TCDD for responsive cells was less than 0.5 nM, while the two nonresponsive cells lines had an ED_{50} of greater than 100 nM (Niwa *et al.,* 1975,

Guenthner and Nebert, 1977). It was also determined that the number of receptors capable of binding TCDD was approximately the same for all of the four cell types tested (Guenthner and Nebert, 1977). These results confirm that AhR binds TCDD and is the receptor responsible for the induction of CYP1A1 activity. The phenotypic differences in PAH responsiveness in various mouse strains was later elucidated and the existence of four forms of the AhR with key amino acid mutations was shown to be the cause of the discrepancy in PAH response (Okey *et al.,* 1989; Poland *et al.,* 1994).

The AhR was purified successfully upon the development of a photoaffinity ligand that was used to monitor the receptor (Poland *et al.,* 1986) and enabled for the subsequent cloning and characterization of the receptor (Ema *et al.,* 1992, Burbach *et al.,* 1992). The AhR deduced amino acid sequence reveals a structural organization that is representative of a family of transcription factors called the basic helix-loop-helix Per-ARNT-Sim (bHLH/PAS) (Schmidt and Bradfield, 1996; Hankinson, 1995). The Per-ARNT-Sim domain of AhR was characterized based on the sequence similarity to known *Drosophila* proteins Per and Sim, and the heterodimer partner of AhR termed ARNT. The Per protein in *Drosophila* is known to be important in the maintenance of circadian rhythms (Crews *et al.,* 1988), and the Sim protein is involved in the specification of cell fate during midline cell differentiation (Nambu *et al.,* 1990; Namub *et al.,* 1991). ARNT, the heterodimer partner of AhR, was originally thought to be important for the nuclear translocation of AhR (Hoffman *et al.,* 1991). The N-terminal region of the AhR contains the basic residues which contributes to DNA binding, and the HLH domain facilitates protein-protein dimerization with other proteins and transcription factors (Murre *et al.,* 1989a; Murre *et al.,* 1989b; Davis *et al.,* 1990). The N-terminal region also contains the

AhR nuclear localization signal and a nuclear export signal sequence (Ikuta *et al.,* 1998). The C-terminal portion contains the PAS region composed of two subdomains, PAS A and PAS B, which are enriched in polar residues and influence protein-protein interactions, DNA recognition, and ligand binding. Deletion mutants of AhR demonstrated the existence of discrete functional domains. Photoaffinity labeled dioxin was shown to bind a fragment containing amino acids 232-334 within the PAS B repeat, indicating that ligand binding is localized to this region (Burbach *et al.,* 1992). The PAS domain also contains the contact region for Hsp90. (Denis *et al.,* 1988; Perdew, 1988). One Hsp 90 molecule appears to bind within the PAS region and the other interacts with the helix-loop-helix region (Fukunaga *et al.,* 1995; Reisz-Porszasz *et al.,* 1994). The Hsp90 interaction is hypothesized to be important for maintaining AhR in a high affinity ligand binding conformation and to repress DNA-binding affinity (Dolwick *et al.,* 1993). The basic region was determined to be important for binding to DNA response elements but not pertinent for dimerization. The deletion of the C-terminal portion had no affect on DNA binding but eliminated biological activity suggesting this region contains the transactivation domain consisting of stimulatory and inhibitory subdomains (Ko *et al.,* 1996; Ko *et al.,* 1997).

Molecular Mechanism of CYP1A1 Induction

The model for AhR signaling to induce CYP1A1 expression begins with the exposure to a lipophilic ligand, such as TCDD, which can easily diffuse across a cell membrane and enter the cell. Immunofluorescence microscopy using AhR specific antibodies reveals that the unoccupied receptor is localized in the cytosol (Pollenz *et al.,*

1994). The unbound AhR exists in the cytosol complexed with a dimer of heat shock proteins, Hsp90, which maintains the AhR in a high affinity ligand binding state and prevents nuclear translocation and dimerization with ARNT, one molecule of the co-chaperone protein p23, and one molecule of XAP2, an immunophilin-related protein involved in the regulation of AhR turnover (Perdew, 1992; Meyer *et al.,* 1998, Meyer and Perdew, 1999; Heid *et al.,* 2000; Dull *et al.,* 2002). Ligand binding to the receptor induces a conformational change that results in increase affinity for DNA binding and decrease rate of ligand dissociation (Bradfield *et al.,* 1988) resulting in translocation of the ligand bound AhR to the nucleus and subsequent heterodimerization with its partner ARNT (Whitlock, 1999; Gonzalez *et al.,* 1996, Schmidt and Bradfield, 1996; Hankinson *et al.,* 1995; Okey *et al.,* 1994). ARNT was termed the AhR nuclear translocator protein, although it is now known that it is not required for nuclear translocation of the AhR (Reyes *et al.,* 1992). Two theories exist for the formation of the heterodimer complex with ARNT. The first model is that the ligand induces dissociation of chaperone proteins from the AhR resulting in the exposure of the nuclear localization signal, followed by nuclear uptake and heterodimerization with ARNT. The second view suggests that the ligand binding induces nuclear translocation of the entire core complex and dissociation occurs upon heterodimerization with ARNT (Petrulis and Perdew, 2002). The exact chain of events leading to translocation into the nucleus is still under debate.

The AhR/ARNT heterodimer complex recognizes and binds to distinct DNA sequences called xenobiotic response elements (XREs) leading to the transactivation and induction of target genes, such as CYP1A1, that contain XREs in their promoter region. The DNA recognition region is located in the HLH and PAS domains of both proteins.

Heterodimerization orients the basic regions of the proteins towards the XRE sequences in the major groove of DNA (Bacsi *et al.,* 1995). Electrophoretic mobility shift assays indicate that the liganded AhR recognizes a specific DNA motif containing the following XRE sequence 5' TGCGTG 3' (Denison *et al.,* 1989). XRE consensus sequences were initially identified by using short segments of upstream regions of mouse and rat *CYP1A1* genes fused to the chloramphenicol acetyl transferase (CAT) reporter gene that became activated upon TCDD or PAH treatment (Fujisawa-Sehara *et al.,* 1987; Denison *et al.,* 1988). Five functional XREs were identified within the 1218 bp 5' to the cap site of the mouse *CYP1A1* gene (Lusska *et al.,* 1993), and the human *CYP1A1* gene was found to have at least seven XREs within the first 1300 bp of the 5' upstream flanking region (Fisher *et al.,* 1990; Kubota *et al.,* 1991).

The AhR/ARNT heterodimer complex binds XRE elements and is also able to recruit and bind nuclear co-activators to mediate transcriptional activation. Chromatin immunoprecipitation experiments indicate that NCoA-1, NCoA-2, NCoA-3, p/CIP, CBP/p300, and RIP140 interact with *CYP1A1* enhancer region in a TCDD-dependent fashion, (Beischlag *et al.,* 2002; Kobayashi *et al.,* 1997; Kumar *et al.,* 1999a). These cofactors interact with the AhR via its C-terminal transactivation domain (Kuma *et al.,* 1999b). These cofactors are involved in the recruitment of additional proteins to form bridges between several classes of transcription factors and the core transcription initiation complex (Beischlag *et al.,* 2002), as well as ATP-dependent chromatin remodeling and acetylation of promoter histones (Hestermann *et al.,* 2003). The presence of these proteins results in the relaxation of the chromatin and the recruitment of RNA polymerase to initiate transcription of target genes, such as CYP1A1.

FIGURE 1-1

Mechanism of CYP1A1 Induction

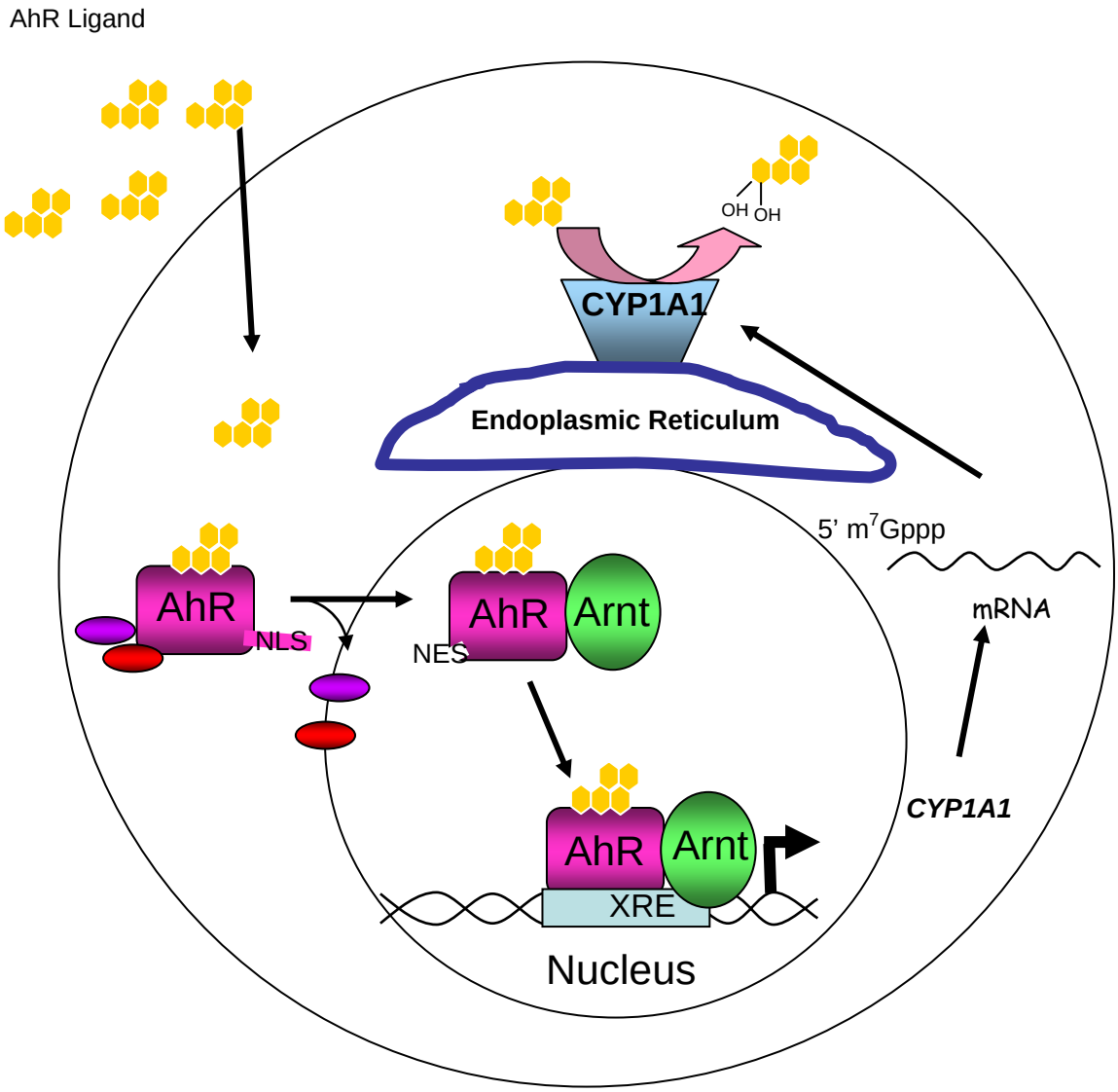


FIGURE 1-1. Mechanism of CYP1A1 induction. Normally CYP1A1 is not basally expressed and its expression is induced upon exposure to xenobiotics, such as BaP. CYP1A1 induction is primarily regulated by the AhR, which resides in the cytosol bound by chaperone proteins. Upon exposure to a ligand, the AhR translocates to the nucleus and disassociates from its chaperone proteins and heterodimerizes with its partner Arnt. This heterodimer complex is then able to bind the xenobiotic responsive element (XRE) in the promoter region *CYP1A1*.

CYP1A1 Induction is a Biomarker for Exposure to Environmental Contaminants

The induction of CYP1A1 activity is widely used as biomarker for exposure to various classes of chemicals including TCDD and PAHs. The oxidation of the substrate 7-ethoxyresorufin to resorufin is specifically mediated by CYP1A1 and CYP1A2 (Burke and Mayer, 1975; Nebert and Gelboin, 1968a; Johnson *et al.,* 1979). This reaction was used to develop a fluorimetric assay by Burke and Mayer to easily measure the ethoxyresorufin O-deethylase (EROD) activity from microsomal preparations in order to sensitively monitor induction of CYP1A1 upon xenobiotic treatment (Burke and Mayer, 1974; Pohl and Fouts, 1980). The EROD assay is a useful bioassay to evaluate the relative biological and toxicological potency of compounds and complex mixtures containing potential AhR ligands (Casterline *et al.,* 1983; Tillitt *et al.,* 1988; Tillitt *et al.,* 1991; Safe *et al.,* 1986). However, the EROD assay exhibits several disadvantages that limit the capacity for widespread application as a screening method. For instance, there are intra- and inter-species differences in response to halogenated aromatic hydrocarbons (Denison *et al.,* 1986; Denison *et al.,* 1995). More importantly, many AhR ligands are substrates of CYP1A1 which results in competitive inhibition of EROD activity, as well as potentially inactivating the CYP1A1 enzyme (Hahn *et al.,* 1993). To address these issues, an alternative class of in vitro assays was designed to determine enzymatic activity based on AhR activation and induction of a reporter gene (Aarts *et al.,* 1995).

The use of a reporter construct containing the firefly luciferase gene under the transcriptional control of XREs has proven to be a sensitive tool to detect the presence of AhR agonists (Postlind *et al.,* 1993; Denison *et al.,* 1993; Garrison *et al.,* 1996; Yueh *et*

al., 2004). These chemically activated luciferase expression (CALUX) bioassays have high correlation between EROD activity and the CALUX bioassay. However, the CALUX method is more sensitive and is not limited by CYP1A1 substrate inhibition. In addition, The CALUX assay enables the determination of total toxic equivalents (TEQs) relative to TCDD as a comparison and identification of AhR ligands (Aarts *et al.,* 1993, Anderson and Fisher, 1995; Sanderson *et al.,* 1996). Although TEQs have been determined for many TCDD-like compounds and PAHs, the exact values can vary greatly depending on specific species (Safe *et al.,* 1994; Ahlborg *et al.,* 1994). Various CALUX cell lines were constructed by stably transfecting plasmids containing small regions of the *CYP1A1* gene containing several XRE elements fused upstream of the firefly luciferase gene into several types of mammalian cell lines including mouse Heap1c1c, rat H4IIE, guinea pig GPC16, Hamster AHL, Human HepG2, MCF7, and LS180 cells (Denison *et al.,* 1993; Garrison *et al.,* 1996; Aarts *et al.,* 1993; Postlind *et al.,* 1993; Yueh *et al.,* 2004). These cell lines allow for a species specific comparison of sensitivity and response to known AhR agonists and complex mixtures of compounds (Long *et al.,* 2003).

Although the CALUX bioassays that have been developed are quite sensitive and useful for the identification and characterization of AhR ligands, there are cost effective problems which restrict their adaptation into high-throughput screening bioassays. A new generation of recombinant cell bioassays for the detection of AhR activation were developed that employs the use of the enhanced green fluorescent protein (EGFP) reporter gene under the control of XREs (Nagy *et al.,* 2002a; Nagy *et al.,* 2002b). Exposure of these recombinant cells to TCDD and other AhR agonists leads to an induction of EGFP in a dose, time, and substrate dependent manner (Nagy *et al.,* 2002a).

The use of an EGFP based reporter system to identify AhR ligands is cost efficient because EGFP can be directly measured in intact cells without the addition of any necessary reagents and therefore can be easily adapted for rapid screening of large chemical libraries that can activate the AhR signaling cascade resulting in induced EGFP expression (Nagy *et al.*, 2002b).

In addition to the in vitro cell culture bioassays, several transgenic mouse models expressing large portions of the *CYP1A1* promoter region fused to a reporter gene, as well as the entire human *CYP1A1* gene including the regulatory regions have been generated (Galijatovic *et al.,* 2004; Campbell *et al.,* 1996). The transgenes were inducible upon treatment with PAHs and the pattern of expression in various tissues correlated with the expected regulation of the CYP1A1 protein. Initial construction of transgenic mouse lines expressing smaller fragments of the *CYP1A1* promoter region led to variable basal activities and inconsistencies in the pattern of tissue specific expression of the transgenes (Jones *et al.,* 1991; Smith *et al.,* 1995; Galijatovic *et al.,* 2004), however, these issues were resolved when much larger promoter regions were incorporated into the transgene (Campbell *et al.,* 1996). This suggests that important regulatory regions may exist in the *CYP1A1* promoter that are distal from the transcriptional start site. Although several transgenic mouse models exist that provide information on transcriptional activation of the *CYP1A1* gene, a model that allows for the simple and rapid screening of inducible and functional human CYP1A1 protein is currently lacking.

Phase II Metabolism and the Process of Glucuronidation

Phase II drug metabolizing enzymes work in concert with Phase I enzymes to detoxify and eliminate endogenous and exogenous compounds from the body. Phase II reactions are referred to as conjugative reactions which include glucuronidation, sulfation, acetylation, methylation, and conjugation with glutathione and amino acids. Phase II reactions involve a large polar molecule that is derived from the body to be covalently linked to a substrate, resulting in a conjugated metabolite that is more polar and readily excretable from the body. The most important Phase II enzymes for the detoxification of drugs are the udp-glucuronosyltransferases (UGTs), and approximately 80% of therapeutic drugs are eliminated via the glucuronidation pathway.

The process of glucuronidation is catalyzed by a family of enzymes called UPD-glucuronosyltransferases (UGTs). UGTs utilize the co-substrate uridine diphospho-glucuronic acid (UDPGA) and transfer the glucuronic acid moiety to a variety of endogenous compounds and xenobiotics to form the metabolite called the glucuronide. In 1855 Schmid reported the first compound characterized as a glucuronide, euxanthic acid, which was isolated from the urine of cows that fed on mango leaves, and this glucuronide was used as a major component of the dye Indian yellow (Dutton, 1980). While studying the metabolism of the compound camphor, Schmiedeberg and Meyer isolated a camphor conjugate from the urine of dogs and characterized the sugar moiety as glucuronic acid (Schmiedeberg and Meyer, 1879). A landmark discovery was made in 1953, when Dutton and Storey discovered a thermostable cofactor in the liver that was required for the formation of a phenol glucuronide in cell-free preparations (Dutton and Storey, 1953; Dutton and Storey, 1954). This compound was isolated and identified as UDPGA and

shown to act as a co-substrate in the reaction in which glucuronic acid was transferred to an acceptor substrate, forming the glucuronide metabolite (Dutton and Storey, 1954; Storey and Dutton, 1955; Smith and Mills, 1954).

Purification and Characterization of UGTs

The heterogeneous substrates that are subject to glucuronidation fueled the debate over the existence of a single UGT enzyme with a promiscuous active site or a population of numerous UGT enzymes (Axelrod *et al.,* 1957; Mulder, 1971). The isolation and purification of UGTs was of critical importance in order to determine distinct populations of UGTs and their substrate specificities. However, UGTs are inherently difficult to purify due to their relative instability in the high concentrations of detergent required for solubilization and phospholipid dependence (Burchell and Coughtrie, 1989). In 1975, the first successful separation of UGT activities was reported by Villar *et al.* when activities toward morphine and p-nitrophenol were resolved from rat liver microsomes, demonstrating distinct and separate populations of UGTs capable of glucuronidating specific substrates (Villar *et al*., 1975). This purification technique utilized DEAE-cellulose column chromatography and was adapted from the method described by Sato *et al.* that was used to resolve microsomal cytochrome P450 and other components of the hepatic mixed function oxidase system (Sato *et al*., 1973). This technique was further validated by Bock *et al*. as they were able to separate two rat liver UGT activities which catalyzed either the glucuronidation of morphine or the glucuronidation of morphine and 1-napthol (Bock et al., 1977). The development of a UGT purification technique using affinity chromatography with UDP-hexanolamine Sepharose beads attached to the

column enabled for the successful purification of UGT enzymes with much higher specific activity (Gorski and Kasper, 1977). This method led to the purification of UGT enzymes including 3-MC-inducible UGT and phenobarbital-inducible UGT (Burchell, 1978; Bock *et al.,* 1980), oestrone-UGT and p-nitrophenol-UGT (Tukey *et al.,* 1978), and testosterone-UGT (Weatherill and Burchell, 1980). It was quickly observed that partially purified delipidated enzymes were catalytically inactive, but activities could be restored upon addition of phospholipids or phosphatidylcholine mixtures, indicating that enzyme activity was dependent on the presence of phospholipids (Tukey *et al.,* 1979, Tukey and Tephly, 1980; Gorski and Kasper, 1978). The combination of purification techniques utilizing chromatofocusing in conjunction with UDP-hexanolamine Sepharose became the method of choice to separate UGTs more readily. This method was initially implemented by Falany and Tephly and resulted in the isolation of three UGT isoforms: 4-nitrophenol-UGT, 3-hydroxyandrogen-UGT, and 17-hydroxysteroid-UGT (Falany and Tephly, 1983). Chowdury and co-workers also isolated six UGTs using this method (Chowdhury et al., 1986). Substrate specificity analysis of UGT isoforms illustrated that 4-nitrophenol-UGT was active toward specific planar phenols but did not have activity for morphine or steroids. 17-hydroxysteroid-UGT demonstrated activity towards several phenols, as well as testosterone and β-estradiol, while 3-hydroxyandrogen-UGT was found to only have activity towards androsterone and etiocholanolone (Falany and Tephly, 1983). Further substrate specificity analysis showed that 17-hydroxysteroid-UGT and 3-hydroxyandrogen-UGT exhibited marked regioselectivity and stereoselectivity of conjugation towards bile acids and steroids (Falany *et al*., 1986). These results demonstrated distinct and overlapping substrate specificity of UGTs.

Physical characterization of the purified enzymes was conducted to determine the homology among the isoforms. Using peptide mapping and amino acid analysis it was observed that 17-hydroxysteroid-UGT and 3-hydroxyandrogen-UGT, both of which have activity towards steroids, were quite homologous but 4-nitriphenol-UGT was found to be quite different in amino acid composition and peptide mapping (Falany *et al*., 1986). This suggested that these UGTs may represent two different subfamilies and this was later confirmed through comparison of nucleotide sequences of the cloned cDNAs encoding for these UGT isoforms (Jackson and Burchell, 1986; Mackenzie, 1986; Mackenzie, 1987; Harding *et al*., 1987; Iyanagi *et al*., 1986).

The UGTs are classified into two distinct gene families, UGT1 and UGT2 (Mackenzie *et al.,* 1997). The UGT2 subfamily is composed of individual genes located in a gene cluster on chromosome 4 at 4q13-q21 and encodes 7 functional UGT2B proteins and 3 UGT2A proteins which have not been functionally characterized (Monaghan *et al.,* 1994; Beaulieu *et al.,* 1997; Chen *et al.,* 1993). The UGT2B members, which include UGT2B4, 2B7, 2B10, 2B11, 2B15, 2B17, and 2B28, primarily conjugate endogenous compounds such as bile acids (Monaghan *et al.,* 1997), steroids (Belanger *et al.,* 1998; Hum *et al.,* 1999), and hormones (Jin *et al.,* 1997; Guillemette *et al.,* 2004; Thibaudeau *et al.,* 2006), but are also important for the elimination of therapeutic drugs (Coffman *et al.,* 1997; Davies *et al.,* 2003). In contrast, the UGT1 subfamily is primarily involved in metabolizing exogenous compounds (Dutton, 1980; Kiang *et al.,* 2004). Although Ritter and co-workers reported isolation and characterization of two human cDNA clones encoding for UGT1s having activity for the endogenous compound bilirubin (Ritter *et al*., 1990), however, it was later discovered that only UGT1A1 was the

only UGT capable of efficiently conjugating bilirubin (Bosma *et al.,* 1994). Serendipitously, during the search for the gene encoding for the bilirubin transferase, Ritter and co-workers stumbled upon a novel gene locus encoding for the *UGT1* family. They initially identified six different gene products from the locus composed of unique exon 1s and a series of transcriptional start sites and shared c-terminal exons (Ritter *et al.,* 1992a). Subsequently, the same group extended the *UGT1* complex to 200 kb and additionally uncovered UGT1A7, UGT1A8, UGT1A9, UGT1A10, and several pseudo genes (Gong *et al*., 2001). It is now known that the UGT1 family consists of nine functional isoforms, UGT1A1 and UGT1A3-UGT1A10, derived from a single gene locus resulting from gene duplication events (Mackenzie *et al.,* 1997; Ritter *et al.,* 1992a) located on chromosome 2 at 2q37 (Harding *et al.,* 1990). Through a process called exon sharing, the first exon is combined with common exons 2-5. This genomic organization results in a diverse set of functional *UGT1* gene products that have a variable amino terminus encoded by the unique exon 1 and an identical carboxyl terminus encoded by exons 2-5 (Wooster *et al.,* 1991; Ritter *et al.,* 1992a). A recent study has identified a novel UGT1A1 isoform called UGT1A1_i2 that is generated by alternative splicing of a newly discovered exon 5 resulting in a truncated and inactive form of the protein, and this splicing event presumably also leads to other inactive UGT1 isoforms containing this truncated exon 5 (Levesque *et al.,* 2007).

FIGURE 1-2

Genomic Organization of the Human *UGT1A* Locus

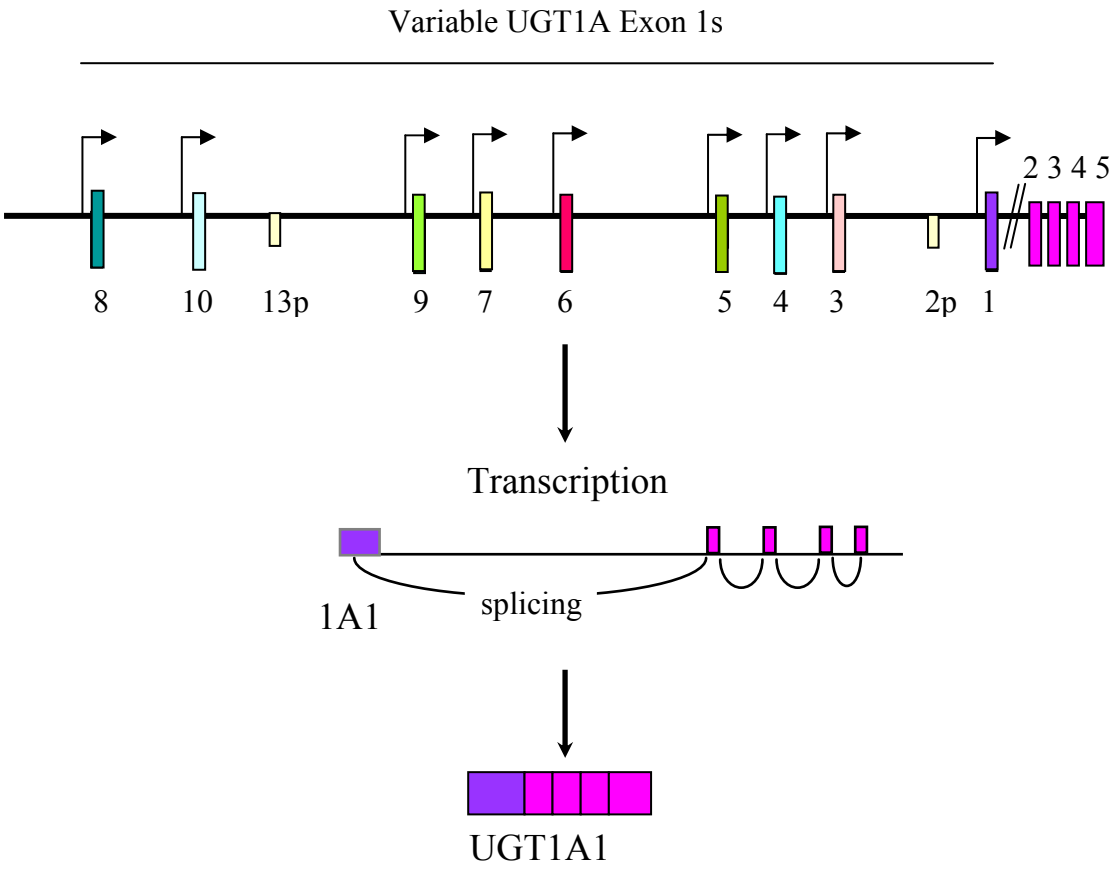


FIGURE 1-2. Genomic organization of the human UGT1A locus. The *UGT1A* locus on chromosome 2 spans 200 kb and is controlled by 13 unique promoters which regulate the independent expression of 9 UGT1A isoforms. Through the process of exon sharing all of the UGT1A isoforms have identical 2-5 exons and a variable exon 1.

The improved biochemical techniques to obtain homogenous UGT preparations led to the production of antibodies raised against purified UGTs (Mackenzie *et al.,* 1984a). These antibodies were used to specifically recognize and immunoprecipitate UGTs that were newly synthesized proteins being translated from polysomes and allowed for the isolation of the first mouse UGT mRNAs. This in vitro translation and specific immunoadsorption method led to the cloning and characterization of several rat liver UGTs (Mackenzie *et al.,* 1984b; Jackson *et al.,* 1985; Mackenzie, 1986). Comparison of the mRNA sequences of the isolated UGTs confirmed the heterogeneous population of the UGT enzymes. This method opened the flood gates for isolation and characterization of UGT enzymes from various species including rat, mouse, and human. The sequences of the enzymes were analyzed and guidelines were set for standardized nomenclature based on evolutionary divergence (Burchell *et al.,* 1991).

Cloning of the UGT cDNAs enabled the expression of recombinant proteins using heterologous cell culture tools and analysis of substrate specificities of the expressed isoforms. Methods of choice included standard transient transfection of recombinant DNA (Mackenzie *et al.,* 1984b; Mackenzie, 1986; Remmel and Burchell, 1993) or stable transfection of the DNA (Wooster *et al*., 1993) into the genome of the COS cells which express minimal levels of UGTs. Other laboratories also utilized the expression of UGTs in insect SF-9 cells following infection with UGT-recombinant AcMNPV virus (Strassburg *et al*., 1996; Strassburg *et al*., 1998a; Strassburg *et al*., 1999, Nguyen and Tukey, 1997). After transfection cells were harvested 48-72 hours later and enzyme activity towards various substrates were measured using radiolabeled co-substrate UDPGA followed by thin layer chromatography. There have been hundreds of known

agents that have been identified as substrates for the expressed UGTs (Tukey and Strassburg, 2000). The structurally divergent compounds include a wide breadth of chemical classes including alcohols, flavones, coumarins, carboxylic acids, amines, opioids, and steroids (Tukey and Strassburg, 2000; Tukey and Strassburg, 2001). The reactive functional groups associated with these compounds are found in our daily dietary constituents, as well as pharmaceutical agents. These xenobiotic agents are ingested and undergo detoxification mechanisms that likely include glucuronidation by UGT enzymes.

Despite the differences in primary amino acid sequences between the two UGT families, the C-terminal domains of the proteins have very high sequence identity, implicating the conserved function of UDPGA binding, (Burchell and Coughtrie, 1989; Ritter *et al*., 1992a; Tephly and Burchell, 1990). The N-terminal domain of all UGTs is highly divergent and catalytic activity analysis of chimeric UGT proteins suggests that this region is responsible for the substrate specificity (Mackenzie, 1990). Substrate specificity varies among UGT isoforms with some having strict specificity, while others accept a wide range of structurally unrelated substrates. Small molecules that form phenolic-hydroxy glucuronides such as, 4-nitrophenol, 1-napthol, and the coumarin derivative 4-methylumbelliferone serve as substrates for most of the UGTs but are catalyzed most efficiently by the UGT1 proteins, except for UGT1A4 (Tukey and Strassburg, 2000). There is considerable substrate specific redundancy in phenolic glucuronidation among UGT1A1, UGT1A3, UGT1A7, UGT1A8, UGT1A9, and UGT1A10 (Tukey and Strassburg, 2000; Meech and Mackenzie, 1997). Meanwhile, some substrates are glucuronidated by specific isoforms, as exhibited by UGT1A1-specific bilirubin glucuronidation (Bosma *et al.,* 1994) and the UGT1A3- and UGT1A4-

specific formation of quaternary ammonium glucuronides (Green *et al*., 1998; Green *et al*., 1995). The glucuronidation of morphine and other structurally similar opioids is mainly catalyzed by UGT2B7, although UGT1A1 (Coffman *et al*., 1995) and UGT1A8 (Cheng *et al*., 1998) do exhibit some activity towards morphine.

The metabolism of substrates via the glucuronidation pathway was originally thought to occur mainly in the liver (Dutton, 1980). However, more recent studies have identified UGT activity toward bile acids, phenols, and bilirubin in numerous organs including the intestine, kidney, and colon (Matern *et al.,* 1984; Pacifici *et al.,* 1986; Parquet *et al.,* 1985; Peters *et al.,* 1988; Peters *et al.,* 1989; Peters *et al.,* 1991; Pacifici *et al.,* 1988; McDonnell *et al.,* 1996). Characterization of UGT expression in various tissues has been complicated by the high degree of sequence homology of the *UGT* gene products. For example, sequence homology exceeding 93% among UGT1A3, UGT1A4, and UGT1A5, as well as among UGT1A7, UGT1A8, UGT1A9 and UGT1A10 limits the ability to use DNA fragments as probes in hybridization techniques such as Northern blot analysis (Strassburg *et al*., 1997b). The use of antibodies raised against purified UGTs to detect expression patterns in target tissues has also limited specificity due to recognition of conserved epitopes within the UGT proteins (Strassburg *et al*., 1998a). The refinement of specific reverse transcriptase (RT)-PCR technique has made it possible to detect single base pair changes in DNA sequence which allowed for the identification of highly homologous *UGT* gene transcripts.

The use of RT-PCR was a major breakthrough in the characterization of UGT expression patterns in the liver and throughout the gastrointestinal tract (GI) (Strassburg *et al*., 1997a, Strassburg *et al*., 1997b). In addition, this method allowed for the semi-

quantification of relative mRNA abundance of UGT transcripts in different tissues. The expression pattern of the human UGT1A enzymes indicates that they are expressed and regulated in a tissue-specific manner. There are 17 UGT enzymes that have been shown to be expressed in humans, nine functional UGT1 isoforms (UGT1A1, UGT1A3, UGT1A4, UGT1A5, UGT1A6, UGT1A7, UGT1A8, UGT1A9, UGT1A10), seven proteins encoded by *UGT2B* genes (UGT2B4, UGT2B7, UGT2B11, UGT2B15, UGT2B17, UGT2B28) and one UGT2A enzyme (UGT2A1) (Tukey and Strassburg, 2000). The majority of the UGT1 proteins are expressed in the liver and include UGT1A1, UGT1A3, UGT1A4, UGT1A6, and UGT1A9 (Strassburg *et al.,* 1997a). Interestingly, UGT1A7, UGT1A8, and UGT1A10 are exclusively extrahepatic (Strassburg *et al.,* 1997b; Strassburg *et al.,* 1998a). UGT1A8 and UGT1A10 are ubiquitously found throughout the GI tract, particularly in the small and large intestine, whereas UGT1A7 is expressed primarily in the proximal areas of the GI tract, such as the esophagus and stomach (Strassburg *et al.,* 1997a; Strassburg *et al.,* 1998a; Strassburg *et al.,* 1998b). Analysis of extrahepatic expression outside of the GI tract indicates expression of UGT1A9 in the kidney (McGurk *et al.,* 1998) and UGT1A6 in the rat brain (Suleman *et al.,* 1998). The expression of the human *UGT1* locus in transgenic mice revealed that the UGT1A enzymes are differentially expressed in the liver and the GI tract, similar to the expression pattern observed in humans (Chen *et al.,* 2005). In addition, the tissue-specific expressed UGTs were inducible upon treatment with pregnenolone-16α-carbonitrile and TCDD. These finding indicate that the human *UGT1* locus is differentially regulated, with a unique complement of gene transcripts found in the different tissues.

UGT2 genes are also regulated in a tissue specific manner, however, distinct differences in hepatic and extrahepatic isoform expression patterns have not been observed. All of the *UGT2B* gene products have been found in the liver (Tukey and Strassburg, 2000). The most distinct differential expression pattern of the UGT2 genes is the localization of the UGT2A1 which seems to be restricted to the sensory tissues, such as olfactory mucosa, and not expressed in the liver or GI tract (Jedlitschky *et al*., 1999). Many of the UGT2Bs are abundantly expressed in the colon such as UGT2B7, UGT2B10, and UGT2B15, whereas UGT2B4 expression is absent (Strassburg *et al*., 2000). UGT2B7, UGT2B10, UGT2B15, and UGT2B17 can be found throughout the GI tract and also in steroid sensitive target tissues (Beaulieu *et al*., 1996; Beaulieu *et al*., 1997; Levesque *et al*., 1997).

The GI tract and liver are the primary organs responsible for the metabolic deactivation of dietary constituents and therapeutic drugs. The liver is comprised mainly of hepatocytes which represents the major metabolic cell type of the liver. As epithelial cells, hepatocytes have a basolateral membrane that faces the circulation where uptake mechanisms allow for compounds to be directed to cellular sites for metabolism (Wilton and Mathews, 1996). Clearance of metabolites occurs via the apical membrane by specific transport processes (Konig *et al*., 1999; Kullack-Ublick *et al*., 2000), and the exported conjugates are transported to the duodenum via the bile ducts. The human digestive tract comprises one of the largest surface areas of the body. Food and xenobiotic compounds are immediately targeted for metabolism upon contact with squamous cells in the oral cavity. In addition, the proximal portions of the GI tract play important roles in resorption and metabolism of drugs. It is therefore not surprising that

drug metabolizing enzymes, such as the UGTs, are specifically regulated and expressed in these target tissues that come in contact with xenobiotics (Tukey and Strassburg, 2001).

Implications in Disease and Toxicity Due to Glucuronidation Deficiency

The large interindividual variability of UGT expression in various tissues is an important determinant of response to drugs and xenobiotics that are primarily eliminated by the glucuronidation process (Burchell *et al*., 2000). In many cases, decreased expression of a specific UGT enzyme may result in adverse metabolic consequences by diverting a compound into pathways that produce bioactive intermediates that can covalently bind proteins and nucleic acids. An example of such an event occurs when deficiency in glucuronidation leads to the altered biotransformation of the commonly used analgesic drug, acetaminophen. Acetaminophen is primarily cleared via the glucuronidation pathway, and reduced UGT activity would allow for the accumulation of acetaminophen which can be bioactivated by cytochrome P450s. At normal doses the bioactivated acetaminophen metabolite is detoxified by glutathione conjugation, however, high concentrations of the toxic metabolite readily depletes glutathione. This results in the accumulation of the toxic acetaminophen metabolite that is capable of covalently binding proteins and cause hepatic and renal damage (Hinson, 1980). A study conducted by de Morais and coworkers illustrated that Gunn rats, which are genetically deficient in UGT1 proteins, had greater susceptibility to acetaminophen-induced toxicity as compared to Wistar rats which are the parent strain of Gunn animals (de Morais *et al*.,

1992). These results support the hypothesis that deficiency in the activity of UGT1 isoforms can be a phenotypic determinant of acetaminophen toxicity.

The molecular mechanism for the large interindividual phenotypic variations in UGT activity is not well understood. However, evidence suggests that polymorphisms present in genes encoding for UGTs may significantly impact drug response and disease susceptibility. Initial evidence suggesting alterations in *UGT* genes as a genetic risk factor of cancer was observed in a study where polymorphisms of the *UGT1A1* candidate gene were assessed (Guillemette *et al*., 2000a). UGT1A1 is abundantly expressed in mammary tissue and is involved in the inactivation of estradiol and it catechol-reactive metabolites (Senafi *et al*., 1994; Guillemette *et al*., 2000a). It was hypothesized that the presence of the common genetic variant in the *UGT1A1* gene, which entails a di-nucleotide repeat polymorphism in the atypical TATA-box region of the *UGT1A1* promoter, would result in increased levels of estrogen exposure and consequently increased estrogen-related cancer risk. It was observed that women who were carriers of the polymorphic UGT1A1*28 and UGT1A1*34 alleles had elevated estradiol levels, and these alleles were associated with increased risk of developing invasive breast cancer in premenopausal African American women (Guillemette *et al*., 2000a).

Glucuronidation is known to be a major pathway for the detoxification of environmental contaminants, such as PAHs found in cigarette smoke, which are known to cause cancer (Bock *et al*., 1999). Therefore, the efficiency of specific UGT isoforms is critical in protecting against toxicity. It has been shown that polymorphic variation in UGTs has the potential to alter sensitivity to PAHs that are present in the diet and the environment (Hu and Wells, 1994). In particular, UGT1A7 is an important extrahepatic

UGT which has been shown to be active towards numerous carcinogens, such as BaP metabolites (Guillemette *et al*., 2000b). UGT1A7 was found to be expressed ubiquitously throughout the oral cavity, which are tissues in direct contact with cigarette smoke (Zheng *et al*., 2001). It was observed that the UGT1A7 allele with low activity was associated with increased risk of otolaryngeal cancer. In addition, polymorphisms resulting in decreased activity of UGT1A7 was also found to be associated with increased risk of liver and colon cancer (Vogel *et al*., 2001; Zheng *et al*., 2001; Strassburg *et al*., 2002).

Perhaps the best known effects of glucuronidation deficiency occur within the UGT1 family of proteins which are generally regarded as xenobiotic detoxifying enzymes. In addition to its wide array of xenobiotic substrates, UGT1A1 is known to be the only isoform that significantly contributes to the conjugation and detoxification of the endogenous compound bilirubin (Bosma *et al.,* 1994). Bilirubin is the metabolic by-product of the catabolism of heme, which is derived from hemoglobin, cytochromes, catalase, peroxidase, and other hemoproteins (Tenhunen *et al.,* 1969). Bilirubin is present in the plasma tightly bound to albumin and is taken up into the liver partly through a carrier mediated mechanism (Cui *et al*., 2001) where it is conjugated by UGT1A1 to form mono- and di-glucuronides. Defects in clearance of bilirubin lead to excessive levels of unconjugated bilirubin which saturates the capacity of albumin for high affinity binding. Unbound bilirubin can leave the plasma and enter cells causing cellular toxicity via unknown mechanisms. A genetic model of unconjugated hyperbilirubinemia in the rat was discovered by Gunn in 1938 (Gunn, 1938) and it was determined that the rats lacked the functional enzyme to conjugate bilirubin (Lathe and Walker, 1957). Sequencing of

the Gunn rat UGT1A1 cDNA revealed that single base pair deletion located in the common exon region resulted in a C-terminal truncation of the protein (Iyanagi *et al.,* 1989). In humans, functional deficiency of UGT1A1 results in an accumulation of unconjugated bilirubin in the plasma. The degree of hyperbilirubinemia is classified based upon three grades of UGT1A1 deficiency that occurs in humans, Crigler-Najjar syndrome type I (CN-1), Crigler-Najjar syndrome type II (CN-2), and Gilbert syndrome (Kadakol *et al.,* 2000). CN-1 syndrome was originally described in 1952 and is characterized by potentially lethal levels of bilirubin in the plasma (serum bilirubin 20-50 mg/dL) (Crigler and Najjar, 1952). The mechanism was later identified as the complete absence of hepatic glucuronidation (Seppen *et al.,* 1994), due to lack of UGT1A1 activity. Phototherapy has been used as a treatment option and has extended life expectancy but liver transplant is the only curative therapy currently available (Gourley *et al.,* 1997). CN-2 syndrome was first described by Arias in 1962 (Arias *et al.,* 1962) and is characterized by intermediate levels of hyperbilirubinemia (7-20 mg/dL) due to a severe decrease in UGT1A1 activity (Seppen *et al.,* 1994). CN-2 syndrome can be partly treated by phenobarbital administration and subsequent induction of UGT1A1 activity, resulting in decreased serum bilirubin levels (Arias *et al.,* 1969). Both CN-1 and CN-2 syndromes result from mutations in the coding regions of the exons, as well as TA insertion in the promoter (Ciotti *et al.,* 1995; Ciotti *et al.,* 1998; Ritter *et al.,* 1992b; Costa, 2006). Sustained levels of unconjugated hyperbilirubinemia results in a wide array of neurological defects known as bilirubin encephalopathy. Accumulation and deposition of bilirubin in the focal brain regions is believed to cause cell death and neural dysfunction (Wennberg, 2000; Roger *et al*., 1995).

Gilbert syndrome is the mildest form of inherited unconjugated hyperbilirubinemia and is considered to be harmless. Gilbert syndrome is associated with a structurally functional coding region for *UGT1A1*, but has a variant promoter region that contains an extra TA insertion in the TATAA element of the promoter which results in decreased UGT1A1 transcription by 70% (Bosma *et al.,* 1995). Homozygosity for the variant promoter is required for Gilbert syndrome. Some Japanese studies indicate that Gilbert syndrome associated with an aberration in the TATAA element is less frequent in the Japanese population but instead heterozygous mutations in the coding regions of *UGT1A1* may be the cause of the mild unconjugated hyperbilirubinemia, consistent with Gilbert syndrome diagnosis (Koiwai *et al.,* 1995; Soeda *et al.,* 1995). The inheritance of CN-1 and CN-2 generally follow an autosomal recessive pattern (Crigler, 1952) because heterozygous carriers can sufficiently maintain bilirubin plasma levels within normal concentrations. However, heterozygous carriers of certain *UGT1A1* mutations exhibit mild to moderate levels of hyperbilirubinemia, suggesting an autosomal dominant pattern of inheritance (Koiwai *et al.,* 1996). This suggests that UGT1A1 mutants could be acting as a dominant negative protein toward the functional UGT1A1 wild type protein.

Proposed Structure of UGTs

UGTs are type I topology membrane bound proteins localized to the endoplasmic reticulum (ER) (Vanstapel and Blanckaert, 1988; Shepherd *et al.,* 1989) and the nuclear envelope (Radominska *et al.,* 2002). UGTs are synthesized as pre-proteins with a signal peptide sequence in the N-terminus that mediates integration into the ER (Mackenzie and Owens, 1984; Harding *et al.,* 1987). The mature protein predominantly resides in the

lumen of the ER with a single transmembrane spanning domain near the C-terminus (Iyanagi *et al.,* 1986) followed by a 20 amino acid carboxyl tail that contains the ER retention signal and protrudes into the cytosol (Nilsson *et al.,* 1989; Meech and Mackenzie, 1997; Barre *et al.,* 2005). It has been suggested that UGT-dependent glucuronidation in the microsomal membranes is regulated in a complex manner that may be due to the compartmentation of the UGTs in the ER (Ikushiro *et al.,* 1997). It is known that glucuronidation activity in intact microsomes is much lower than membrane-disrupted microsomes via sonication or the addition of a detergent (Zakim & Dannenberg, 1992). This phenomenon, termed latency, is believed to be due to UGT membrane topology which requires translocation of the co-substrate UDPGA by a transport protein into the ER (Hauser *et al.,* 1988). An alternative hypothesis, based on kinetic data of UGTs in microsomes and in reconstituted systems, is that UGTs in the membrane can exist in multiple conformational states resulting in different activities (Dannenberg *et al.,* 1990). UGT activity may be inhibited due to a repressive conformation and the functional states of UGTs in the membrane could be affected by the formation of oligomers among the UGTs (Ikushiro *et al.,* 1997).

Potential Protein-Protein Interaction Among the UGTs

Numerous observations support the theory of UGT oligomerization in the ER. Purification of UGTs from rat liver using chromatofocusing and UDP-hexanolamine affinity chromatography illustrated inseparable testosterone-UGT and androsterone-UGT protein aggregates (Matsui *et al.,* 1986). Purification via gel filtration of chenodeoxycholic-UGT isozyme also appeared to exist as an aggregate (Matern *et al.,*

1982). Radiation inactivation analysis to determine the molecular mass of membrane-bound proteins indicated that the dimer and/or tetramer of UGTs may be the active form for enzymatic activity (Peters *et al.,* 1984; Vessey and Kempner, 1989). It is also postulated that the formation of monoglucuronide phenols is catalyzed by a dimeric form of UGT, while diglucuronidation of phenols is catalyzed by the tetramer (Gschaidmeier *et al.,* 1994). Purification of a UGT from pig liver based on p-nitrophenol activity was performed and it exhibited three bands around 58 kDa with an intensity ratio of 1:2:1 on SDS-PAGE, further providing support that UGTs can form tetrameric structures (Hochman and Zakim, 1983). Cross-linking of rat microsomal proteins followed by immunopurification with a UGT1-specific anti-peptide antibody suggested hetero-oligomerization of UGT1A subfamily with UGT2B1 (Ikushiro *et al.,* 1997). These observations provide evidence that UGTs may exist as oligomeric complexes in the ER, however, studies providing concrete evidence for in vivo protein-protein interactions among UGTs are lacking. Very little is also known about the structure of the UGTs because they are membrane-bound proteins and have eluded crystallization analysis. Therefore, more intensive research is required in this area to understand the nature of the UGT protein interactions.

Objectives of the Dissertation

At the advent of my thesis work, the molecular mechanism of CYP1A1 induction by xenobiotic compounds was well established (Whitlock, 1999). The induction of CYP1A1 following exposure to various classes of environmental contaminants, such as PAHs, is a protective mechanism in which the harmful substrate leads to the

transcriptional activation and ultimately in the increased CYP1A1 protein. This regulatory feedback loop prevents accumulation of the toxic compound by the virtue that the substrate induces its own metabolism, thus, allowing the system to return to the basal state once the compound has been efficiently cleared. The molecular details that govern this signaling cascade have been well studied in vitro and have been extremely useful in identifying and characterizing the protein components and DNA regulatory elements required in *CYP1A1* gene regulation. The transcriptional activation pathway of the *CYP1A1* gene has been widely implemented as a biomarker for exposure to large number of environmental chemicals that can bind to the AhR, the key mediator in CYP1A1 regulation. Numerous bioassays based on AhR-dependent induction of CYP1A1 have been developed. However, these cell culture based models do not resemble the physiological conditions that occur in vivo when one is exposed to these xenobiotic compounds. Thus, our lab has embarked on a quest to generate and characterize a transgenic mouse model that expresses a chimeric transgene that can be used to monitor both the transcriptional activation and the function of CYP1A1 protein. Our transgenic mouse model would allow for the exploration of human *CYP1A1* gene regulation in vivo, as well as the functional CYP1A1^{GFP} chimeric protein.

During my work on the characterization of the CYP1A1^{GFP} transgenic mouse I learned a great deal about fluorescence microscopy and its potential applications in other aspects of my thesis work. After attending the UGT Glucuronidation Workshop meeting that was held in Dundee, Scotland in September of 2004, I was exposed to several posters providing preliminary observations that UGTs were forming higher molecular aggregates. After returning from this conference I became intrigued about the possibility

that UGTs were forming oligomer complexes in the ER and decided to pursue this avenue of research. At this time there was very little concrete evidence that UGTs were indeed dimerizing. The majority of the work being done at this time was limited to biochemical analysis using gel filtration columns. I chose to address the question of UGT dimerization by applying the fluorescence microscopy techniques, in conjunction with biochemical evidence, to test if UGTs were capable of forming homo/heterodimers. The focus of the majority of my thesis work has been to explore the intermolecular interactions of the UGTs in living cells using fluorescence resonance energy transfer (FRET). FRET is a non-invasive spectroscopic method that can be used in live cells to monitor spatial and temporal intermolecular interactions of chimeric proteins that have acceptor and donor fluorophores attached. To further complement the in vivo analysis of UGT protein-protein interactions by FRET, co-immunoprecipitation experiments were also implemented to provide further evidence to support the existence of UGT1A protein dimers. After discovering that the UGT1A proteins were forming homodimers, as well as heterodimers, I began to extend my inquiries into the structural aspects of these proteins. I became interested in isolating the structural domains involved in facilitating oligomerization of the UGT1A proteins. Through use of truncation analysis of the UGT1A1 protein and comparative homology modeling, I attempted to dissect out critical areas of the protein that were important for protein-protein interactions and also to build models the of quaternary UGT complexes.

References

Aarts JM, Denison MS, Cox MA, Schalk MA, Garrison PM, Tullis K, de Haan LH, Brouwer A. Species-specific antagonism of Ah receptor action by 2,2',5,5'-tetrachloro- and 2,2',3,3'4,4'-hexachlorobiphenyl. Eur J Pharmacol. 1995 Dec 7;293(4):463-74.

Ahlborg UG, Brouwer A, Fingerhut MA, Jacobson JL, Jacobson SW, Kennedy SW, Kettrup AA, Koeman JH, Poiger H, Rappe C, et al. Impact of polychlorinated dibenzo-p-dioxins, dibenzofurans, and biphenyls on human and environmental health, with special emphasis on application of the toxic equivalency factor concept. Eur J Pharmacol. 1992 Dec 1;228(4):179-99. Review.

Anderson DR, Fisher R. Sources of dioxins in the United Kingdom: the steel industry and other sources. Chemosphere. 2002 Jan;46(3):371-81.

ARIAS IM. Chronic familial nonhemolytic jaundice with conjugated bilirubin in the serum. Gastroenterology. 1962 Nov;43:588-90.

Arias IM, Gartner LM, Cohen M, Ben-Ezzer J, Levi AJ. Chronic nonhemolytic unconjugated hyperbilirubinemia with glucuronyl transferase deficiency: evidence for genetic heterogeneity. Trans Assoc Am Physicians. 1968;81:66-75.

AXELROD J, KALCKAR HM, MAXWELL ES, STROMINGER JL. Enzymatic formation of uridine diphosphoglucuronic acid. J Biol Chem. 1957 Jan;224(1):79-90.

Bacsi SG, Reisz-Porszasz S, Hankinson O. Orientation of the heterodimeric aryl hydrocarbon (dioxin) receptor complex on its asymmetric DNA recognition sequence. Mol Pharmacol. 1995 Mar;47(3):432-8.

Bailey DG, Spence JD, Edgar B, Bayliff CD, Arnold JM. Ethanol enhances the hemodynamic effects of felodipine. Clin Invest Med. 1989 Dec;12(6):357-62.

Bailey DG, Spence JD, Munoz C, Arnold JM. Interaction of citrus juices with felodipine and nifedipine. Lancet. 1991 Feb 2;337(8736):268-9.

Barre L, Fournel-Gigleux S, Finel M, Netter P, Magdalou J, Ouzzine M. Substrate specificity of the human UDP-glucuronosyltransferase UGT2B4 and UGT2B7. Identification of a critical aromatic amino acid residue at position 33. FEBS J. 2007 Mar;274(5):1256-64. Epub 2007 Jan 29.

Beaulieu M, Lévesque E, Hum DW, Bélanger A. Isolation and characterization of a novel cDNA encoding a human UDP-glucuronosyltransferase active on C19 steroids. J Biol Chem. 1996 Sep 13;271(37):22855-62.

Beaulieu M, Levesque E, Tchernof A, Beatty BG, Belanger A, Hum DW. Chromosomal localization, structure, and regulation of the UGT2B17 gene, encoding a C19 steroid metabolizing enzyme. DNA Cell Biol. 1997 Oct;16(10):1143-54.

Beischlag TV, Wang S, Rose DW, Torchia J, Reisz-Porszasz S, Muhammad K, Nelson WE, Probst MR, Rosenfeld MG, Hankinson O. Recruitment of the NCoA/SRC-1/p160 family of transcriptional coactivators by the aryl hydrocarbon receptor/aryl hydrocarbon receptor nuclear translocator complex. Mol Cell Biol. 2002 Jun;22(12):4319-33.

Bélanger A, Hum DW, Beaulieu M, Lévesque E, Guillemette C, Tchernof A, Bélanger G, Turgeon D, Dubois S. Characterization and regulation of UDP-glucuronosyltransferases in steroid target tissues. J Steroid Biochem Mol Biol. 1998 Apr;65(1-6):301-10. Review.

BLEIBERG J, WALLEN M, BRODKIN R, APPLEBAUM IL. INDUSTRIALLY ACQUIRED PORPHYRIA. Arch Dermatol. 1964 Jun;89:793-7.

Bock KW, von Clausbruch UC, Josting D, Ottenwälder H. Separation and partial purification of two differentially inducible UDP-glucuronyltransferases from rat liver. Biochem Pharmacol. 1977 Jun 1;26(11):1097-100.

Bock KW, von Clausbruch UC, Kaufmann R, Lilienblum W, Oesch F, Pfeil H, Platt KL. Functional heterogeneity of UDP-glucuronyltransferase in rat tissues. Biochem Pharmacol. 1980 Feb 15;29(4):495-500.

Bock KW, Raschko FT, Gschaidmeier H, Seidel A, Oesch F, Grove AD, Ritter JK. Mono- and Diglucuronide formation from benzo[a]pyrene and chrysene diphenols by AHH-1 cell-expressed UDP-glucuronosyltransferase UGT1A7. Biochem Pharmacol. 1999 Mar 15;57(6):653-6.

Borgen A, Darvey H, Castagnoli N, Crocker TT, Rasmussen RE, Wang IY. Metabolic conversion of benzo(a)pyrene by Syrian hamster liver microsomes and binding of metabolites to deoxyribonucleic acid. J Med Chem. 1973 May;16(5):502-6.

Bosma PJ, Chowdhury JR, Bakker C, Gantla S, de Boer A, Oostra BA, Lindhout D, Tytgat GN, Jansen PL, Oude Elferink RP, et al., The genetic basis of the reduced expression of bilirubin UDP-glucuronosyltransferase 1 in Gilbert's syndrome. N Engl J Med. 1995 Nov 2;333(18):1171-5.

Bosma PJ, Seppen J, Goldhoorn B, Bakker C, Oude Elferink RP, Chowdhury JR, Chowdhury NR, Jansen PL. Bilirubin UDP-glucuronosyltransferase 1 is the only relevant bilirubin glucuronidating isoform in man. J Biol Chem. 1994 Jul 8;269(27):17960-4. Erratum in: J Biol Chem 1994 Oct 14;269(41):2542.

Bradfield CA, Kende AS, Poland A. Kinetic and equilibrium studies of Ah receptor-ligand binding: use of [125I]2-iodo-7,8-dibromodibenzo-p-dioxin. Mol Pharmacol. 1988 Aug;34(2):229-37.

British Broadcasting Corp. (BBC), 2004. Deadly dioxin used on Yushchenko. Retrieved February 14, 2005, from http: //news.-bbc.co.uk/1/hi/world/Europe/4105035.stm.

Burbach KM, Poland A, Bradfield CA. Cloning of the Ah-receptor cDNA reveals a distinctive ligand-activated transcription factor. Proc Natl Acad Sci U S A. 1992 Sep 1;89(17):8185-9.

Burchell B. Substrate specificity and properties of uridine diphosphate glucuronyltransferase purified to apparent homogeneity from phenobarbital-treated rat liver. Biochem J. 1978 Sep 1;173(3):749-57.

Burchell B, Coughtrie MW. UDP-glucuronosyltransferases. Pharmacol Ther. 1989;43(2):261-89. Review.

Burchell B, Nebert DW, Nelson DR, Bock KW, Iyanagi T, Jansen PL, Lancet D, Mulder GJ, Chowdhury JR, Siest G, et al., The UDP glucuronosyltransferase gene superfamily: suggested nomenclature based on evolutionary divergence. DNA Cell Biol. 1991 Sep;10(7):487-94. Review.

Burchell B, Soars M, Monaghan G, Cassidy A, Smith D, Ethell B. Drug-mediated toxicity caused by genetic deficiency of UDP-glucuronosyltransferases. Toxicol Lett. 2000 Mar 15;112-113:333-40. Review.

Burke MD, Mayer RT. Ethoxyresorufin: direct fluorimetric assay of a microsomal O-dealkylation which is preferentially inducible by 3-methylcholanthrene. Drug Metab Dispos. 1974 Nov-Dec;2(6):583-8.

Burke MD, Mayer RT. Inherent specificities of purified cytochromes P-450 and P-448 toward biphenyl hydroxylation and ethoxyresorufin deethylation. Drug Metab Dispos. 1975 Jul-Aug;3(4):245-53.

Campbell SJ, Carlotti F, Hall PA, Clark AJ, Wolf CR. Regulation of the CYP1A1 promoter in transgenic mice: an exquisitely sensitive on-off system for cell specific gene regulation. J Cell Sci. 1996 Nov;109 (Pt 11):2619-25.

Casterline JL Jr, Bradlaw JA, Puma BJ, Ku Y. Screening of fresh water fish extracts for enzyme-inducing substances by an aryl hydrocarbon hydroxylase induction bioassay technique. J Assoc Off Anal Chem. 1983 Sep;66(5):1136-9.

Chen S, Beaton D, Nguyen N, Senekeo-Effenberger K, Brace-Sinnokrak E, Argikar U, Remmel RP, Trottier J, Barbier O, Ritter JK, Tukey RH. Tissue-specific, inducible, and

hormonal control of the human UDP-glucuronosyltransferase-1 (UGT1) locus. J Biol Chem. 2005 Nov 11;280(45):37547-57. Epub 2005 Sep 9.

Chen F, Ritter JK, Wang MG, McBride OW, Lubet RA, Owens IS. Characterization of a cloned human dihydrotestosterone/androstanediol UDP-glucuronosyltransferase and its comparison to other steroid isoforms. Biochemistry. 1993 Oct 12;32(40):10648-57.

Cheng Z, Radominska-Pandya A, Tephly TR. Cloning and expression of human UDP-glucuronosyltransferase (UGT) 1A8. Arch Biochem Biophys. 1998 Aug 15;356(2):301-5.

Chivers, C.J., A dinner in Ukraine made for Agatha Christie. New York Times, New York. December 20, 2004.

Chowdhury NR, Arias IM, Lederstein M, Chowdhury JR. Substrates and products of purified rat liver bilirubin UDP-glucuronosyltransferase. Hepatology. 1986 Jan-Feb;6(1):123-8.

Ciotti M, Chen F, Rubaltelli FF, Owens IS. Coding defect and a TATA box mutation at the bilirubin UDP-glucuronosyltransferase gene cause Crigler-Najjar type I disease. Biochim Biophys Acta. 1998 Jul 1;1407(1):40-50.

Ciotti M, Yeatman MT, Sokol RJ, Owens IS. Altered coding for a strictly conserved di-glycine in the major bilirubin UDP-glucuronosyltransferase of a Crigler-Najjar type I patient. J Biol Chem. 1995 Feb 17;270(7):3284-91.

Coffman BL, Rios GR, King CD, Tephly TR. Human UGT2B7 catalyzes morphine glucuronidation. Drug Metab Dispos. 1997 Jan;25(1):1-4.

Coffman BL, Green MD, King CD, Tephly TR. Cloning and stable expression of a cDNA encoding a rat liver UDP-glucuronosyltransferase (UDP-glucuronosyltransferase 1.1) that catalyzes the glucuronidation of opioids and bilirubin. Mol Pharmacol. 1995 Jun;47(6):1101-5.

Conney AH. Induction of microsomal enzymes by foreign chemicals and carcinogenesis by polycyclic aromatic hydrocarbons: G. H. A. Clowes Memorial Lecture. Cancer Res. 1982 Dec;42(12):4875-917. Review.

CONNEY AH, MILLER EC, MILLER JA. Substrate-induced synthesis and other properties of benzpyrene hydroxylase in rat liver. J Biol Chem. 1957 Oct;228(2):753-66.

Cook JW, Hewett CL, Heiger I. The isolation of a cancer producing hydrocarbon from coal tar. (II) Isolation of 1,2- and 4,5-benopyrenes, perylene and 1,2-benzanthracene. J Chem Soc 1933;296-298.

COOPER DY, ESTABROOK RW, ROSENTHAL O. The stoichiometry of C21 hydroxylation of steroids by adrenocortical microsomes. J Biol Chem. 1963 Apr;238:1320-3.

Costa E. Hematologically important mutations: bilirubin UDP-glucuronosyltransferase gene mutations in Gilbert and Crigler-Najjar syndromes. Blood Cells Mol Dis. 2006 Jan-Feb;36(1):77-80. Epub 2005 Dec 28. Review.

Crews ST, Thomas JB, Goodman CS. The Drosophila single-minded gene encodes a nuclear protein with sequence similarity to the per gene product. Cell. 1988 Jan 15;52(1):143-51.

CRIGLER JF Jr, NAJJAR VA. Congenital familial nonhemolytic jaundice with kernicterus. Pediatrics. 1952 Aug;10(2):169-80.

Cui Y, König J, Leier I, Buchholz U, Keppler D. Hepatic uptake of bilirubin and its conjugates by the human organic anion transporter SLC21A6. J Biol Chem. 2001 Mar 30;276(13):9626-30.

Danielson PB. The cytochrome P450 superfamily: biochemistry, evolution and drug metabolism in humans. Curr Drug Metab. 2002 Dec;3(6):561-97. Review.

Dannenberg AJ, Kavecansky J, Scarlata S, Zakim D. Organization of microsomal UDP-glucuronosyltransferase. Activation by treatment at high pressure. Biochemistry. 1990 Jun 26;29(25):5961-7.

Davies NM, Teng XW, Skjodt NM. Pharmacokinetics of rofecoxib: a specific cyclo-oxygenase-2 inhibitor. Clin Pharmacokinet. 2003;42(6):545-56. Review.

Davis RL, Cheng PF, Lassar AB, Weintraub H. The MyoD DNA binding domain contains a recognition code for muscle-specific gene activation. Cell. 1990 Mar 9;60(5):733-46.

Denis M, Cuthill S, Wikström AC, Poellinger L, Gustafsson JA. Association of the dioxin receptor with the Mr 90,000 heat shock protein: a structural kinship with the glucocorticoid receptor. Biochem Biophys Res Commun. 1988 Sep 15;155(2):801-7.

Denison, M. S., El-Fouly, M. H., Aarts, J. M. M. J. G., Brouwer, A., Richter, C., and Giesy, J. P. (1993). Production of a novel recombinant- cell line bioassay system for the detection of 2,3,7,8-tetrachlorodibenzo-*p*-dioxin-like chemicals. Short paper. *Dioxin ‘* 93, 365–368.

Denison MS, Fisher JM, Whitlock JP Jr. Protein-DNA interactions at recognition sites for the dioxin-Ah receptor complex. J Biol Chem. 1989 Oct 5;264(28):16478-82.

Denison MS, Fisher JM, Whitlock JP Jr. Inducible, receptor-dependent protein-DNA interactions at a dioxin-responsive transcriptional enhancer. Proc Natl Acad Sci U S A. 1988 Apr;85(8):2528-32.

Denison MS, Vella LM, Okey AB. Structure and function of the Ah receptor for 2,3,7,8-tetrachlorodibenzo-p-dioxin. Species difference in molecular properties of the receptors from mouse and rat hepatic cytosols. J Biol Chem. 1986 Mar 25;261(9):3987-95.

Denison MS, Whitlock JP Jr. Xenobiotic-inducible transcription of cytochrome P450 genes. J Biol Chem. 1995 Aug 4;270(31):18175-8. Review.

Dolwick KM, Swanson HI, Bradfield CA. In vitro analysis of Ah receptor domains involved in ligand-activated DNA recognition. Proc Natl Acad Sci U S A. 1993 Sep 15;90(18):8566-70.

Dorado P, Peñas-Lledó EM, Llerena A. CYP2D6 polymorphism: implications for antipsychotic drug response, schizophrenia and personality traits. Pharmacogenomics. 2007 Nov;8(11):1597-1608.

Dull AB, Carlson DB, Petrulis JR, Perdew GH. Characterization of the phosphorylation status of the hepatitis B virus X-associated protein 2. Arch Biochem Biophys. 2002 Oct 15;406(2):209-21.

Dutton, G.J. (1980) Glucuronidation of Drugs and Other Compounds. CRC Press, Boca Raton, Fla, USA

DUTTON GJ, STOREY ID. The isolation of a compound of uridine diphosphate and glucuronic acid from liver. Biochem J. 1953 Mar;53(4):xxxvii-xxxviii.

DUTTON GJ, STOREY ID. Uridine compounds in glucuronic acid metabolism. I. The formation of glucuronides in liver suspensions. Biochem J. 1954 Jun;57(2):275-83.

Ema M, Sogawa K, Watanabe N, Chujoh Y, Matsushita N, Gotoh O, Funae Y, Fujii-Kuriyama Y. cDNA cloning and structure of mouse putative Ah receptor. Biochem Biophys Res Commun. 1992 Apr 15;184(1):246-53.

ESTABROOK RW, COOPER DY, ROSENTHAL O. THE LIGHT REVERSIBLE CARBON MONOXIDE INHIBITION OF THE STEROID C21-HYDROXYLASE SYSTEM OF THE ADRENAL CORTEX. Biochem Z. 1963;338:741-55.

Falany CN, Green MD, Swain E, Tephly TR. Substrate specificity and characterization of rat liver p-nitrophenol, 3 alpha-hydroxysteroid and 17 beta-hydroxysteroid UDP-glucuronosyltransferases. Biochem J. 1986 Aug 15;238(1):65-73.

Falany CN, Tephly TR. Separation, purification and characterization of three isoenzymes of UDP-glucuronyltransferase from rat liver microsomes. Arch Biochem Biophys. 1983 Nov;227(1):248-58.

Fisher JM, Wu L, Denison MS, Whitlock JP Jr. Organization and function of a dioxin-responsive enhancer. J Biol Chem. 1990 Jun 15;265(17):9676-81.

Fisslthaler B, Popp R, Kiss L, Potente M, Harder DR, Fleming I, Busse R. Cytochrome P450 2C is an EDHF synthase in coronary arteries. Nature. 1999 Sep 30;401(6752):493-7.

Floren LC, Bekersky I, Benet LZ, Mekki Q, Dressler D, Lee JW, Roberts JP, Hebert MF. Tacrolimus oral bioavailability doubles with coadministration of ketoconazole. Clin Pharmacol Ther. 1997 Jul;62(1):41-9.

Fujisawa-Sehara A, Sogawa K, Yamane M, Fujii-Kuriyama Y. Characterization of xenobiotic responsive elements upstream from the drug-metabolizing cytochrome P-450c gene: a similarity to glucocorticoid regulatory elements. Nucleic Acids Res. 1987 May 26;15(10):4179-91.

Fukunaga BN, Probst MR, Reisz-Porszasz S, Hankinson O. Identification of functional domains of the aryl hydrocarbon receptor. J Biol Chem. 1995 Dec 8;270(49):29270-8.

Galijatovic A, Beaton D, Nguyen N, Chen S, Bonzo J, Johnson R, Maeda S, Karin M, Guengerich FP, Tukey RH. The human CYP1A1 gene is regulated in a developmental and tissue-specific fashion in transgenic mice. J Biol Chem. 2004 Jun 4;279(23):23969-76.

GARFINKEL D. Studies on pig liver microsomes. I. Enzymic and pigment composition of different microsomal fractions. Arch Biochem Biophys. 1958 Oct;77(2):493-509.

Garrison PM, Tullis K, Aarts JM, Brouwer A, Giesy JP, Denison MS. Species-specific recombinant cell lines as bioassay systems for the detection of 2,3,7,8-tetrachlorodibenzo-p-dioxin-like chemicals. Fundam Appl Toxicol. 1996 Apr;30(2):194-203.

Geyer HJ, Schramm KW, Feicht EA, Behechti A, Steinberg C, Brüggemann R, Poiger H, Henkelmann B, Kettrup A. Half-lives of tetra-, penta-, hexa-, hepta-, and octachlorodibenzo-p-dioxin in rats, monkeys, and humans--a critical review. Chemosphere. 2002 Aug;48(6):631-44. Review.

Goldstein JA, de Morais SM. Biochemistry and molecular biology of the human CYP2C subfamily. Pharmacogenetics. 1994 Dec;4(6):285-99. Review.

Gong QH, Cho JW, Huang T, Potter C, Gholami N, Basu NK, Kubota S, Carvalho S, Pennington MW, Owens IS, Popescu NC. Thirteen UDPglucuronosyltransferase genes are encoded at the human UGT1 gene complex locus. Pharmacogenetics. 2001 Jun;11(4):357-68.

Gonzalez FJ, Fernandez-Salguero P, Ward JM. The role of the aryl hydrocarbon receptor in animal development, physiological homeostasis and toxicity of TCDD. J Toxicol Sci. 1996 Dec;21(5):273-7. Review.

Gonzalez FJ, Nebert DW. Evolution of the P450 gene superfamily: animal-plant 'warfare', molecular drive and human genetic differences in drug oxidation. Trends Genet. 1990 Jun;6(6):182-6. Review.

Gonzalez FJ, Tukey RH, Nebert DW. Structural gene products of the Ah locus. Transcriptional regulation of cytochrome P1-450 and P3-450 mRNA levels by 3-methylcholanthrene. Mol Pharmacol. 1984 Jul;26(1):117-21.

Gorski JP, Kasper CB. Purification and properties of microsomal UDP-glucuronosyltransferase from rat liver. J Biol Chem. 1977 Feb 25;252(4):1336-43.

Gorski JP, Kasper CB. UDP-glucuronosyltransferase: phospholipid dependence and properties of the reconstituted apoenzyme. Biochemistry. 1978 Oct 31;17(22):4600-5.

Gourley GR. Bilirubin metabolism and kernicterus. Adv Pediatr. 1997;44:173-229. Review.

Green MD, Bishop WP, Tephly TR. Expressed human UGT1.4 protein catalyzes the formation of quaternary ammonium-linked glucuronides. Drug Metab Dispos. 1995 Mar;23(3):299-302.

Green MD, King CD, Mojarrabi B, Mackenzie PI, Tephly TR. Glucuronidation of amines and other xenobiotics catalyzed by expressed human UDP-glucuronosyltransferase 1A3. Drug Metab Dispos. 1998 Jun;26(6):507-12.

Gschaidmeier H, Bock KW. Radiation inactivation analysis of microsomal UDP-glucuronosyltransferases catalysing mono- and diglucuronide formation of 3,6-dihydroxybenzo(a)pyrene and 3,6-dihydroxychrysene. Biochem Pharmacol. 1994 Oct 18;48(8):1545-9.

Guengerich FP. Roles of cytochrome P-450 enzymes in chemical carcinogenesis and cancer chemotherapy. Cancer Res. 1988 Jun 1;48(11):2946-54.

Guengerich FP. Cytochrome P450s and other enzymes in drug metabolism and toxicity. AAPS J. 2006 Mar 10;8(1):E101-11. Review.

Guengerich FP, MacDonald TL. Mechanisms of cytochrome P-450 catalysis. FASEB J. 1990 May;4(8):2453-9. Review.

Guenthner TM, Nebert DW. Cytosolic receptor for aryl hydrocarbon hydroxylase induction by polycyclic aromatic compounds. Evidence for structural and regulatory variants among established cell cultured lines. J Biol Chem. 1977 Dec 25;252(24):8981-9.

Guillemette C, Bélanger A, Lépine J. Metabolic inactivation of estrogens in breast tissue by UDP-glucuronosyltransferase enzymes: an overview. Breast Cancer Res. 2004;6(6):246-54. Epub 2004 Sep 27. Review.

Guillemette C, Millikan RC, Newman B, Housman DE. Genetic polymorphisms in uridine diphospho-glucuronosyltransferase 1A1 and association with breast cancer among African Americans. Cancer Res. 2000a Feb 15;60(4):950-6.

Guillemette C, Ritter JK, Auyeung DJ, Kessler FK, Housman DE. Structural heterogeneity at the UDP-glucuronosyltransferase 1 locus: functional consequences of three novel missense mutations in the human UGT1A7 gene. Pharmacogenetics. 2000 Oct;10(7):629-44.

Gunn CH. Hereditary alcoholuric jaundice. J Hered 1938; 29:137.
Hahn ME, Lamb TM, Schultz ME, Smolowitz RM, and Stegeman J. Cytochrome P4501A induction and inhibition by 3,3',4,4'-tetrachlorobiphenyl in an Ah receptor-containing fish hepatoma cell line (PLHC-1). Aquat. Toxicol. 1993. 26, 185-208.

Hankinson O. The aryl hydrocarbon receptor complex. Annu Rev Pharmacol Toxicol. 1995;35:307-40. Review.

Haque M, Anreola F. The cloning and characterization of a novel cytochrome P450 family, CYP26, with specificity toward retinoic acid. Nutr Rev. 1998 Mar;56(3):84-5. Review.

Harding D, Jeremiah SJ, Povey S, Burchell B. Chromosomal mapping of a human phenol UDP-glucuronosyltransferase, GNT1. Ann Hum Genet. 1990 Jan;54 (Pt 1):17-21.

Harding D, Wilson SM, Jackson MR, Burchell B, Green MD, Tephly TR. Nucleotide and deduced amino acid sequence of rat liver 17 beta-hydroxysteroid UDP-glucuronosyltransferase. Nucleic Acids Res. 1987 May 11;15(9):3936.

Hauser SC, Ziurys JC, Gollan JL. A membrane transporter mediates access of uridine 5'-diphosphoglucuronic acid from the cytosol into the endoplasmic reticulum of rat hepatocytes: implications for glucuronidation reactions. Biochim Biophys Acta. 1988 Nov 17;967(2):149-57.

Heid SE, Pollenz RS, Swanson HI. Role of heat shock protein 90 dissociation in mediating agonist-induced activation of the aryl hydrocarbon receptor. Mol Pharmacol. 2000 Jan;57(1):82-92.

Hestermann EV, Brown M. Agonist and chemopreventative ligands induce differential transcriptional cofactor recruitment by aryl hydrocarbon receptor. Mol Cell Biol. 2003 Nov;23(21):7920-5.

Hildebrand CE, Gonzalez FJ, McBride OW, Nebert DW. Assignment of the human 2,3,7,8-tetrachlorodibenzo-p-dioxin-inducible cytochrome P1-450 gene to chromosome 15. Nucleic Acids Res. 1985 Mar 25;13(6):2009-16.

Hinson JA, Pohl LR, Monks TJ, Gillette JR, Guengerich FP. 3-Hydroxyacetaminophen: a microsomal metabolite of acetaminophen. Evidence against an epoxide as the reactive metabolite of acetaminophen. Drug Metab Dispos. 1980 Sep-Oct;8(5):289-94.

Hochman Y, Zakim D. A comparison of the kinetic properties of two different forms of microsomal UDPglucuronyltransferase. J Biol Chem. 1983 Apr 10;258(7):4143-6.

Hoffman FL. THE ACCURACY OF AMERICAN CANCER MORTALITY STATISTICS. Am J Public Health (N Y). 1915 Jun;5(6):526-37.

Hoffman EC, Reyes H, Chu FF, Sander F, Conley LH, Brooks BA, Hankinson O. Cloning of a factor required for activity of the Ah (dioxin) receptor. Science. 1991 May 17;252(5008):954-8.

Hsu MH, Savas U, Griffin KJ, Johnson EF. Human cytochrome p450 family 4 enzymes: function, genetic variation and regulation. Drug Metab Rev. 2007;39(2-3):515-38. Review.

Hu Z, Wells PG. Modulation of benzo[a]pyrene bioactivation by glucuronidation in lymphocytes and hepatic microsomes from rats with a hereditary deficiency in bilirubin UDP-glucuronosyltransferase. Toxicol Appl Pharmacol. 1994 Aug;127(2):306-13.

Hum DW, Bélanger A, Lévesque E, Barbier O, Beaulieu M, Albert C, Vallée M, Guillemette C, Tchernof A, Turgeon D, Dubois S. Characterization of UDP-glucuronosyltransferases active on steroid hormones. J Steroid Biochem Mol Biol. 1999 Apr-Jun;69(1-6):413-23. Review.

Ikushiro S, Emi Y, Iyanagi T. Protein-protein interactions between UDP-glucuronosyltransferase isozymes in rat hepatic microsomes. Biochemistry. 1997 Jun 10;36(23):7154-61.

Ikuta T, Eguchi H, Tachibana T, Yoneda Y, Kawajiri K. Nuclear localization and export signals of the human aryl hydrocarbon receptor. J Biol Chem. 1998 Jan 30;273(5):2895-904.

Institute of Medicine (IOM), 2005. Veterans and Agent Orange: Update 2004. National Academic Press, Washington, DC.

Isin EM, Guengerich FP. Complex reactions catalyzed by cytochrome P450 enzymes. Biochim Biophys Acta. 2007 Mar;1770(3):314-29.

Iyanagi T, Haniu M, Sogawa K, Fujii-Kuriyama Y, Watanabe S, Shively JE, Anan KF. Cloning and characterization of cDNA encoding 3-methylcholanthrene inducible rat mRNA for UDP-glucuronosyltransferase. J Biol Chem. 1986 Nov 25;261(33):15607-14.

Iyanagi T, Watanabe T, Uchiyama Y. The 3-methylcholanthrene-inducible UDP-glucuronosyltransferase deficiency in the hyperbilirubinemic rat (Gunn rat) is caused by a -1 frameshift mutation. J Biol Chem. 1989 Dec 15;264(35):21302-7.

Jackson MR, Burchell B. The full length coding sequence of rat liver androsterone UDP-glucuronyltransferase cDNA and comparison with other members of this gene family. Nucleic Acids Res. 1986 Jan 24;14(2):779-95.

Jackson MR, McCarthy LR, Corser RB, Barr GC, Burchell B. Cloning of cDNAs coding for rat hepatic microsomal UDP-glucuronyltransferases. Gene. 1985;34(2-3):147-53.

Jaiswal AK, Gonzalez FJ, Nebert DW. Human dioxin-inducible cytochrome P1-450: complementary DNA and amino acid sequence. Science. 1985 Apr 5;228(4695):80-3.

Jedlitschky G, Cassidy AJ, Sales M, Pratt N, Burchell B. Cloning and characterization of a novel human olfactory UDP-glucuronosyltransferase. Biochem J. 1999 Jun 15;340 (Pt 3):837-43.

Jin CJ, Mackenzie PI, Miners JO. The regio- and stereo-selectivity of C19 and C21 hydroxysteroid glucuronidation by UGT2B7 and UGT2B11. Arch Biochem Biophys. 1997 May 15;341(2):207-11.

Johnson EF, Schwab GE, Muller-Eberhard U. Multiple forms of cytochrome P-450: catalytic differences exhibited by two homogeneous forms of rabbit cytochrome P-450. Mol Pharmacol. 1979 May;15(3):708-18.

Johnson WW. Cytochrome p450 inactivation by pharmaceuticals and phytochemicals: therapeutic relevance. Drug Metab Rev. 2008;40(1):101-47.

Jones SN, Jones PG, Ibarguen H, Caskey CT, Craigen WJ. Induction of the Cyp1a-1 dioxin-responsive enhancer in transgenic mice. Nucleic Acids Res. 1991 Dec 11;19(23):6547-51.

Kadakol A, Ghosh SS, Sappal BS, Sharma G, Chowdhury JR, Chowdhury NR. Genetic lesions of bilirubin uridine-diphosphoglucuronate glucuronosyltransferase (UGT1A1) causing Crigler-Najjar and Gilbert syndromes: correlation of genotype to phenotype. Hum Mutat. 2000 Oct;16(4):297-306. Review.

Kalsotra A, Strobel HW. Cytochrome P450 4F subfamily: at the crossroads of eicosanoid and drug metabolism. Pharmacol Ther. 2006 Dec;112(3):589-611. Epub 2006 Aug 22. Review.

Kiang TK, Ensom MH, Chang TK. UDP-glucuronosyltransferases and clinical drug-drug interactions. Pharmacol Ther. 2005 Apr;106(1):97-132. Epub 2005 Jan 12. Review.

Kiani J, Imam SZ. Medicinal importance of grapefruit juice and its interaction with various drugs. Nutr J. 2007 Oct 30;6:33. Review.

KIMMIG J, SCHULZ KH. Occupational acne (so-called chloracne) due to chlorinated aromatic cyclic ethers. Dermatologica. 1957 Oct;115(4):540-6.

Kivistö KT, Kantola T, Neuvonen PJ. Different effects of itraconazole on the pharmacokinetics of fluvastatin and lovastatin. Br J Clin Pharmacol. 1998 Jul;46(1):49-53.
Kivistö KT, Lamberg TS, Kantola T, Neuvonen PJ. Plasma buspirone concentrations are greatly increased by erythromycin and itraconazole. Clin Pharmacol Ther. 1997 Sep;62(3):348-54.

KLINGENBERG M. Pigments of rat liver microsomes. Arch Biochem Biophys. 1958 Jun;75(2):376-86.

Ko HP, Okino ST, Ma Q, Whitlock JP Jr. Dioxin-induced CYP1A1 transcription in vivo: the aromatic hydrocarbon receptor mediates transactivation, enhancer-promoter communication, and changes in chromatin structure. Mol Cell Biol. 1996 Jan;16(1):430-6.

Ko HP, Okino ST, Ma Q, Whitlock JP Jr. Transactivation domains facilitate promoter occupancy for the dioxin-inducible CYP1A1 gene in vivo. Mol Cell Biol. 1997 Jul;17(7):3497-507.

Kobayashi T, Sugimoto T, Saijoh K, Fujii M, Chihara K. Cloning and characterization of the 5'-flanking region of the mouse diastrophic dysplasia sulfate transporter gene. Biochem Biophys Res Commun. 1997 Sep 29;238(3):738-43.

Koiwai O, Aono S, Adachi Y, Kamisako T, Yasui Y, Nishizawa M, Sato H. Crigler-Najjar syndrome type II is inherited both as a dominant and as a recessive trait. Hum Mol Genet. 1996 May;5(5):645-7.

Koiwai O, Nishizawa M, Hasada K, Aono S, Adachi Y, Mamiya N, Sato H. Gilbert's syndrome is caused by a heterozygous missense mutation in the gene for bilirubin UDP-glucuronosyltransferase. Hum Mol Genet. 1995 Jul;4(7):1183-6.

König J, Nies AT, Cui Y, Leier I, Keppler D. Conjugate export pumps of the multidrug resistance protein (MRP) family: localization, substrate specificity, and MRP2-mediated drug resistance. Biochim Biophys Acta. 1999 Dec 6;1461(2):377-94. Review.

Kubota M, Sogawa K, Kaizu Y, Sawaya T, Watanabe J, Kawajiri K, Gotoh O, Fujii-Kuriyama Y. Xenobiotic responsive element in the 5'-upstream region of the human P-450c gene. J Biochem. 1991 Aug;110(2):232-6.

Kumar MB, Perdew GH. Nuclear receptor coactivator SRC-1 interacts with the Q-rich subdomain of the AhR and modulates its transactivation potential. Gene Expr. 1999b;8(5-6):273-86.

Kumar MB, Tarpey RW, Perdew GH. Differential recruitment of coactivator RIP140 by Ah and estrogen receptors. Absence of a role for LXXLL motifs. J Biol Chem. 1999a Aug 6;274(32):22155-64.

Kullak-Ublick GA, Beuers U, Paumgartner G. Hepatobiliary transport. J Hepatol. 2000;32(1 Suppl):3-18. Review.

Lathe GH, Walker M. An enzyme defect in human neonatal jaundice and in Gunn’s strain of jaundiced rats. Biochem. J 1957;9p.

Lévesque E, Beaulieu M, Green MD, Tephly TR, Bélanger A, Hum DW. Isolation and characterization of UGT2B15(Y85): a UDP-glucuronosyltransferase encoded by a polymorphic gene. Pharmacogenetics. 1997 Aug;7(4):317-25.

Lévesque E, Girard H, Journault K, Lépine J, Guillemette C. Regulation of the UGT1A1 bilirubin-conjugating pathway: role of a new splicing event at the UGT1A locus. Hepatology. 2007 Jan;45(1):128-38.

Long M, Laier P, Vinggaard AM, Andersen HR, Lynggaard J, Bonefeld-Jørgensen EC. Effects of currently used pesticides in the AhR-CALUX assay: comparison between the human TV101L and the rat H4IIE cell line. Toxicology. 2003 Dec 15;194(1-2):77-93.

Loomis, WF. (1988) *Four Billion Years, An Essay on the Evolution of Genes and Organisms*., Sinauer Associates, Inc., Sunderland, Massachusetts, pp.286.

Lundahl J, Regårdh CG, Edgar B, Johnsson G. Effects of grapefruit juice ingestion--pharmacokinetics and haemodynamics of intravenously and orally administered felodipine in healthy men. Eur J Clin Pharmacol. 1997;52(2):139-45.

Lusska A, Shen E, Whitlock JP Jr. Protein-DNA interactions at a dioxin-responsive enhancer. Analysis of six bona fide DNA-binding sites for the liganded Ah receptor. J Biol Chem. 1993 Mar 25;268(9):6575-80.

Ma Q, Lu AY. CYP1A induction and human risk assessment: an evolving tale of in vitro and in vivo studies. Drug Metab Dispos. 2007 Jul;35(7):1009-16. Epub 2007 Apr 12. Review.

Macdonald TL, Gutheim WG, Martin RB, Guengerich FP. Oxidation of substituted N,N-dimethylanilines by cytochrome P-450: estimation of the effective oxidation-reduction potential of cytochrome P-450. Biochemistry. 1989 Mar 7;28(5):2071-7.

Mackenzie PI. Rat liver UDP-glucuronosyltransferase. Sequence and expression of a cDNA encoding a phenobarbital-inducible form. J Biol Chem. 1986 May 5;261(13):6119-25.

Mackenzie PI. Rat liver UDP-glucuronosyltransferase. Identification of cDNAs encoding two enzymes which glucuronidate testosterone, dihydrotestosterone, and beta-estradiol. J Biol Chem. 1987 Jul 15;262(20):9744-9.

Mackenzie PI. Expression of chimeric cDNAs in cell culture defines a region of UDP glucuronosyltransferase involved in substrate selection. J Biol Chem. 1990 Feb 25;265(6):3432-5.

Mackenzie PI, Gonzalez FJ, Owens IS. Cell-free translation of mouse liver mRNA coding for two forms of UDP glucuronosyltransferase. Arch Biochem Biophys. 1984a May 1;230(2):676-80.

Mackenzie PI, Gonzalez FJ, Owens IS. Cloning and characterization of DNA complementary to rat liver UDP-glucuronosyltransferase mRNA. J Biol Chem. 1984b Oct 10;259(19):12153-60.

Mackenzie PI, Owens IS. Cleavage of nascent UDP glucuronosyltransferase from rat liver by dog pancreatic microsomes. Biochem Biophys Res Commun. 1984 Aug 16;122(3):1441-9.

Mackenzie PI, Owens IS, Burchell B, Bock KW, Bairoch A, Belanger A, Fournel-Gigleux S, Green M, Hum DW, Iyanagi T, Lancet D, Louisot P, Magdalou J, Chowdhury JR, Ritter JK, Schachter H, Tephly TR, Tipton KF, Nebert DW. The UDP glycosyltransferase gene superfamily: recommended nomenclature update based on evolutionary divergence. Pharmacogenetics. 1997 Aug;7(4):255-69. Review.

Matern S, Matern H, Farthmann EH, Gerok W. Hepatic and extrahepatic glucuronidation of bile acids in man. Characterization of bile acid uridine 5'-diphosphate-glucuronosyltransferase in hepatic, renal, and intestinal microsomes. J Clin Invest. 1984 Aug;74(2):402-10.

Matern H, Matern S, Gerok W. Isolation and characterization of rat liver microsomal UDP-glucuronosyltransferase activity toward chenodeoxycholic acid and testosterone as a single form of enzyme. J Biol Chem. 1982 Jul 10;257(13):7422-9.

Matsui M, Nagai F. Genetic deficiency of androsterone UDP-glucuronosyltransferase activity in Wistar rats is due to the loss of enzyme protein. Biochem J. 1986 Feb 15;234(1):139-44.

McDonnell WM, Hitomi E, Askari FK. Identification of bilirubin UDP-GTs in the human alimentary tract in accordance with the gut as a putative metabolic organ. Biochem Pharmacol. 1996 Feb 23;51(4):483-8.

McGurk KA, Brierley CH, Burchell B. Drug glucuronidation by human renal UDP-glucuronosyltransferases. Biochem Pharmacol. 1998 Apr 1;55(7):1005-12.

Meech R, Mackenzie PI. Structure and function of uridine diphosphate glucuronosyltransferases. Clin Exp Pharmacol Physiol. 1997 Dec;24(12):907-15. Review.

Meyer BK, Perdew GH. Characterization of the AhR-hsp90-XAP2 core complex and the role of the immunophilin-related protein XAP2 in AhR stabilization. Biochemistry. 1999 Jul 13;38(28):8907-17.

Meyer BK, Pray-Grant MG, Vanden Heuvel JP, Perdew GH. Hepatitis B virus X-associated protein 2 is a subunit of the unliganded aryl hydrocarbon receptor core complex and exhibits transcriptional enhancer activity. Mol Cell Biol. 1998 Feb;18(2):978-88.

Monaghan G, Burchell B, Boxer M. Structure of the human UGT2B4 gene encoding a bile acid UDP-glucuronosyltransferase. Mamm Genome. 1997 Sep;8(9):692-4.

Monaghan G, Clarke DJ, Povey S, See CG, Boxer M, Burchell B. Isolation of a human YAC contig encompassing a cluster of UGT2 genes and its regional localization to chromosome 4q13. Genomics. 1994 Sep 15;23(2):496-9.

de Morais SM, Chow SY, Wells PG. Biotransformation and toxicity of acetaminophen in congenic RHA rats with or without a hereditary deficiency in bilirubin UDP-glucuronosyltransferase. Toxicol Appl Pharmacol. 1992 Nov;117(1):81-7.

Mulder GJ. The heterogeneity of uridine diphosphate glucuronyltransferase from rat liver. Biochem J. 1971 Nov;125(1):9-15.

Murre C, McCaw PS, Baltimore D. A new DNA binding and dimerization motif in immunoglobulin enhancer binding, daughterless, MyoD, and myc proteins. Cell. 1989a Mar 10;56(5):777-83.

Murre C, McCaw PS, Vaessin H, Caudy M, Jan LY, Jan YN, Cabrera CV, Buskin JN, Hauschka SD, Lassar AB, et al., Interactions between heterologous helix-loop-helix proteins generate complexes that bind specifically to a common DNA sequence. Cell. 1989b Aug 11;58(3):537-44.

Nagy SR, Liu G, Lam KS, Denison MS. Identification of novel Ah receptor agonists using a high-throughput green fluorescent protein-based recombinant cell bioassay. Biochemistry. 2002b Jan 22;41(3):861-8.

Nagy SR, Sanborn JR, Hammock BD, Denison MS. Development of a green fluorescent protein-based cell bioassay for the rapid and inexpensive detection and characterization of ah receptor agonists. Toxicol Sci. 2002a Feb;65(2):200-10.

Nakamura M, Negishi M, Altieri M, Chen YT, Ikeda T, Tukey RH, Nebert DW. Structure of the mouse cytochrome P1-450 genomic gene. Eur J Biochem. 1983 Jul 15;134(1):19-25.

Nambu JR, Franks RG, Hu S, Crews ST. The single-minded gene of Drosophila is required for the expression of genes important for the development of CNS midline cells. Cell. 1990 Oct 5;63(1):63-75.

Nambu JR, Lewis JO, Wharton KA Jr, Crews ST. The Drosophila single-minded gene encodes a helix-loop-helix protein that acts as a master regulator of CNS midline development. Cell. 1991 Dec 20;67(6):1157-67.

Nebert DW, Considine N, Owens IS. Genetic expression of aryl hydrocarbon hydroxylase induction. VI. Control of other aromatic hydrocarbon-inducible mono-oxygenase activities at or near the same genetic locus. Arch Biochem Biophys. 1973a Jul;157(1):148-59.

Nebert DW, Dalton TP. The role of cytochrome P450 enzymes in endogenous signalling pathways and environmental carcinogenesis. Nat Rev Cancer. 2006 Dec;6(12):947-60. Review.

Nebert DW, Dieter MZ. The evolution of drug metabolism. Pharmacology. 2000 Sep;61(3):124-35. Review.

Nebert DW, Felton JS. Evidence for the activation of 3-methylcholanthrene as a carcinogen in vivo and asa mutagen in vitro by P1 -450 from inbred strains of mice. Adv Exp Med Biol. 1975;58(00):127-49.

Nebert DW, Feyereisen, R. (1994) In Cytochrome P450, Biochemistry, Biophysics and Molecular Biology, (Lechner M.C. Ed.), Libbey Eurotext, London, pp. 3-13.

Nebert DW, Gelboin HV. Substrate-inducible microsomal aryl hydroxylase in mammalian cell culture. II. Cellular responses during enzyme induction. J Biol Chem. 1968a Dec 10;243(23):6250-61.

Nebert DW, Gelboin HV. Substrate-inducible microsomal aryl hydroxylase in mammalian cell culture. I. Assay and properties of induced enzyme. J Biol Chem. 1968b Dec 10;243(23):6242-9.

Nebert DW, Gielen JE. Aryl hydrocarbon hydroxylase induction in mammalian liver cell culture. II. Effects of actinomycin D and cycloheximide on induction processes by phenobarbital or polycyclic hydrocarbons. J Biol Chem. 1971 Sep 10;246(17):5199-206.

Nebert DW, Gonzalez FJ. P450 genes: structure, evolution, and regulation. Annu Rev Biochem. 1987;56:945-93.

Nebert DW, Heidema JK, Strobel HW, Coon MJ. Genetic expression of aryl hydrocarbon hydroxylase induction. Genetic specificity resides in the fraction containing cytochromes P448 and P450. J Biol Chem. 1973b Nov 25;248(22):7631-6.

Negishi M, Nebert DW. Structural gene products of the Ah locus. Genetic and immunochemical evidence for two forms of mouse liver cytochrome P-450 induced by 3-methylcholanthrene. J Biol Chem. 1979 Nov 10;254(21):11015-23.

Negishi M, Nebert DW. Structural gene products of the Ah complex. Increases in large mRNA from mouse liver associated with cytochrome P1-450 induction by 3-methylcholanthrene. J Biol Chem. 1981 Mar 25;256(6):3085-91.

Negishi M, Swan DC, Enquist LW, Nebert DW. Isolation and characterization of a cloned DNA sequence associated with the murine Ah locus and a 3-methylcholanthrene-induced form of cytochrome P-450. Proc Natl Acad Sci U S A. 1981 Feb;78(2):800-4.

Nguyen N, Tukey RH. Baculovirus-directed expression of rabbit UDP-glucuronosyltransferases in Spodoptera frugiperda cells. Drug Metab Dispos. 1997 Jun;25(6):745-9.

Nilsson T, Jackson M, Peterson PA. Short cytoplasmic sequences serve as retention signals for transmembrane proteins in the endoplasmic reticulum. Cell. 1989 Aug 25;58(4):707-18.

Niwa A, Kumaki K, Nebert DW, Poland AP. Genetic expression of aryl hydrocarbon hydroxylase activity in the mouse. Distinction between the "responsive" homozygote and heterozygote at the Ah locus. Arch Biochem Biophys. 1975 Feb;166(2):559-64.

Niznik HB, Tyndale RF, Sallee FR, Gonzalez FJ, Hardwick JP, Inaba T, Kalow W. The dopamine transporter and cytochrome P45OIID1 (debrisoquine 4-hydroxylase) in brain: resolution and identification of two distinct [3H]GBR-12935 binding proteins. Arch Biochem Biophys. 1990 Feb 1;276(2):424-32.

Norlin M, Wikvall K. Enzymes in the conversion of cholesterol into bile acids. Curr Mol Med. 2007 Mar;7(2):199-218. Review.

Norris D. A Note on the Bases of Gasworks Coal-tar which are believed to be the Predisposing Cause of Pitch Cancer, with Special Reference to their Action on Lymphocytes, together with a Method for their Inactivation: Part I: Auxetic Action. Biochem J. 1914 Jun;8(3):253-60.

Okey AB, Riddick DS, Harper PA. The Ah receptor: mediator of the toxicity of 2,3,7,8-tetrachlorodibenzo-p-dioxin (TCDD) and related compounds. Toxicol Lett. 1994 Jan;70(1):1-22. Review.

Okey AB, Vella LM, Harper PA. Detection and characterization of a low affinity form of cytosolic Ah receptor in livers of mice nonresponsive to induction of cytochrome P1-450 by 3-methylcholanthrene. Mol Pharmacol. 1989 Jun;35(6):823-30.

Pacifici GM, Giuliani L, Calcaprina R. Glucuronidation of 1-naphthol in nuclear and microsomal fractions of the human intestine. Pharmacology. 1986;33(2):103-9.

Parquet M, Pessah M, Sacquet E, Salvat C, Raizman A, Infante R. Glucuronidation of bile acids in human liver, intestine and kidney. An in vitro study on hyodeoxycholic acid. FEBS Lett. 1985 Sep 23;189(2):183-7.

Perdew GH. Association of the Ah receptor with the 90-kDa heat shock protein. J Biol Chem. 1988 Sep 25;263(27):13802-5.

Perdew GH. Chemical cross-linking of the cytosolic and nuclear forms of the Ah receptor in hepatoma cell line 1c1c7. Biochem Biophys Res Commun. 1992 Jan 15;182(1):55-62.

Peters WH, Allebes WA, Jansen PL, Poels LG, Capel PJ. Characterization and tissue specificity of a monoclonal antibody against human uridine 5'-diphosphate-glucuronosyltransferase. Gastroenterology. 1987 Jul;93(1):162-9.

Peters WH, Jansen PL. Immunocharacterization of UDP-glucuronyltransferase isoenzymes in human liver, intestine and kidney. Biochem Pharmacol. 1988 Feb 1;37(3):564-7.

Peters WH, Jansen PL, Nauta H. The molecular weights of UDP-glucuronyltransferase determined with radiation-inactivation analysis. A molecular model of bilirubin UDP-glucuronyltransferase. J Biol Chem. 1984 Oct 10;259(19):11701-5.

Peters WH, Kock L, Nagengast FM, Kremers PG. Biotransformation enzymes in human intestine: critical low levels in the colon? Gut. 1991 Apr;32(4):408-12.

Peters WH, Nagengast FM, van Tongeren JH. Glutathione S-transferase, cytochrome P450, and uridine 5'-diphosphate-glucuronosyltransferase in human small intestine and liver. Gastroenterology. 1989 Mar;96(3):783-9.

Petrulis JR, Perdew GH. The role of chaperone proteins in the aryl hydrocarbon receptor core complex. Chem Biol Interact. 2002 Sep 20;141(1-2):25-40. Review.

Pohl RJ, Fouts JR. A rapid method for assaying the metabolism of 7-ethoxyresorufin by microsomal subcellular fractions. Anal Biochem. 1980 Sep 1;107(1):150-5

Poland A, Glover E. Comparison of 2,3,7,8-tetrachlorodibenzo-p-dioxin, a potent inducer of aryl hydrocarbon hydroxylase, with 3-methylcholanthrene. Mol Pharmacol. 1974 Mar;10(2):349-59.

Poland, A. & Glover, E. Genetic expression of aryl hydrocarbon hydroxylase by 2, 3, 7, 8-tetrachlorodibenzo-p-dioxin: Evidence for a receptor mutation in genetically nonresponsive mice. Mol. Pharmacol. 1975 11, 389-398.

Poland A, Glover E, Ebetino FH, Kende AS. Photoaffinity labeling of the Ah receptor. J Biol Chem. 1986 May 15;261(14):6352-65.

Poland A, Glover E, Kende AS. Stereospecific, high affinity binding of 2,3,7,8-tetrachlorodibenzo-p-dioxin by hepatic cytosol. Evidence that the binding species is receptor for induction of aryl hydrocarbon hydroxylase. J Biol Chem. 1976 Aug 25;251(16):4936-46.

Poland AP, Glover E, Robinson JR, Nebert DW. Genetic expression of aryl hydrocarbon hydroxylase activity. Induction of monooxygenase activities and cytochrome P1-450 formation by 2,3,7,8-tetrachlorodibenzo-p-dioxin in mice genetically "nonresponsive" to other aromatic hydrocarbons. J Biol Chem. 1974 Sep 10;249(17):5599-606.

Poland A, Palen D, Glover E. Analysis of the four alleles of the murine aryl hydrocarbon receptor. Mol Pharmacol. 1994 Nov;46(5):915-21.

Pollenz RS, Sattler CA, Poland A. The aryl hydrocarbon receptor and aryl hydrocarbon receptor nuclear translocator protein show distinct subcellular localizations in Hepa 1c1c7 cells by immunofluorescence microscopy. Mol Pharmacol. 1994 Mar;45(3):428-38.

Postlind H, Vu TP, Tukey RH, Quattrochi LC. Response of human CYP1-luciferase plasmids to 2,3,7,8-tetrachlorodibenzo-p-dioxin and polycyclic aromatic hydrocarbons. Toxicol Appl Pharmacol. 1993 Feb;118(2):255-62.

Proctor RN. Tobacco and the global lung cancer epidemic. Nat Rev Cancer. 2001 Oct;1(1):82-6. Review.

Prosser DE, Jones G. Enzymes involved in the activation and inactivation of vitamin D. Trends Biochem Sci. 2004 Dec;29(12):664-73. Review.

Radominska-Pandya A, Pokrovskaya ID, Xu J, Little JM, Jude AR, Kurten RC, Czernik PJ. Nuclear UDP-glucuronosyltransferases: identification of UGT2B7 and UGT1A6 in human liver nuclear membranes. Arch Biochem Biophys. 2002 Mar 1;399(1):37-48.

Reisz-Porszasz S, Probst MR, Fukunaga BN, Hankinson O. Identification of functional domains of the aryl hydrocarbon receptor nuclear translocator protein (ARNT). Mol Cell Biol. 1994 Sep;14(9):6075-86.

Remmel RP, Burchell B. Validation and use of cloned, expressed human drug-metabolizing enzymes in heterologous cells for analysis of drug metabolism and drug-drug interactions. Biochem Pharmacol. 1993 Aug 17;46(4):559-66. Review.

Rendic S. Summary of information on human CYP enzymes: human P450 metabolism data. Drug Metab Rev. 2002 Feb-May;34(1-2):83-448. Review.

Reyes H, Reisz-Porszasz S, Hankinson O. Identification of the Ah receptor nuclear translocator protein (Arnt) as a component of the DNA binding form of the Ah receptor. Science. 1992 May 22;256(5060):1193-5.

Ritter JK, Chen F, Sheen YY, Tran HM, Kimura S, Yeatman MT, Owens IS. A novel complex locus UGT1 encodes human bilirubin, phenol, and other UDP-glucuronosyltransferase isozymes with identical carboxyl termini. J Biol Chem. 1992a Feb 15;267(5):3257-61.

Ritter JK, Crawford JM, Owens IS. Cloning of two human liver bilirubin UDP-glucuronosyltransferase cDNAs with expression in COS-1 cells. J Biol Chem. 1991 Jan 15;266(2):1043-7.

Ritter JK, Yeatman MT, Ferreira P, Owens IS. Identification of a genetic alteration in the code for bilirubin UDP-glucuronosyltransferase in the UGT1 gene complex of a Crigler-Najjar type I patient. J Clin Invest. 1992b Jul;90(1):150-5.

Roger C, Koziel V, Vert P, Nehlig A. Mapping of the consequences of bilirubin exposure in the immature rat: local cerebral metabolic rates for glucose during moderate and severe hyperbilirubinemia. Early Hum Dev. 1995 Oct 2;43(2):133-44.

Ryner LC, Swain A. Sex in the '90s. Cell. 1995 May 19;81(4):483-93.

Safe SH. Comparative toxicology and mechanism of action of polychlorinated dibenzo-p-dioxins and dibenzofurans. Annu Rev Pharmacol Toxicol. 1986;26:371-99. Review.

Safe SH. Polychlorinated biphenyls (PCBs): environmental impact, biochemical and toxic responses, and implications for risk assessment. Crit Rev Toxicol. 1994;24(2):87-149. Review.

Sanderson JT, Aarts JM, Brouwer A, Froese KL, Denison MS, Giesy JP. Comparison of Ah receptor-mediated luciferase and ethoxyresorufin-O-deethylase induction in H4IIE cells: implications for their use as bioanalytical tools for the detection of polyhalogenated aromatic hydrocarbons. Toxicol Appl Pharmacol. 1996 Apr;137(2):316-25.

Sato R, Satake H, Imai Y. Partial purification and some spectral properties of hepatic microsomal cytochrome P-450. Drug Metab Dispos. 1973 Jan-Feb;1(1):6-13.

Schecter A, Päpke O, Tung KC, Joseph J, Harris TR, Dahlgren J. Polybrominated diphenyl ether flame retardants in the U.S. population: current levels, temporal trends, and comparison with dioxins, dibenzofurans, and polychlorinated biphenyls. J Occup Environ Med. 2005 Mar;47(3):199-211.

Schlezinger JJ, White RD, Stegeman JJ. Oxidative inactivation of cytochrome P-450 1A (CYP1A) stimulated by 3,3',4,4'-tetrachlorobiphenyl: production of reactive oxygen by vertebrate CYP1As. Mol Pharmacol. 1999 Sep;56(3):588-97.

Schmidt JV, Bradfield CA. Ah receptor signaling pathways. Annu Rev Cell Dev Biol. 1996;12:55-89. Review.

Schmiedeberg O, and Meyer H. Z.Physiol.Chem. 3:422 (1879)

SCHULZ KH. Clinical & experimental studies on the etiology of chloracne. Arch Klin Exp Dermatol. 1957;206:589-96.

Schwetz BA, Norris JM, Sparschu GL, Rowe UK, Gehring PJ, Emerson JL, Gerbig CG. Toxicology of chlorinated dibenzo-p-dioxins. Environ Health Perspect. 1973 Sep;5:87-99.

Senafi SB, Clarke DJ, Burchell B. Investigation of the substrate specificity of a cloned expressed human bilirubin UDP-glucuronosyltransferase: UDP-sugar specificity and involvement in steroid and xenobiotic glucuronidation. Biochem J. 1994 Oct 1;303 (Pt 1):233-40.

Seppen J, Bosma PJ, Goldhoorn BG, Bakker CT, Chowdhury JR, Chowdhury NR, Jansen PL, Oude Elferink RP. Discrimination between Crigler-Najjar type I and II by expression of mutant bilirubin uridine diphosphate-glucuronosyltransferase. J Clin Invest. 1994 Dec;94(6):2385-91.

Shepherd SR, Baird SJ, Hallinan T, Burchell B. An investigation of the transverse topology of bilirubin UDP-glucuronosyltransferase in rat hepatic endoplasmic reticulum. Biochem J. 1989 Apr 15;259(2):617-20.

Shimada T, Fujii-Kuriyama Y. Metabolic activation of polycyclic aromatic hydrocarbons to carcinogens by cytochromes P450 1A1 and 1B1. Cancer Sci. 2004 Jan;95(1):1-6. Review.

Shimada T, Nakamura S. Cytochrome P-450-mediated activation of procarcinogens and promutagens to DNA-damaging products by measuring expression of umu gene in Salmonella typhimurium TA1535/pSK1002. Biochem Pharmacol. 1987 Jun 15;36(12):1979-87.

Sims P, Grover PL, Swaisland A, Pal K, Hewer A. Metabolic activation of benzo(a)pyrene proceeds by a diol-epoxide. Nature. 1974 Nov 22;252(5481):326-8.

SMITH EE, MILLS GT. Uridine nucleotide compounds of liver. Biochim Biophys Acta. 1954 Mar;13(3):386-400.

Smith JD, Wong E, Ginsberg M. Cytochrome P450 1A1 promoter as a genetic switch for the regulatable and physiological expression of a plasma protein in transgenic mice. Proc Natl Acad Sci U S A. 1995 Dec 5;92(25):11926-30.

Soeda Y, Yamamoto K, Adachi Y, Hori T, Aono S, Koiwai O, Sato H. Predicted homozygous mis-sense mutation in Gilbert's syndrome. Lancet. 1995 Dec 2;346(8988):1494.

STOREY ID, DUTTON GJ. Uridine compounds in glucuronic acid metabolism. 2. The isolation and structure of 'uridine-diphosphate-glucuronic acid'. Biochem J. 1955 Feb;59(2):279-88.

Strassburg CP, Kneip S, Topp J, Obermayer-Straub P, Barut A, Tukey RH, Manns MP.

Polymorphic gene regulation and interindividual variation of UDP-glucuronosyltransferase activity in human small intestine. J Biol Chem. 2000 Nov 17;275(46):36164-71.

Strassburg CP, Manns MP, Tukey RH. Differential down-regulation of the UDP-glucuronosyltransferase 1A locus is an early event in human liver and biliary cancer. Cancer Res. 1997b Jul 15;57(14):2979-85.

Strassburg CP, Manns MP, Tukey RH. Expression of the UDP-glucuronosyltransferase 1A locus in human colon. Identification and characterization of the novel extrahepatic UGT1A8. J Biol Chem. 1998a Apr 10;273(15):8719-26.

Strassburg CP, Nguyen N, Manns MP, Tukey RH. UDP-glucuronosyltransferase activity in human liver and colon. Gastroenterology. 1999 Jan;116(1):149-60.

Strassburg CP, Obermayer-Straub P, Alex B, Durazzo M, Rizzetto M, Tukey RH, Manns MP. Autoantibodies against glucuronosyltransferases differ between viral hepatitis and autoimmune hepatitis. Gastroenterology. 1996 Dec;111(6):1576-86.

Strassburg CP, Nguyen N, Manns MP, Tukey RH. Polymorphic expression of the UDP-glucuronosyltransferase UGT1A gene locus in human gastric epithelium. Mol Pharmacol. 1998b Oct;54(4):647-54.

Strassburg CP, Oldhafer K, Manns MP, Tukey RH. Differential expression of the UGT1A locus in human liver, biliary, and gastric tissue: identification of UGT1A7 and UGT1A10 transcripts in extrahepatic tissue. Mol Pharmacol. 1997a Aug;52(2):212-20.

Strassburg CP, Vogel A, Kneip S, Tukey RH, Manns MP. Polymorphisms of the human UDP-glucuronosyltransferase (UGT) 1A7 gene in colorectal cancer. Gut. 2002 Jun;50(6):851-6.

Suleman FG, Abid A, Gradinaru D, Daval JL, Magdalou J, Minn A. Identification of the uridine diphosphate glucuronosyltransferase isoform UGT1A6 in rat brain and in primary cultures of neurons and astrocytes. Arch Biochem Biophys. 1998 Oct 1;358(1):63-7.

Tenhunen R, Marver HS, Schmid R. The enzymatic conversion of hemoglobin to bilirubin. Trans Assoc Am Physicians. 1969;82:363-71

Tephly TR, Burchell B. UDP-glucuronosyltransferases: a family of detoxifying enzymes. Trends Pharmacol Sci. 1990 Jul;11(7):276-9. Review.

Thibaudeau J, Lépine J, Tojcic J, Duguay Y, Pelletier G, Plante M, Brisson J, Têtu B, Jacob S, Perusse L, Bélanger A, Guillemette C. Characterization of common UGT1A8, UGT1A9, and UGT2B7 variants with different capacities to inactivate mutagenic 4-hydroxylated metabolites of estradiol and estrone. Cancer Res. 2006 Jan 1;66(1):125-33.

Tillitt DE, Ankley GT, Verbrugge DA, Giesy JP, Ludwig JP, Kubiak TJ. H4IIE rat hepatoma cell bioassay-derived 2,3,7,8-tetrachlorodibenzo-p-dioxin equivalents in colonial fish-eating waterbird eggs from the Great Lakes. Arch Environ Contam Toxicol. 1991 Jul;21(1):91-101.

Tillitt DE, Giesy JP, Fromm PO. In vitro mitogenesis of peripheral blood lymphocytes from rainbow trout (Salmo gairdneri). Comp Biochem Physiol A. 1988;89(1):25-35.

Tukey RH, Billings RE, Autor AP, Tephly TR. Phospholipid-dependence of oestrone UDP-glucuronyltransferase and p-nitrophenol UDP-glucuronyltransferase. Biochem J. 1979 Apr 1;179(1):59-65.

Tukey RH, Billings RE, Tephly TR. Separation of oestrone UDP-glucuronyltransferase and p-nitrophenol UDP-glucuronyltransferase activities. Biochem J. 1978 Jun 1;171(3):659-63

Tukey RH, Lalley PA, Nebert DW. Localization of cytochrome P1-450 and P3-450 genes to mouse chromosome 9. Proc Natl Acad Sci U S A. 1984 May;81(10):3163-6.

Tukey RH, Nebert DW, Negishi M. Structural gene product of the [Ah] complex. Evidence for transcriptional control of cytochrome P1-450 induction by use of a cloned DNA sequence. J Biol Chem. 1981 Jul 10;256(13):6969-74.

Tukey RH, Strassburg CP. Human UDP-glucuronosyltransferases: metabolism, expression, and disease. Annu Rev Pharmacol Toxicol. 2000;40:581-616. Review.

Tukey RH, Strassburg CP. Genetic multiplicity of the human UDP-glucuronosyltransferases and regulation in the gastrointestinal tract. Mol Pharmacol. 2001 Mar;59(3):405-14. Review.

Tukey R, Tephly T. Phospholipid dependency of purified estrone and p-nitrophenol UDP-glucuronyltransferases. Life Sci. 1980 Dec 22-29;27(25-26):2471-6.

Urlacher V, Schmid RD. Biotransformations using prokaryotic P450 monooxygenases. Curr Opin Biotechnol. 2002 Dec;13(6):557-64. Review.

Vanstapel F, Blanckaert N. Topology and regulation of bilirubin UDP-glucuronyltransferase in sealed native microsomes from rat liver. Arch Biochem Biophys. 1988 May 15;263(1):216-25.

Vessey DA, Kempner ES. In situ structural analysis of microsomal UDP-glucuronyltransferases by radiation inactivation. J Biol Chem. 1989 Apr 15;264(11):6334-8.

Vogel A, Kneip S, Barut A, Ehmer U, Tukey RH, Manns MP, Strassburg CP. Genetic link of hepatocellular carcinoma with polymorphisms of the UDP-glucuronosyltransferase UGT1A7 gene. Gastroenterology. 2001 Nov;121(5):1136-44.

Del Villar E, Sanchez E, Autor AP, Tephly TR. Morphine metabolism. III. Solubilization and separation of morphine and p-nitrophenol uridine diphosphoglucuronyltransferases. Mol Pharmacol. 1975 Mar;11(2):236-40.

Weatherill PJ, Burchell B. The separation and purification of rat liver UDP-glucuronyltransferase activities towards testosterone and oestrone. Biochem J. 1980 Aug 1;189(2):377-80.

Weisburger EK. Metabolism and activation of chemical carcinogens. Mol Cell Biochem. 1980 Sep 15;32(2):95-104. Review.

Wennberg RP. The blood-brain barrier and bilirubin encephalopathy. Cell Mol Neurobiol. 2000 Feb;20(1):97-109. Review.

Whitlock JP Jr. Induction of cytochrome P4501A1. Annu Rev Pharmacol Toxicol. 1999;39:103-25. Review.

Williams JA, Hyland R, Jones BC, Smith DA, Hurst S, Goosen TC, Peterkin V, Koup JR, Ball SE. Drug-drug interactions for UDP-glucuronosyltransferase substrates: a pharmacokinetic explanation for typically observed low exposure (AUCi/AUC) ratios. Drug Metab Dispos. 2004 Nov;32(11):1201-8. Epub 2004 Aug 10. Review.

Williams, R.T. Detoxication Mechanisms: The Metabolism of Drugs and Allied Organic Compounds. Chapman and Hall, London, 1949.

Williams, R.T. The metabolism of certain drugs and food chemicals in man. Ann. N.Y. Acad. Sci. 179, 141-154. 1971.

Wilton JC, Matthews GM. Polarised membrane traffic in hepatocytes. Bioessays. 1996 Mar;18(3):229-36. Review.

Wooster R, Ebner T, Sutherland L, Clarke D, Burchell B. Drug and xenobiotic glucuronidation catalysed by cloned human liver UDP-Glucuronosyltransferases stably expressed in tissue culture cell lines. Toxicology. 1993 Oct 5;82(1-3):119-29. Review.

Wooster R, Sutherland L, Ebner T, Clarke D, Da Cruz e Silva O, Burchell B. Cloning and stable expression of a new member of the human liver phenol/bilirubin: UDP-glucuronosyltransferase cDNA family. Biochem J. 1991 Sep 1;278 (Pt 2):465-9.

Yamagiwa K, Ichikawa K. Experimental study of the pathogenesis of carcinoma. CA Cancer J Clin. 1977 May-Jun;27(3):174-81.

Yamazaki H, Degawa M, Funae Y, Imaoka S, Inui Y, Guengerich FP, Shimada T. Roles of different cytochrome P450 enzymes in bioactivation of the potent hepatocarcinogen 3-methoxy-4-aminoazobenzene by rat and human liver microsomes. Carcinogenesis. 1991 Jan;12(1):133-9.

Yueh MF, Kawahara M, Raucy J. Cell-based high-throughput bioassays to assess induction and inhibition of CYP1A enzymes. Toxicol In Vitro. 2005 Mar;19(2):275-87.

Zakim D, Dannenberg AJ. How does the microsomal membrane regulate UDP-glucuronosyltransferases? Biochem Pharmacol. 1992 Apr 1;43(7):1385-93. Review.

Zheng Z, Park JY, Guillemette C, Schantz SP, Lazarus P. Tobacco carcinogen-detoxifying enzyme UGT1A7 and its association with orolaryngeal cancer risk. J Natl Cancer Inst. 2001 Sep 19;93(18):1411-8.

CHAPTER 2

Human CYP1A1^{GFP} Expression in Transgenic Mice Serves as a Biomarker for Environmental Toxicant Exposure

INTRODUCTION

Exposure of mice to classical aryl hydrocarbon receptor (AhR) ligands, such as 2,3,7,8-tetrachlorodibenzo-*p*-dioxin (TCDD) or any of the family of polycyclic aromatic hyrdrocarbons (PAHs) like benzo[a]pyrene (BaP), results in activation of the AhR (Tukey *et al.*, 1982; Okino *et al.*, 1992) and induction of selective target genes such as those represented by the family of CYP1 proteins (Nelson *et al.*, 1996). The transcriptional mechanism of CYP1 induction begins with ligand binding to the AhR and culminates in translocation to the nucleus where the AhR dimerizes with the aryl-hydrocarbon receptor nuclear translocator (ARNT) (Hoffman *et al.*, 1991; Reyes *et al.*, 1992). The AhR/ARNT complex binds to highly conserved DNA enhancer sequences known as xenobiotic response elements (Gonzalez and Nebert, 1985; Fujisawa-Sehara *et al.*, 1986), resulting in the propagation of the induction signal to the promoter region, alteration of chromatin structure (Okino and Whitlock, 1995; Wu and Whitlock, Jr., 1992) and subsequent enhanced gene expression.

Induction of the CYP1A family of proteins, in particular CYP1A1, is a hallmark of exposure to combustion products and other environmental contaminants that activate the AhR. Cell based assays expressing portions of the *CYP1A1* promoter region (Postlind *et al.*, 1993; Anderson *et al.*, 1995) or dioxin responsive elements (El-Fouly *et al.*, 1995; Yueh *et al.*, 2005; Nagy *et al.*, 2002) fused to reporter genes have been used to screen for potential AhR ligands. These cell based assays are sensitive, and for the most part can be used to identify agonists/antagonists capable of interacting with the AhR. To complement this approach, transgenic mice expressing reporter genes driven by AhR enhancer elements have also proven to be useful in equating gene expression patterns when mice

have been exposed to AhR ligands (Campbell *et al.*, 1996; Galijatovic *et al.*, 2004). Based upon the route of administration, induction of reporter gene activity in vivo is the end result of not only AhR activation, but also reflects the contribution of circulating and activated humoral factors towards those processes involved in gene expression. The only potential drawback with the use of reporter gene assays in vivo is that they monitor only transcriptional activity and are based upon the steady-state levels of the selected reporter that is being analyzed.

As an additional tool to examine the regulation of the human *CYP1A1* gene, we have generated a transgenic mouse line expressing the human *CYP1A1* gene fused in frame to a *GFP* reporter gene inserted at the last codon located in exon 7 (Tg-*CYP1A1*^{GFP}). This transgenic model serves as a biological tool to explore the mechanisms associated with the regulation and expression of the human *CYP1A1* gene in vivo as well as in cultured cells by measuring GFP fluorescence. Since the measurement of induction results from the cellular accumulation of the human CYP1A1 protein, measurement of induction is based upon transcriptional response and the steady-state balance of protein accumulation. These mice allow for the visualization of spatial and temporal induction of human CYP1A1^{GFP}, which can be used as a biomarker for environmental toxicant exposure to substances that serve as AhR ligands.

MATERIALS AND METHODS

Reagents. 2,3,7,8-Tetrachlorodibenzo-*p*-dioxin (TCDD) was purchased from Wellington Laboratories (Guelph, Ontario, Canada). Benzo[a]pyrene (BaP), 3-methylcholanthrene and β-naphthoflavone (βNF) and an anti-β-actin antibody were purchased from Sigma-Aldrich (St. louis, MO). Human HepG2 cells were purchased from American Type Tissue Culture (http://www.atcc.org/). The anti-human CYP1A1 antibody (Soucek *et al.*, 1995) was kindly provided by Dr. Fred Guengerich (Vanderbilt University) and the anti-human UGT1A1, UGT1A4 and UGT1A6 antibodies (Ritter *et al.*, 1999; Chen *et al.*, 2005) from Dr. Joseph Ritter (Virginia Commonwealth University).

Generation of the CYP1A1^{GFP} Transgenic Mice. The human *CYP1A1* gene was cloned previously from a human liver genomic library constructed in the replacement vector λ-EMBL-3 (McManus *et al.*, 1990) and the 15 kb insert removed by SalI digestion followed by cloning into pBluescript II (Stratagene, La Jolla, CA). A selective mutation was made at the stop codon located in exon 7 and the gene subcloned into the peGFP-N2 vector, generating a chimeric gene that encoded the full length *CYP1A1* gene fused in frame with the *GFP* reporter gene (**Figure 1**). The CYP1A1^{GFP} plasmid DNA was purified from *E. coli* using Qiagen Plasmid Purification columns (Qiagen, Valencia, CA) followed by linearization with Sal I digest. The linearized DNA was microinjected into fertilized $CB6F_1$ mouse eggs and transplanted into the oviduct of pseudopregnant C57BL/6N mice for the production of transgenic mice. All procedures for the generation of the transgenic mice were carried out by the UCSD Superfund Transgenic Core

Facility. For genotype analysis, DNA from tail clippings was screened by PCR using specific GFP sense 5'-cacatgaagcagcacgactt-3' and antisense 5'-tgctcaggtagtggttgtcg-3' primers. For PCR analysis, DNA was amplified in a 50 µl reaction containing 25 µl of Qiagen Hotstart Master Mix (following manufacturer's instructions), 5 ng of template DNA, and 0.4 µM concentration of each primer. A 15 minute activation of the polymerase was carried out at 95 °C followed by 30 cycles from 95 °C for 30 s to 58 °C for 30 s and 72 °C for 45 s followed by final extension at 72 °C for 7 min. PCR reactions were carried out in a PerkinElmer Life Sciences GeneAmp DNA thermocycler PCR system. From 13 litters and 57 offspring, 12 founders were *CYP1A1*^{GFP} positive and 5 of the founders were bred to produce F_1 offspring. Three out of the five founders had F_1 offspring that produced inducible hepatic CYP1A1^{GFP} protein following a single intraperitoneal (i.p.) dose of 16 µg/ kg TCDD.

Animal studies. Animal studies were perfomed in compliance with the rules and regulations for the care and use of laboratory animals from the National Institutes of Health. All animals were 8-12 weeks of age and fed a standard chow diet. TCDD was dissolved in DMSO and given as a single i.p. dose of 16 µg/kg. Benzo[a]pyrene was dissolved in DMSO:corn oil (50:50 v/v) and was given as an single i.p. dose of 100 mg/kg or 100 mg/kg as an oral dose (p.o.) following administration using an oral dosing needle and syringe.

Generation of G418-resistant CYP1A1^{GFP} cells. HepG2 and hepa1c1c7 cells were cultured as previously described (Chen *et al.*, 2003) and transfected with the

CYP1A1^{GFP} expression plasmid and after 48 hours were trypsinized and plated at 1/10 volume. The cells were then exposed to media containing 0.8 mg/ml G418. After approximately 2-3 weeks, individual colonies were selected and re-cultured with continued exposure to G418. A number of the expanded colonies were treated with 5 nM TCDD for 24 h followed by analysis of induced GFP. The generation of cell populations expressing CYP1A1^{GFP} was also calibrated by flow cytometry (Chen *et al.*, 2003).

Microsomal protein isolation. Tissues isolated from 3 mice per treatment group were combined and frozen in liquid nitrogen. Samples were pulverized using a porcelain mortar and pestle under liquid nitrogen. Five volumes of ice cold 1.15 % KCl was added to the pulverized tissue and homogenized using a motorized glass-teflon homogenizer. The tissue homogenate was first centrifuged at 3,000 x g for 10 min at 4 °C. The supernatant was removed and then centrifuged at 10,000 x g for 10 min at 4 °C and the resulting supernatant then centrifuged at 100,000 x g for 60 min at 4 °C. The pellet was resuspened in 20% glycerol, 100 mM potassium phosphate buffer, pH 7.4 containing 10 mM EDTA and 1 mM PMSF.

Western blot analysis. All Western blots were performed using NuPAGE Bis-Tris polyacrylamide gels as outlined by the supplier (Invitrogen, Carlsbad, CA). Protein was heated at 70 °C for 10 min in loading buffer and resolved in 4-12% Bis-Tris gels under denaturing conditions (50 mM MOPS, 50 mM Tris-base, pH 7.7, 0.1% SDS, 1mM EDTA). The resolved protein was transferred onto nitrocellulose membrane using a semi-dry transfer system. The membrane was blocked with 5% nonfat dry milk in 10 mM Tris-

HCl, pH 8, 0.15 M NaCl, and 0.05% Tween 20 (Tris-buffered saline) for 1 h at room temperature. The membrane was washed in the Tris-buffered saline solution and incubated with primary antibodies in Tris-buffered saline, shaking at 4 °C overnight. Membranes were then washed five times with Tris-buffered saline solution and incubated with horseradish peroxidase-conjugated secondary antibodies in Tris-buffered saline solution with 2% nonfat milk for 1 h at room temperature. Membranes were then washed five times with Tris-buffered saline solution and visualized using chemiluminscent reagents according to the manufacturer's instructions (PerkinElmer, Boston, MA)) followed by exposure to X-ray film.

Isolation and treatment of transgenic mouse primary hepatocytes. Primary hepatocytes were isolated from 8-12 week old mice as previously described (Chen *et al.*, 2005c). Mice were anesthetized by isoflurane inhalation. The portal vein was cannulated and perfused with Hank's Balanced Salt Solution (Ca^{2+} free and Mg^{2+} free) containing 0.1 mM EGTA and 10 mM Hepes at pH 7.4 for five minutes at a flow rate of 7 ml/min. The anterior vena cava was cut immediately after the perfusion began to allow for continuous flow of the solution out of the liver. After the five minute initial perfusion, the perfusate was changed to 20 μg/ml Liberase Blendzyme (Roche Applied Science) in Hank's Balanced Salt Solution (with Ca^{2+} and Mg^{2+}) for five minutes at a flow rate of 7 ml/min. The liver was removed and placed in low glucose DMEM media and the hepatocytes were isolated by mechanical dissection followed by filtration through a sterile 70-μm filter. The cells were collected by centrifugation at 50 x g for 30 seconds and washed with low glucose DMEM media. The hepatocytes were cultured in 6-well

collagen-treated plates (Discovery Labware, Bedford, MA) in 3 ml of low glucose DMEM media containing penicillin/streptomycin and supplemented with 10% fetal bovine serum. Three hours after plating the media was removed and replaced with fresh media and the hepatocytes used for subsequent experiments after a 24 h recovery period. The hepatocytes were treated with various chemicals for 48 h and the media containing the chemical compounds refreshed after 24 h. For Western blot analysis, hepatocytes were collected and lysed in a buffer containing 0.05 M Tris-HCl, pH 7.4, 0.15 M NaCl, 0.25% deoxycholic acid and 1% Nonidet P-40 with a compliment of protease and phosphatase cocktail inhibitors (Sigma). After incubation in lysis buffer for 1 h on ice, the supernatant was collected after centrifugation for 20 min in a refrigerated Eppendorf centrifuge at 16,000 x g, and used directly for Western blot analysis.

Tissue section fluorescence microscopy. Transgenic mice were anesthetized with the general anesthetic, nembutol. The mice were then intracardially perfused with Ringer's solution at a rate of 4 ml/min until the liver was clear of blood, followed by perfusion with 4% paraformaldehyde in PBS. The organs were then removed and placed in 4% paraformaldehyde on ice for 2 h to allow for complete fixation. Each organ were sectioned using a vibratome at 100 μm thickness. Tissue sections were washed 3 X with PBS and mounted on glass slides with gelvatol (anti-fade medium). The slides were stored at 4 °C until imaged. Samples were visualized by confocal microscopy using an MRC-1024 system (Bio Rad Laboratories) attached to an Axiovert 35M (Zeiss AG) and a 40 X NA objective. Excitation illumination was with 488 nm light from a krypton/argon

laser. Individual images (1024×1024 pixels) were converted to PICT format and merged as pseudo-color RGB images using Adobe Photoshop (Adobe Systems).

Fluorescence microscopy. Primary hepatocytes were isolated and cultured on collagen treated plates as previously described. Hepatocytes were treated with the following CYP1A1 inducers: TCDD at 0.1, 1 and 10 nM, BaP, 3-methylcholanthrene and βNF at 0.1, 1 and 10 μM. Hepatocytes were treated for 48 h and media changed every 24 h with fresh compound. Cells were then imaged using the Axiovert 200 microscope (Zeiss) with Endow GFP Bandpass filter set.

Measuring tissue fluorescence in microsomal preparations. Fluorescence of 50 μg of microsomal protein from various organs was measured using a Tecan Safire fluorescence plate reader (Tecan) in a 96-well UV plate (Costar). $CYP1A1^{GFP}$ was excited at 488 nm and emission intensity was measured at 525 nm using an excitation and emission slit widths of 5 nm in a top read mode at room temperature.

Measurement of ethoxyresorufin O-deethylase activity. A marker of CYP1A1/CYP1A2 activity, ethoxyresorufin O-deethylase (EROD) activity, was measured using 20 μg of liver microsomes containing 100 mM potassium phosphate buffer (pH 7.4), 5 mM $MgCl_2$, 8 μM 7-ethoxyresorufin and 1 mM NADPH. Reactions were incubated for 15 min at 37 °C and then terminated by the addition of 100 μl cold methanol. The formation of resorufin was measured fluorometrically with an excitation at 530 nm and emission at 590 nm and normalized to a resorufin standard.

RESULTS

Characterization of CYP1A1^{GFP} Tissue Expression in Tg-*CYP1A1*^{GFP} Mice.

We have previously demonstrated that the human *CYP1A1* gene could be regulated in *CYP1A1N* transgenic mice by the identification of TCDD induced human CYP1A1 in tissues such as liver and lung (Galijatovic *et al.*, 2004), but not small intestine. In attempts to design a CYP1A1 marker protein that could be identified by fluorescence, a *CYP1A1-GFP* chimeric gene (*CYP1A1*^{GFP}) was first constructed with the stop codon in exon 7 interrupted and replaced in frame with the *GFP* gene (**Figure 2-1**). This new construct contains 9 kb of regulatory sequence, and when stably integrated into human HepG2 or mouse hepa1c1c7 cells produced a TCDD inducible CYP1A1^{GFP} fusion protein that is detected with either an anti-human CYP1A1 antibody or an anti-GFP antibody (**Figure 2-2**). The anti-CYP1A1 antibody recognizes mouse and human CYP1A1, which can be seen to have slightly different mobilities. The increase in CYP1A1^{GFP} was also represented in the HepG2 cells following a 24 h exposure to TCDD as demonstrated by separation of those cells eliciting fluorescence by flow cytometry (**Figure 2-2**).

FIGURE 2-1

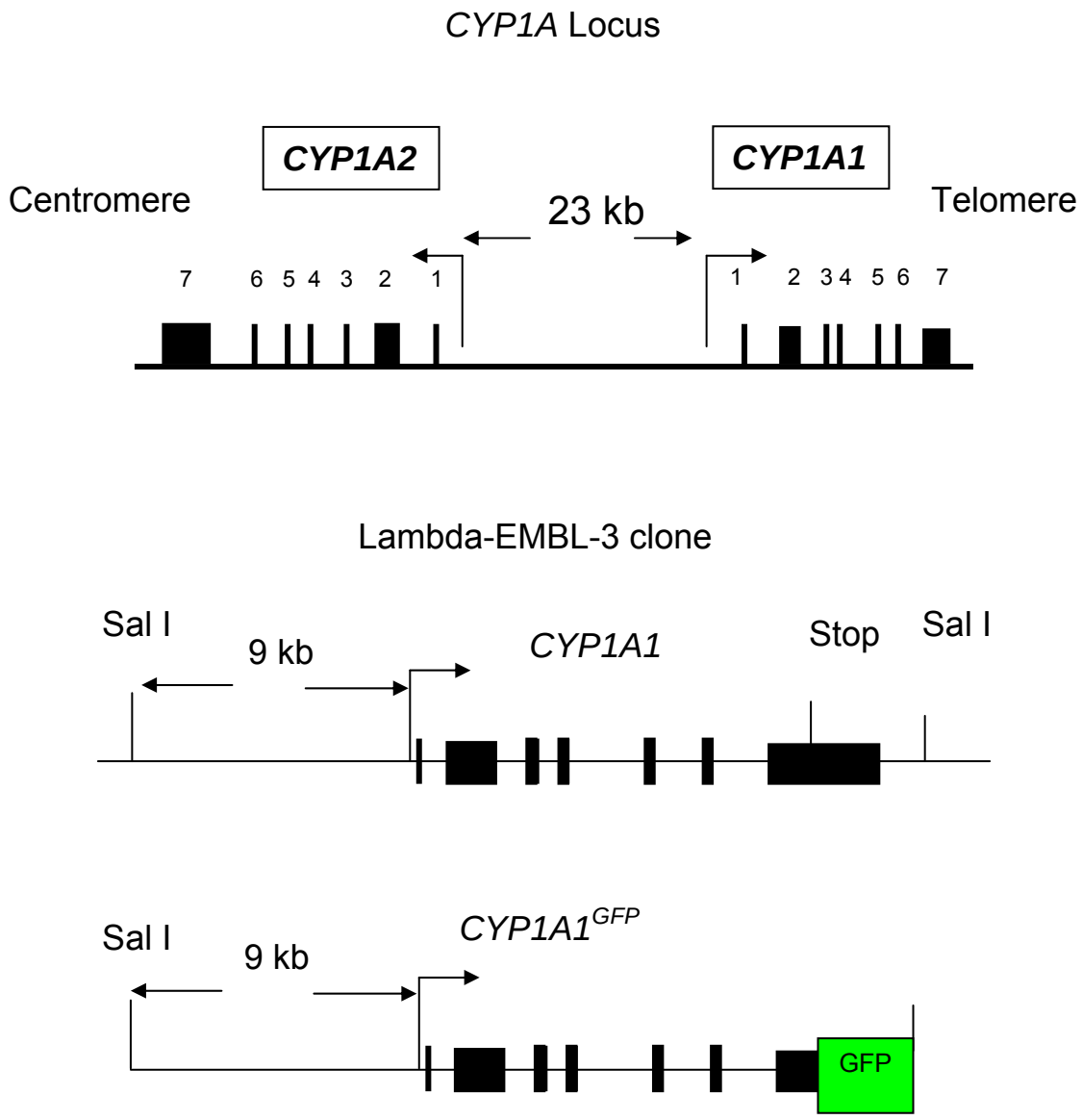


FIGURE 2-1. Representation of the CYP1A1-GFP gene construct used to generate the transgenic *CYP1A1*^{GFP} mice. The organization of the human *CYP1A* locus is shown (Corchero *et al.*, 2001). A lambda-EMBL-3 genomic clone had previously been cloned and characterized (McManus *et al.*, 1990) that contained approximately 9 kb of flanking DNA, as well as exons 1-7 of the *CYP1A1* gene. The DNA insert was removed by SalI digestion from the lambda clone and inserted into a pBluescript (Galijatovic *et al.*, 2004) vector and used to generate a new gene construct where the GFP reporter gene was inserted at the stop codon of the *CYP1A1* gene. The *CYP1A1-GFP* plasmid was used for the generation of the Tg-*CYP1A1*^{GFP} mice.

FIGURE 2-2

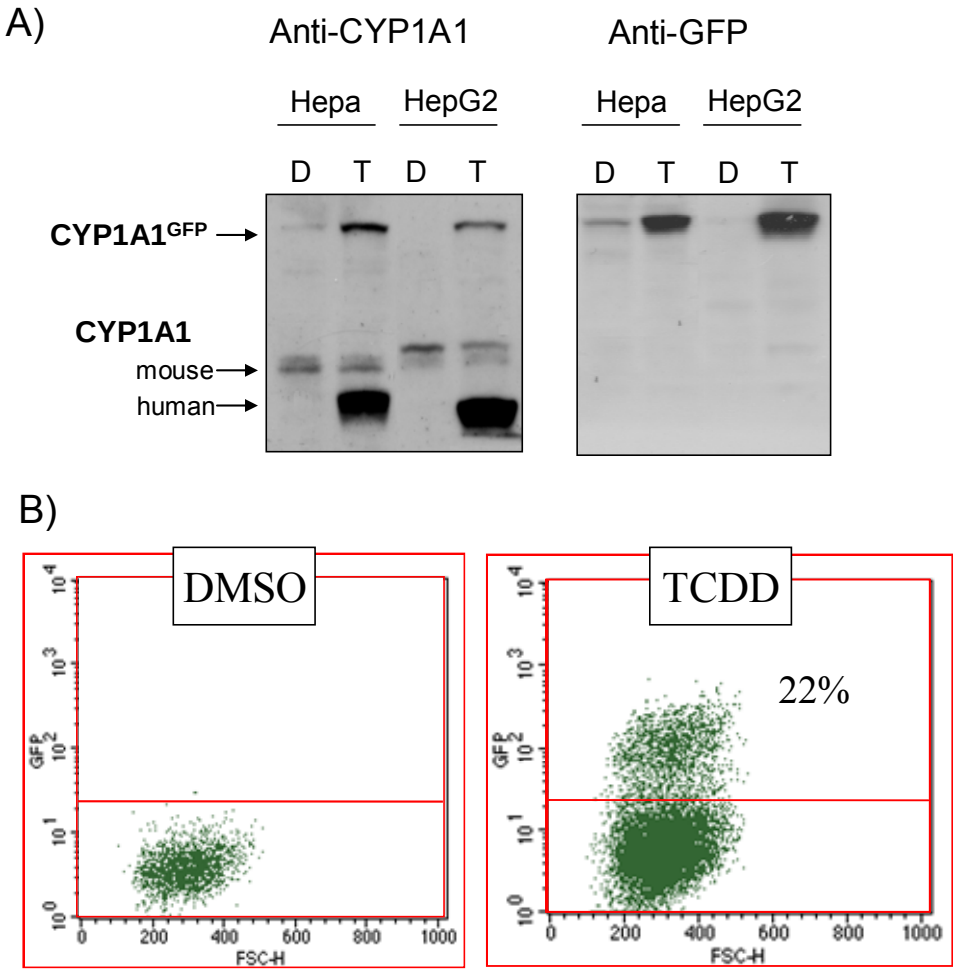


FIGURE 2-2. Expression of CYP1A1^{GFP} in mouse and human hepatoma cells following stable transfection of the *CYP1A1-GFP* gene construct. A) The *CYP1A1-GFP* plasmid construct was transfected into either human HepG2 cells or mouse Hepa1c1c7 (Hepa) cells and stable clones selected in the presence of G418 in the culture media. The selected cells were treated with either DMSO (D) or TCDD (T) for 48 hours, and whole cell lysates used in Western blot analysis to identify CYP1A1^{GFP} expression. Western blots were analyzed with an anti-CYP1A1 or an anti-GFP antibody. The anti-CYP1A1 antibody identified expressed mouse CYP1A1 and human CYP1A1, as indicated by the arrows, as well as induced CYP1A1^{GFP}. **B)** HepG2 cells were subjected to flow cytometry and positive GFP expressing cells identified.

With expression of CYP1A1^{GFP} demonstrated in tissue culture, the *CYP1A1^{GFP}* gene was used to generate transgenic mice (Tg-*CYP1A1^{GFP}*). Following the selection of a transgenic founder line that transmitted the gene, the Tg-*CYP1A1^{GFP}* mice were treated with a single i.p. dose of TCDD and expression of CYP1A1^{GFP} monitored in microsomes from different tissues. The inducibility of CYP1A1^{GFP} was first demonstrated in whole liver when a transgenic mouse was treated with TCDD and the liver exposed and imaged under blue light optics (**Figure 2-3A**). The entire liver was fluorescent green in contrast to the liver from the non-treated transgenic mouse. Isolation of microsomes from TCDD treated mice followed by fluorometry analysis confirmed a four fold increase in liver fluorescence over DMSO treated Tg-*CYP1A1^{GFP}* mice (**Figure 2-3B**). A two fold increase in CYP1A1^{GFP} fluorescence was observed in lung microsomes while no detectable induction of fluorescence was seen in kidney, small intestine, large intestine, brain or spleen.

When Western blots were conducted, TCDD injection led to the prominent induction of mouse CYP1A1 (mCYP1A1) (**Figure 2-4**). In addition, the anti-CYP1A1 antibody detected induction of an 85 kd protein that was also identified with an anti-GFP antibody, confirming that this induced protein represented the CYP1A1^{GFP} fusion protein. TCDD induced mCYP1A1 and CYP1A1^{GFP} was also detected in microsomes from lung tissue. Following the i.p. administration of TCDD, the data indicated that CYP1A1^{GFP} has a similar induction pattern as mCYP1A1.

FIGURE 2-3

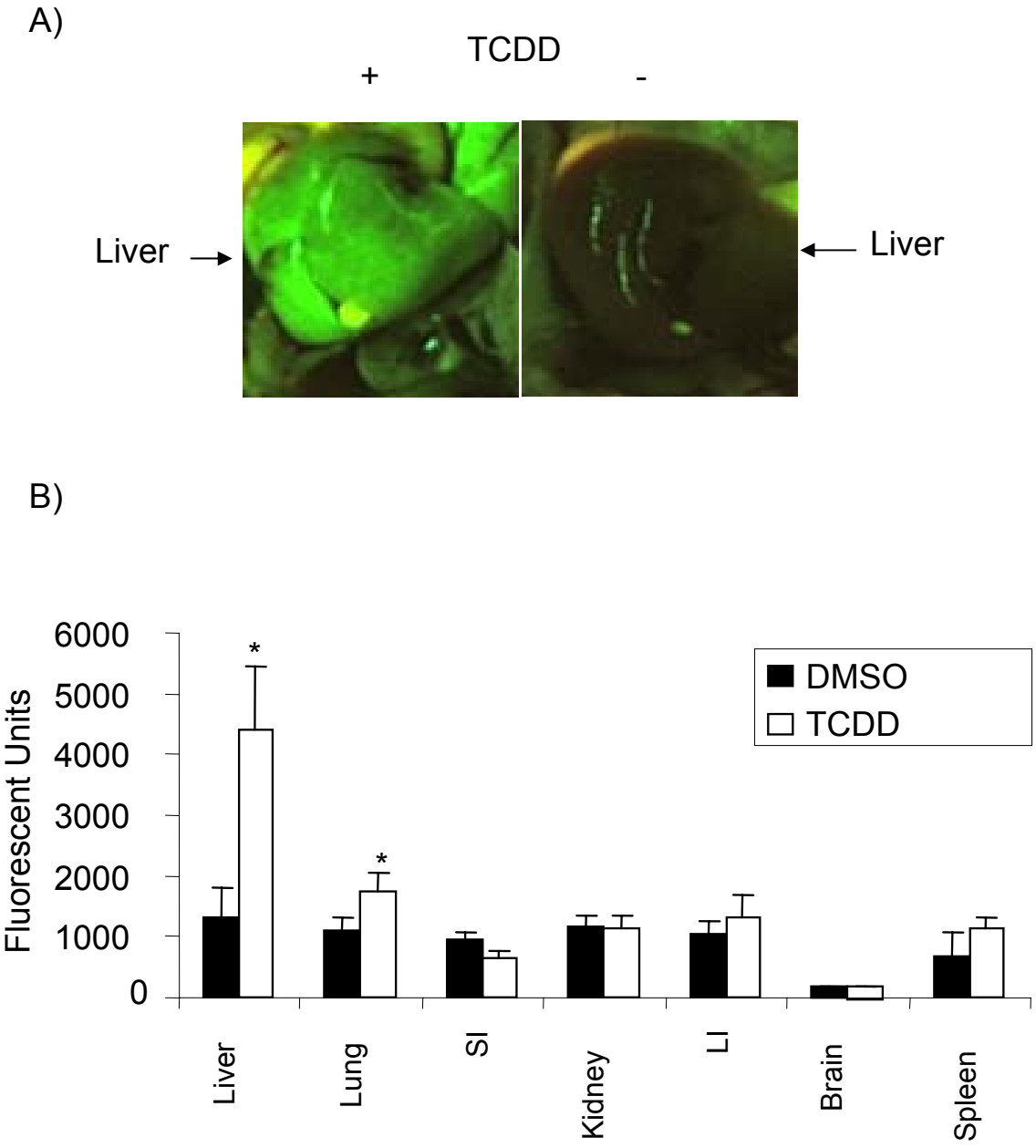


FIGURE 2-3. Analysis of GFP fluorescence in tissues. Tg-*CYP1A1*^{GFP} mice were treated with a single i.p. injection of TCDD or DMSO. **A)** Mice were sacrificed and the liver exposed for imaging using a whole animal fluorescence imaging system to visualize CYP1A1-GFP in liver. **B)** Tissues were combined according to treatment groups (n=3) and microsomes were prepared from each tissue. 100 µg protein was resuspended in PBS and fluorescence was measured using a fluorometer, excitation= 488 nm, emission= 525nm.

FIGURE 2-4

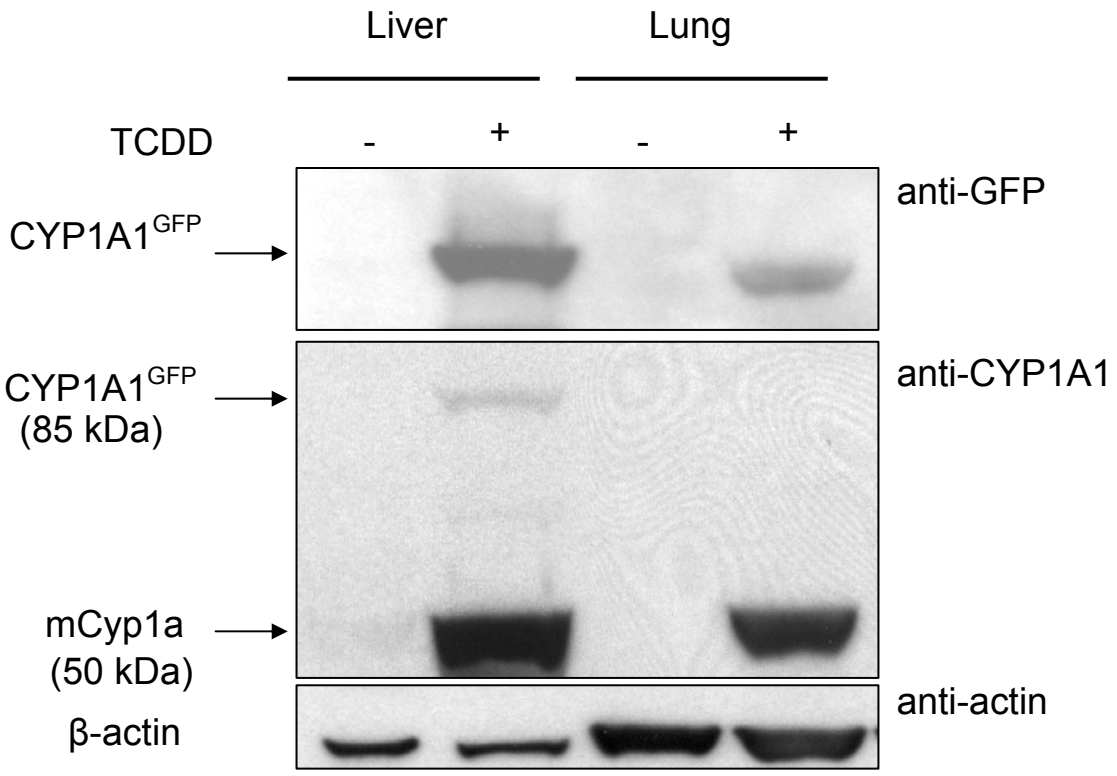


FIGURE 2-4. Induction of CYP1A1^{GFP} in transgenic mice following treatment with TCDD. Transgenic mice (n=3 per group) were treated i.p with 16 µg/kg TCDD or i.p with DMSO for 24 h. Each of the respective tissues were isolated and combined, and microsomes were prepared from each organ. For Western blot analysis, 25 µg of protein from each sample was used. Separate Western blots were generated for analysis with the anti-GFP (α-GFP) and anti-CYP1A1 (α-CYP1A1) antibodies.

Fluorescence Analysis of Tissue Sections of Liver and Lung. The Western blot data and fluorometry data indicated that CYP1A1^{GFP} was inducible in both the liver and the lung. Tissue sections were then performed on these tissues to determine the cellular localization of the GFP fluorescence. Following injection of a single i.p. dose of TCDD (16 μg/kg) for 24 h, the mice were whole body perfused and fixed with 4% formaldehyde. Tissues were sectioned at 100 μm thickness and imaged using confocal microscopy with excitation at 488 nm with a krypton/argon laser. Very little background fluorescence was observed in liver and lung tissue from Tg-*CYP1A1*^{GFP} mice that were treated with DMSO (**Figure 2-5A and 2-5C**). In mice that were treated with TCDD, abundant GFP fluorescence was observed in liver hepatocytes, signifying that activation of the AhR led to adequate expression of CYP1A1^{GFP} (**Figure 2-5B**). When lung tissue was examined, primary fluorescence was noted in a population of cuboidal shaped cells, signifying that induction in the lung is restricted to a selective cell type that morphologically resembles Clara cells (**Figure 2-5D**).

FIGURE 2-5

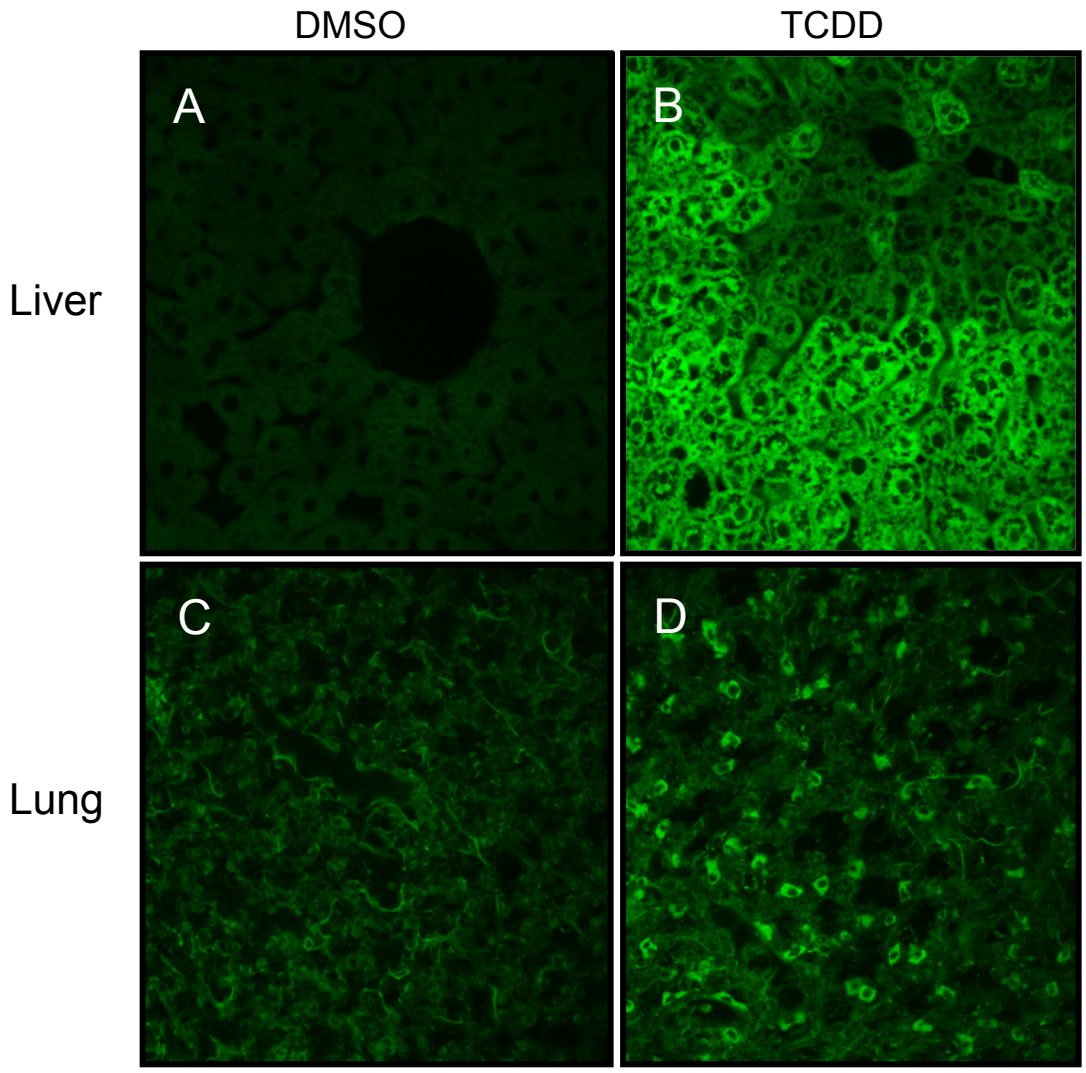


FIGURE 2-5. Confocal microscopy analysis of tissue- and cell-type specific expression of CYP1A1-GFP. Tg-*CYP1A1*^{GFP} mice were treated with 16 µg/kg TCDD or DMSO for 24 h. Intracardial perfusion was performed with 1 X PBS, followed by 4% formaldehyde. Liver and lung were dissected and fixed in 4% formaldehyde overnight at 4 °C. Tissues were sliced at 100 µm thickness using a vibratome and mounted onto slides. Samples were imaged using a confocal microscope with excitation= 488 nm, emission= 525 nm. Panel A and C are DMSO treated liver and lung sections, respectively. Panel B and D are TCDD treated liver and lung sections, respectively.

CYP1A1^{GFP} Expression in Primary Hepatocytes. Since TCDD treatment demonstrated induction of CYP1A1^{GFP} in liver tissue, experiments were conducted to examine the potential for induction in primary hepatocytes. To initiate these experiments, primary hepatocytes were isolated from Tg-*CYP1A1^{GFP}* mice and cultured on collagen coated tissue culture plates. The cells were treated with 10 nM TCDD for 8, 24, and 48 h and fluorescence images were captured following each treatment with a Zeiss inverted microscope using a GFP filter set. As shown in **Figure 2-6**, DMSO treated hepatocytes exhibited very little background fluorescence. At 8 h of TCDD exposure, slight GFP fluorescence was observed compared to the DMSO treated hepatocytes. At 24 h the GFP signal increased and maximum GFP fluorescence was observed following 48 h of exposure to TCDD.

To determine the sensitivity of CYP1A1^{GFP} induction with other AhR agonists, primary hepatocytes were isolated from Tg-*CYP1A1^{GFP}* mice and the cells treated with agents known to activate the AhR. After 48 h of exposure, the cells were collected, resuspended in PBS and fluorescence measured using a 96 well fluorometer (**Figure 2-7A**). TCDD induced maximal fluorescence at 0.1 nM, while BaP and 3-methylcholanthrene induced fluorescence at 1 μM and βNF facilitated induction at 10 μM. The induced fluorescence profiles matched induction of CYP1A1^{GFP} as determined by Western blot analysis (**Figure 2-7B**). In addition, the induction of CYP1A1^{GFP} with each of the AhR agonists was paralleled by increases in mCYP1A1. These results confirm that Tg-*CYP1A1^{GFP}* hepatocytes can be used to examine the potential of chemicals and xenobiotics to induce human CYP1A1.

FIGURE 2-6

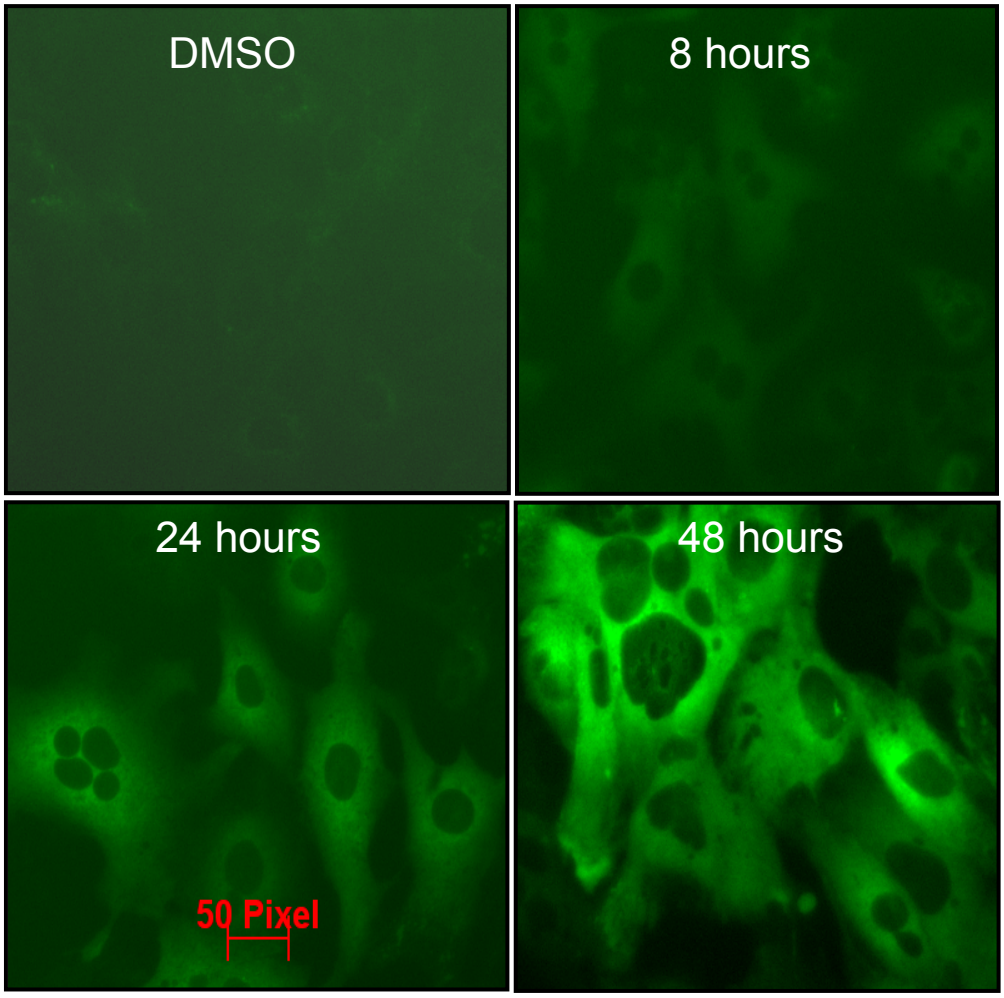


FIGURE 2-6. Time-dependent increase of CYP1A1-GFP expression in primary hepatocytes after TCDD treatment. Primary hepatocytes were isolated from transgenic mice and treated with 10 nM TCDD or DMSO over a 48 h time course. Primary hepatocytes were imaged using an inverted fluorescence microscope with excitation= 488 nm, emission at 525 nm.

FIGURE 2-7

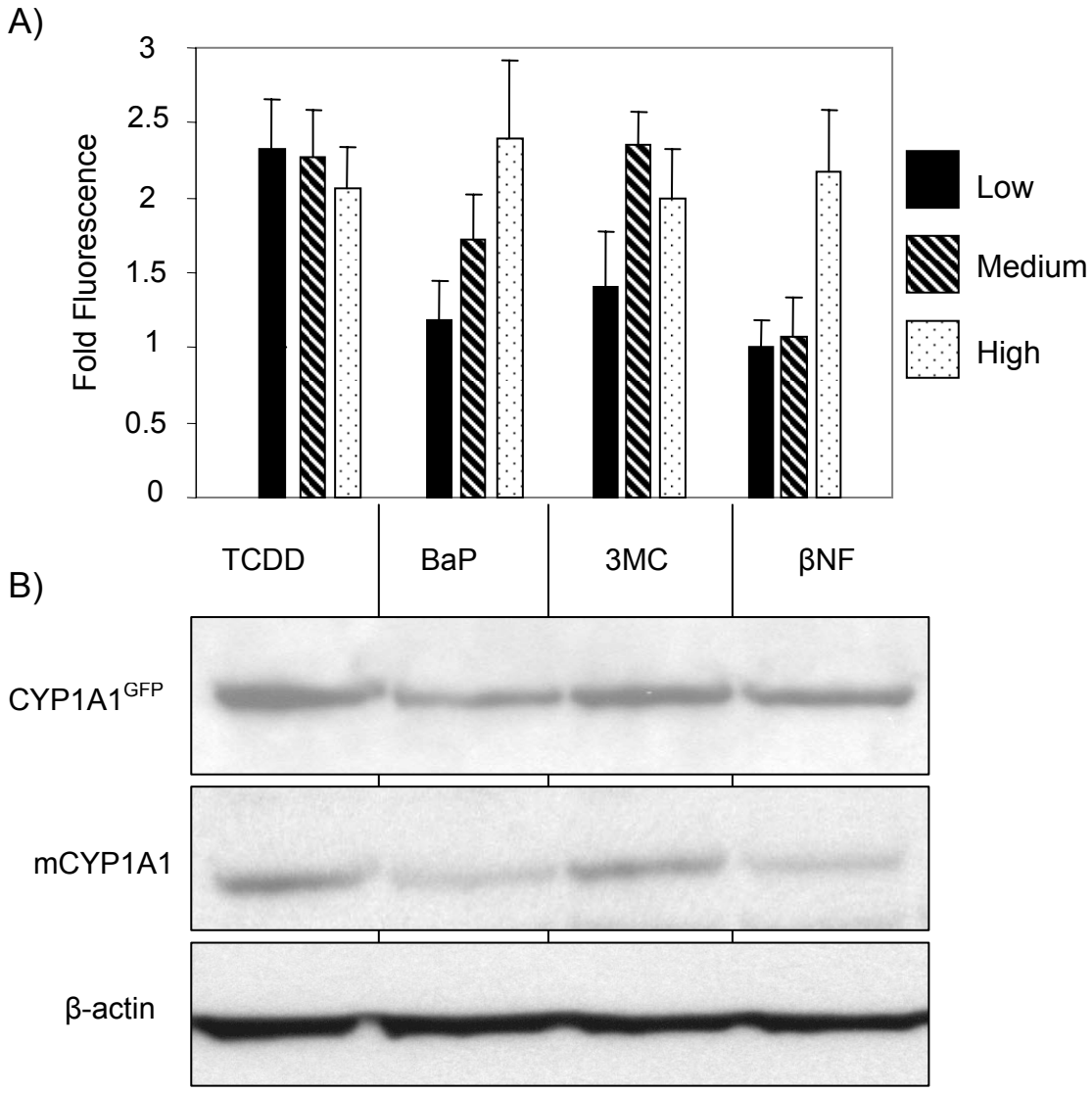


FIGURE 2-7. Dose dependent induction of CYP1A1-GFP in primary hepatocytes using various Ah Receptor ligands. A) Primary hepatocytes from transgenic mice were isolated and placed into culture for 24 hours. Hepatocytes were treated for 48 hours with three different concentrations of inducers indicated as low, medium and high. The inducers were TCDD (0.1, 1.0, 10 nM), BaP (0.1, 1.0, 10 μM), 3-methylcholantrhene (3MC) at (0.1, 1.0, 10 μM), ß-napthoflavone (βNF) at (0.1, 1.0 10 μM). A) Cells were collected and resuspended in 1 X PBS and fluorescence was measured using a fluorometer with excitation = 488 nm, emission= 525 nm. **B)** At the highest concentration of each treatment, cells were collected and total cell lysate used for Western blot analysis using anti-GFP and -CYP1A1 antibodies.

Induction and Function of CYP1A1^{GFP} Following Oral Administration of Benzo[a]pyrene. Following the i.p. injection of BaP into Tg-*CYP1A1^{GFP}* mice, induction of CYP1A1^{GFP} was apparent by detection of the fusion protein by Western blot analysis as well as fluorescence in microsomal preparations. However, the i.p. administration of drugs and other xenobiotics is not representative of normal routes of exposure. To examine the effects of oral BaP administration on CYP1A1^{GFP} induction, Tg-*CYP1A1^{GFP}* mice received BaP (100 mg/kg) every day for three days and tissues collected 24 h after the last dose. Western blots using liver and lung microsomal preparations demonstrated induction of CYP1A1^{GFP} in these tissues as indicated with the anti-GFP and anti-CYP1A1 antibody (**Figure 2-8**). It was interesting to note that minimal induction of mCYP1A1 was observed in liver microsomes after oral administration of BaP although induction was observed in lung. Since mCYP1A1 was not detected in liver at an oral dose of 100 mg/kg, the appearance of CYP1A1^{GFP} at this dose leads us to speculate that the induction of fluorescence in these mice may be a more sensitive indicator of AhR activation than induction of mCYP1A1.

FIGURE 2-8

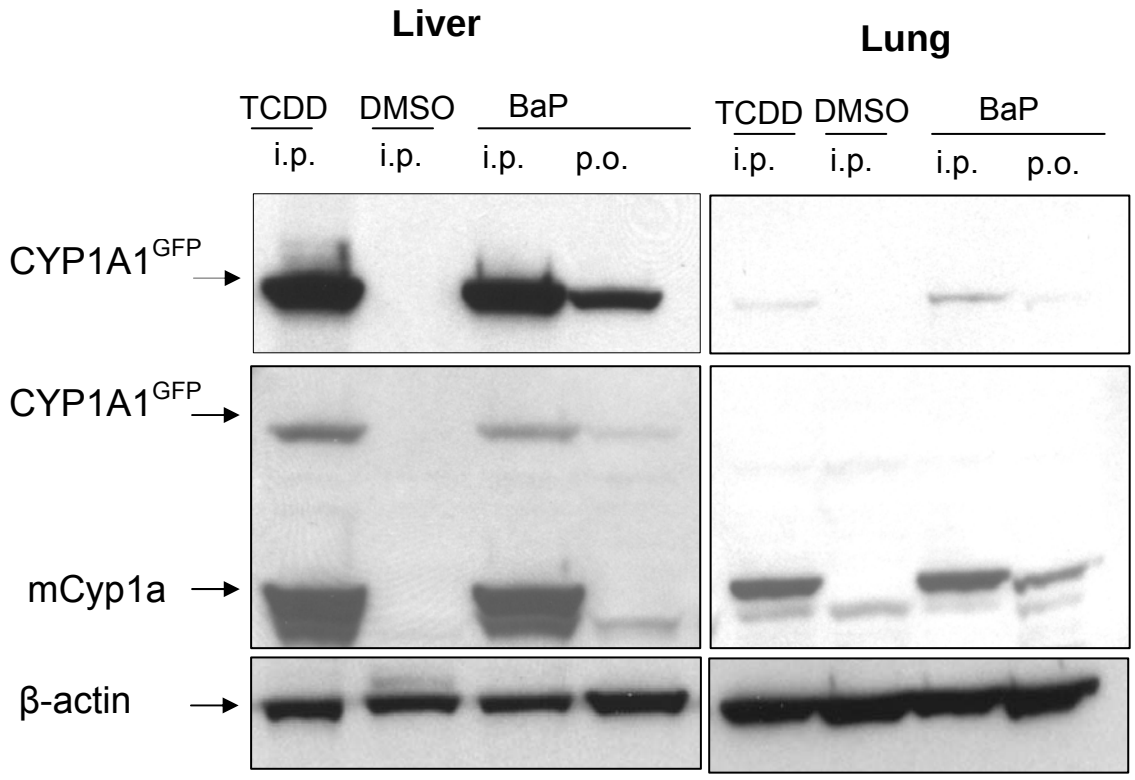


FIGURE 2-8. Differential expression pattern of mCYP1A1 and CYP1A1^{GFP} in transgenic mice after oral vs. i.p. treatment with BaP. Transgenic mice (n=3) for each treatment group were treated 16 μg/kg TCDD by the intraperitoneal route (i.p.). For BaP treatment, 100 mg/kg BaP was injected i.p. for three days, or 100 mg/kg BaP was administered by oral gavage for three days. Control mice received 100 ul of DMSO/corn oil (50:50 v/v) each day for three days. On the fourth day the animals were sacrificed and the small intestine, liver and lung from each animal was collected. The organs from each treatment group were combined and microsomes were prepared. For each Western blot, 20 μg of microsomal protein was used. The anti-CYP1A1 and anti-GFP antibodies were used to detect mCYP1A1 and CYP1A1^{GFP}, respectively. Loading of protein was analyzed by Western blot using an anti-β-actin antibody.

The preferential induction of liver CYP1A1^{GFP} by oral BaP administration led us to examine the contribution of induced CYP1A1^{GFP} toward 7-ethoxyresorufin-O-deethylase (EROD) activity, a relatively specific microsomal monooxygenase activity that has been attributed to expressed CYP1A1/1A2 (Fisher *et al.*, 1992;Sandhu *et al.*, 1994;Guo *et al.*, 1994). When we measured liver microsomal EROD activity from WT litter mates treated orally with BaP, there was a 2-3 fold induction of activity in microsomes (**Table 2-1**). Since we were unable to detect by immunoblot induced mCYP1A1 (**Figure 2-8**), this activity may result from mild induction of a faster mobility band observed by Western blot analysis (**Figure 2-8**, lane 4), which may correspond to mCYP1A2. However, when EROD activity was measured in liver microsomes from Tg-*CYP1A1*^{GFP} mice given BaP by oral administration, EROD activity was induced 8-10 fold over control (**Table 2-1**), and was comparable to those values measured following i.p. treatment with BaP. The contrasting differences in induced EROD activity between WT and Tg-*CYP1A1*^{GFP} mice suggest that induction of CYP1A1^{GFP} by oral BaP is responsible for the majority of the induced EROD activity in transgenic mice, confirming that the fusion protein is functional.

TABLE 2-1

EROD Activity in the Liver (pmol/mg/hr)

	WT	CYP1A1-GFP
Vehicle	13.4 ± 1.1	18.7 ± 1.9
Oral BaP	46.8 ± 2.7	160.7 ± 7.8
IP BaP	137.7 ± 1.9	141.3 ± 22.5

TABLE 2-1. EROD activity in the liver. Transgenic mice n=3 and WT mice n=3 were treated with 100 mg/kg IP BaP, 100 mg/kg oral BaP, and control animals received 100 ul of 50:50 DMSO/corn oil for three days. Livers were isolated, combined, and pulverized with liquid nitrogen according to treatment groups. Microsomes were prepared and 100 ug of protein was used to measure EROD activity in the treatment groups.

As another means to examine the potential of oral BaP to induce other xenobiotic metabolizing proteins, we examined the expression of several human UGT1A proteins in transgenic mice (Tg-*UGT1*) that express the human *UGT1* locus. In Tg-*UGT1* mice, functional expression of all 9 human UGTs have been demonstrated, with expression of the genes targeted by activation of xenobiotic receptors such as the pregnane X-receptor, the liver X-receptor alpha and the AhR (Chen *et al.*, 2005b;Verreault *et al.*, 2006). In previous studies (Chen *et al.*, 2005e), the UGT1A proteins have been shown to be expressed and induced in the GI tract following i.p. treatment with TCDD. When Tg-*UGT1* mice were treated orally with BaP for three days, Western blot analysis using microsomes from the small intestine confirmed the induction of human UGT1A1, UGT1A4 and UGT1A6 (**Figure 2-9**). Interestingly, UGT1A1, UGT1A4 and UGT1A6 were also induced in liver, indicating that adequate concentrations of BaP were being absorbed through the portal circulation to the liver resulting in activation of the AhR. These results indicate that oral BaP treatment is sufficient to induce human *CYP1A1* and *UGT1A* gene expression in liver, but has limited potential to induce mouse CYP1A1 in liver.

FIGURE 2-9

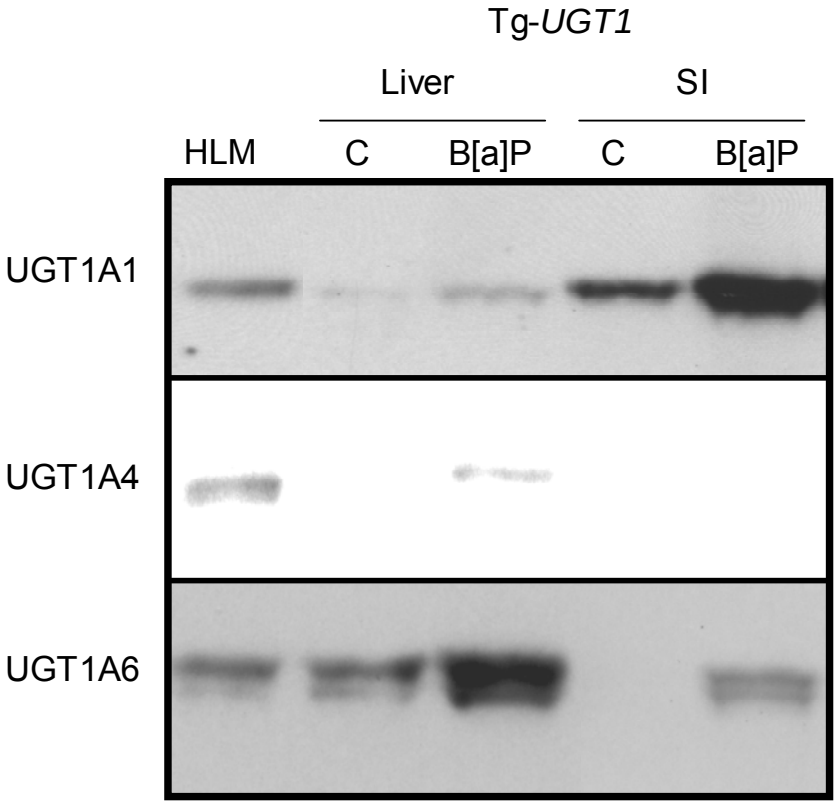


FIGURE 2-9. Induction of UGTs in the liver after oral BaP treatment of Tg-*UGT1* mice. Transgenic *UGT1* (Chen *et al.*, 2005) mice were treated by oral gavage with100 mg/kg BaP for three days. Control Tg-*UGT1* mice received 100 µl of a solution of DMSO/corn oil (50:50 v/v) for three days. Livers were isolated and microsomes were prepared. For Western blot analysis, 20 ug of protein was loaded into each lane. Human liver microsomes (HLM) were used as a positive control for UGT1A expression. Human specific anti-UGT1A1, -UGT1A4, and -UGT1A6 antibodies were used to detect isoform specific UGTs.

DISCUSSION

The development of transgenic mouse strains that express human genes provides a novel opportunity to examine the regulatory properties of the genes but also the functional role of the regulated gene product. The current study demonstrates that the entire human *CYP1A1* gene fused to a reporter GFP gene produces a functional and inducible CYP1A1^{GFP} fusion protein in transgenic mice. Isolation of primary hepatocytes from Tg-*CYP1A1*^{GFP} mice provides a sensitive biological tool to quantitate *CYP1A1* gene induction through the simple and rapid measurement of induced GFP fluorescence. Following the i.p. treatment of Tg-*CYP1A1* ^{GFP} mice with TCDD, induced fluorescence was observed primarily in liver and lung tissue. This corresponded with the induction of human CYP1A1 as previously demonstrated in transgenic mice that express only the human *CYP1A1* gene (Galijatovic *et al.*, 2004). Similar induction patterns were seen when mice were treated by i.p. administration with BaP, confirming that absorption of AhR ligands into circulation through the i.p. cavity serves as an efficient mechanism to examine induction of the *CYP1A1* gene in these tissues. In addition, CYP1A1^{GFP} fluorescence was not observed in the gastrointestinal tract or kidney, similar to the expression patterns of the human *CYP1A1* gene and *CYP1A1*-Luciferase gene in transgenic mice expressing these DNA constructs. Thus, consistency in the induction pattern of the human *CYP1A1* genes in different transgenic strains is corroborated.

One of the unique aspects of undertaking regulatory gene experiments in transgenic mice is the ability examine expression patterns in different tissues following routes of administration that contrast those to classical treatment regimes such as the administration of xenobiotics by the i.p. route. When expression experiments were

conducted following oral administration of BaP, liver CYP1A1^{GFP} levels were slightly less abundant than CYP1A1^{GFP} levels following i.p. administration of BaP. The induced human CYP1A1^{GFP} by oral administration in liver was in contrast to undetectable levels of mCYP1A1 induction, demonstrating that inducibility of the mouse and human *CYP1A1* genes in liver by BaP results from differential sensitivity of these genes to activated AhR. In liver microsomes from WT mice, induced EROD activity was minimal following oral treatment with BaP. Under similar treatment conditions, EROD activity was induced 8-10 fold in liver microsomes from Tg-*CYP1A1*^{GFP} mice. This finding suggests that the human *CYP1A1*^{GFP} gene was more sensitive to AhR activation than the rodent *Cyp1a1/1a2* genes. The increased sensitivity of the *CYP1A1*^{GFP} gene towards response may reflect a gene dosage phenomenon, indicative of the transgene being integrated into the mouse genome in multiple copies. Sufficient concentrations of BaP reach the liver through the portal circulation, a finding which was also confirmed by induction of the AhR dependent family of human *UGT1A* genes in Tg-*UGT1* mice. The reduced induction of mouse CYP1A1 and CYP1A1^{GFP} following oral administration of BaP may in part be a reflection of extensive metabolism in the gastrointestinal tract.

Although other strains of transgenic mice that express *CYP1A1* reporter gene constructs have been developed (Galijatovic *et al.*, 2004; Campbell *et al.*, 1996), expression of CYP1A1^{GFP} in liver and lung provides the opportunity to link gene expression with CYP1A1 protein production, as monitored by fluorescence. Expression of CYP1A1^{GFP} in tissues such as the liver and lung can be used as a biomarker of exposure to agents that regulate the AhR in vivo. Examining expression in whole tissue also results as the culmination of regulatory and signaling processes that are engaged in

control of the AhR, in addition to other humoral processes associated with activation of the human *CYP1A1* gene in vivo.

As a sensitive tool to monitor CYP1A1 induction, primary hepatocytes cultured from Tg-CYP1A1^{GPF} mice can also be cultured on either plastic or collagen coated tissue culture dishes and the induction of fluorescence used as a tool to identify agents that lead to activation of the AhR. Measurement of fluorescence following exposure to several AhR agonists correlated with induction of mCYP1A1, confirming that the increase in CYP1A1^{GFP} was commensurate with regulation of the *Cyp1a1* gene. Primary hepatocytes from Tg-*CYP1A1^{GFP}* mice also allows for the real time monitoring of CYP1A1^{GFP} protein induction and turnover after toxicant exposure, a property that may be useful to assess biological persistence of compounds. The treatment of hepatocytes isolated from transgenic mice with TCDD demonstrated that concentrations as low as 10^{-11} M elicited maximal fluorescence. These values are equal in sensitivity to those reported for induction of reporter gene activities constructed with XRE or CYP1A1 promoter elements (Postlind *et al.*, 1993; Anderson *et al.*, 1995; Nagy *et al.*, 2002), and provide an additional tool for the detection and measurement of potent AhR ligands and environmental toxicants.

Chapter 2, in full, is a reprint of the material as it appears in Operaña TN, Nguyen N, Chen S, Beaton D, Tukey RH. "Human CYP1A1GFP expression in transgenic mice serves as a biomarker for environmental toxicant exposure" *Journal of Toxicological Sciences* (2007) Jan;95(1):98-107. I was the primary investigator and author of this article.

ACKNOWLEDEMENTS: The authors appreciate the technical assistant provided by Dr. Mason Mackey at the UCSD Superfund Imaging Core for help with confocal microscopy, as well as the staff at the Superfund Mouse Transgenic Core for generation of the Tg-*CYP1A1*^{GFP} mice.

REFERENCES

Anderson JW, Rossi S S, Tukey R H, Vu T and Quattrochi L C (1995) A Biomarker, P450 RGS, for Assessing the Induction Potential of Environmental Samples. *Environ Toxicol Chem* **14**: pp 1159-1169.

Campbell SJ, Carlotti F, Hall P A, Clark A J and Wolf C R (1996) Regulation of the *CYP1A1* Promoter in Transgenic Mice: An Exquisitely Sensitive on-Off System for Cell Specific Gene Regulation. *J Cell Sci* **109**: pp 2619-2625.

Chen S, Beaton D, Nguyen N, Senekeo-Effenberger K, Brace-Sinnokrak E, Argikar U, Remmel R P, Trottier J, Barbier O, Ritter J K and Tukey R H (2005) Tissue-Specific, Inducible, and Hormonal Control of the Human UDP-Glucuronosyltransferase-1 (UGT1) Locus. *J Biol Chem* **280**: pp 37547-37557.

Chen S, Nguyen N, Tamura K, Karin M and Tukey R H (2003) The Role of the Ah Receptor and P38 in Benzo[a]Pyrene-7,8-Dihydrodiol and Benzo[a]Pyrene-7,8-Dihydrodiol-9,10-Epoxide-Induced Apoptosis. *J Biol Chem* **278**: pp 19526-19533.

Corchero J, Pimprale S, Kimura S and Gonzalez F J (2001) Organization of the CYP1A Cluster on Human Chromosome 15: Implications for Gene Regulation. *Pharmacogenetics* **11**: pp 1-6.

El-Fouly MH, Richter C, Giesy J P and Denison M S (1995) PRODUCTION OF A NOVEL RECOMBINANT CELL LINE FOR USE AS A BIOASSAY SYSTEM FOR DETECTION OF 2,3,7,8-TETRACHLORODIBENZO-p-DIOXIN-LIKE CHEMICALS. *Environ Toxicol Chem* **13**: pp 1581-1588.

Fisher CW, Caudle D L, Martin-Wixtrom C, Quattrochi L C, Tukey R H, Waterman M R and Estabrook R W (1992) High-Level Expression of Functional Human Cytochrome P450 1A2 in *Escherichia Coli*. *FASEB J* **6**: pp 759-764.

Fujisawa-Sehara A, Sogawa K, Nishi C and Fujii-Kuriyama Y (1986) Regulatory DNA Elements Localized Remotely Upstream From the Drug-Metabolizing Cytochrome P-450c Gene. *Nucleic Acids Res* **14**: pp 1465-1477.

Galijatovic A, Beaton D, Nguyen N, Chen S, Bonzo J, Johnson R, Maeda S, Karin M, Guengerich F P and Tukey R H (2004) The Human CYP1A1 Gene Is Regulated in a Developmental and Tissue-Specific Fashion in Transgenic Mice. *J Biol Chem* **279**: pp 23969-23976.

Gonzalez FJ and Nebert D W (1985) Autoregulation Plus Upstream Positive and Negative Control Regions Associated With Transcriptional Activation of the Mouse P_1-450 Gene. *Nucleic Acids Res* **13**: pp 7269-7288.

Guo Z, Gillam E M J, Ohmori S, Tukey R H and Guengerich F P (1994) Expression of Modified Human Cytochrome P450 1A1 in *Escherichia Coli*: Effects of 5' Substitution, Stabilization, Purification, Spectral Characterization, and Catalytic Properties. *Arch Biochem Biophys* **312**: pp 436-446.

Hoffman EC, Reyes H, Chu F-F, Sander F, Conley L H, Brooks B A and Hankinson O (1991) Cloning of a Factor Required for Activity of the Ah (Dioxin) Receptor. *Science* **252**: pp 954-958.

McManus ME, Burgess W M, Veronese M E, Huggett A, Quattrochi L C and Tukey R H (1990) Metabolism of 2-Acetylaminofluorene, Benzo[a]Pyrene and the Activation of Food Derived Heterocyclic Amine Mutagens by Human Cytochromes P450. *Cancer Res* **50**: pp 3367-3376.

Nagy SR, Sanborn J R, Hammock B D and Denison M S (2002) Development of a Green Fluorescent Protein-Based Cell Bioassay for the Rapid and Inexpensive Detection and Characterization of Ah Receptor Agonists. *Toxicol Sci* **65**: pp 200-210.

Nelson DR, Koymans L, Kamataki T, Stegeman J J, Feyereisen R, Waxman D J, Waterman M R, Gotoh O, Coon M J, Estabrook R W, Gunsalus I C and Nebert D W (1996) P450 Superfamily: Update on New Sequences, Gene Mapping, Accession Numbers and Nomenclature. *Pharmacogenetics* **6**: pp 1-42.

Okino ST, Pendurthi U R and Tukey R H (1992) Phorbol Esters Inhibit the Dioxin Receptor Mediated Transcriptional Activation of the Mouse Cyp1A1 and Cyp1A2 Genes by 2,3,7,8-Tetrachlorodibenzo-p-Dioxin. *J Biol Chem* **267**: pp 6991-6998.

Okino ST and Whitlock J P Jr (1995) Dioxin Induces Localized, Graded Changes in Chromatin Structure: Implications for Cyp1A1 Gene Transcription. *Mol Cell Biol* **15**: pp 3714-3721.

Postlind H, Vu T P, Tukey R H and Quattrochi L C (1993) Response of Human *CYP1*-Luciferase Plasmids to 2,3,7,8- Tetrachlorodibenzo-*p*-Dioxin and Polycyclic Aromatic Hydrocarbons. *Toxicol Appl Pharmacol* **118**: pp 255-262.

Reyes H, Reisz-Porszasz S and Hankinson O (1992) Identification of the Ah Receptor Nuclear Translocator Protein (ARNT) As a Component of the DNA Binding Form of the Ah Receptor. *Science* **256**: pp 1193-1195.

Ritter JK, Kessler F K, Thompson M T, Grove A D, Auyeung D J and Fisher R A (1999) Expression and Inducibility of the Human Bilirubin UDP-Glucuronosyltransferase UGT1A1 in Liver and Cultured Primary Hepatocytes: Evidence for Both Genetic and Environmental Influences. *Hepatology* **30**: pp 476-484.

Sandhu P, Guo Z, Baba T, Martin M V, Tukey R H and Guengerich F P (1994) Expression of Modified Human Cytochrome P450 1A2 in *Escherichia Coli*:

Stabilization, Purification, Spectral Characterization, and Catalytic Activities of the Enzyme. *Arch Biochem Biophys* **309**: pp 168-177.

Soucek P, Martin M V, Ueng Y F and Guengerich F P (1995) Identification of a Common Cytochrome P450 Epitope Near the Conserved Heme-Binding Petide With Antibodies Raised Against Recombinant Cytochrome P450 Family 2 Proteins. *Biochemistry* **34**: pp 16013-16021.

Tukey RH, Hannah R R, Negishi M, Nebert D W and Eisen H J (1982) The Ah Locus: Correlation of Intranuclear Appearance of Inducer-Receptor Complex With Induction of Cytochrome P_1-450 MRNA. *Cell* **31**: pp 275-284.

Verreault M, Senekeo-Effenberger K, Trottier J, Bonzo J A, Belanger J, Kaeding J, Staels B, Caron P, Tukey R H and Barbier O (2006) The Liver X-Receptor Alpha Controls Hepatic Expression of the Human Bile Acid-Glucuronidating UGT1A3 Enzyme in Human Cells and Transgenic Mice. *Hepatology* **44**: pp 368-378.

Wu L and Whitlock J P, Jr. (1992) Mechanism of Dioxin Action: Ah Receptor-Mediated Increase in Promoter Accessibility *in Vivo*. *Proc Natl Acad Sci USA* **89**: pp 4811-4815.

Yueh MF, Kawahara M and Raucy J (2005) Cell-Based High-Throughput Bioassays to Assess Induction and Inhibition of CYP1A Enzymes. *Toxicol In Vitro* **19**: pp 275-287.

CHAPTER 3

Oligomerization of UDP-Glucuronosyltransferase 1A Proteins: Homo- and Heterodimerization Analysis by Fluorescence Resonance Energy Transfer (FRET) and Co-immunoprecipitation

INTRODUCTION

UDP-glucuronosyltransferases (UGTs) are type I membrane bound proteins localized to the endoplasmic reticulum (ER) and play an essential role in the elimination and detoxification of drugs, xenobiotics, and a host of endogenous compounds such as steroids, bile acids, bilirubin and fatty acids (Dutton, 1980). This process proceeds by the transfer of glucuronic acid from UDP-glucuronic acid (UDP-GlcA) to targeted substrates. The addition of the polar glucuronic acid to the lipophilic substrates increases the metabolite's water solubility, thereby facilitating excretion into water compartments of the cell for excretion into either the urine or bile.

The UGTs are classified into two gene families, UGT1 and UGT2 (Mackenzie et al., 1997). The UGT2 subfamily of proteins is encoded by individual genes located in a gene cluster on chromosome 4 at 4q13-q21 (Monaghan et al., 1994; Beaulieu et al., 1997; Chen et al., 1993). These are composed of the UGT2A1 and UGT2A2, along with the UGT2B members, which include UGT2B4, 2B7, 2B10, 2B11, 2B15, 2B17, and 2B28. The UGT2A proteins are localized to the olfactory system, and are felt to be important in eliminating olfactory stimuli (Heydel et al., 2001). The UGT2B proteins are involved in the metabolism of endogenous compounds such as bile acids (Monaghan et al., 1997), steroids (Hum et al., 1999), hormones (Thibaudeau et al., 2006) and fatty acids, but are also important for the elimination of therapeutic drugs (Chouinard et al., 2006). In contrast, the UGT1 locus is located on chromosome 2q37 (Harding et al., 1990) and its gene products are linked to the metabolism of exogenous compounds, although UGT1A1 is the only UGT capable of conjugating the heme byproduct, bilirubin (Bosma et al., 1994). The UGT1 locus encodes nine functional UGT1A proteins (UGT1A1 and

UGT1A3 through UGT1A10) (Mackenzie et al., 1997; Ritter et al., 1992), each derived through a unique process called exon sharing (Tukey and Strassburg, 2001). The UGT1 locus is organized with a tandem array of 9 open reading frames encoding each of the exon 1 regions of the respective UGT1A proteins, flanked by open reading frames encoding exons 2-5. Based upon the start of transcription, each respective first exon sequence is processed with common exons 2-5, resulting in the synthesis of the 9 UGT1A gene products. Thus, each UGT1A protein is composed of a variable amino region (exon 1) and an identical carboxyl region (exons 2-5) (Wooster et al., 1991; Ritter et al., 1992b). The carboxyl region of the UGT1A proteins displays high sequence identity to the same region on the UGT2 proteins, implicating the conserved function of this region for recognition and binding of UDP-GlcA. Within the UGT2 family of proteins, both the amino terminal and the carboxyl region has been shown to play an important role in substrate specificity (Mackenzie, 1990; Li et al., 1997).

Preliminary findings suggest that the family of UGTs may be highly organized within the ER, existing as monomeric proteins, as well as oligomers in homodimeric and heterodimeric states. In rat liver microsomes, UGT2B1 was shown to exist as a functional dimer, with evidence that the amino terminal region was important in the protein-protein interaction of the UGT (Meech and Mackenzie, 1997). In addition, UGT2B1 was also shown to directly heterodimerize with the family of UGT1A proteins (Ikushiro et al., 1997), although identification of the UGT1A proteins involved in the oligomerization were not characterized. Cross-linking studies using expressed human UGT1A1, in addition to a two-hybrid analysis, demonstrated that UGT1A1 formed a homodimer complex. It was also observed that the reduction of disulfide bond formation was shown

to have little impact on UGT1A1 dimerization, and mutagenesis of cysteine 223 to a tyrosine completely abolished UGT1A1 oligomerization, as did the deletion of a membrane embedded region spanning amino acids 152-180. Consistent with the UGT2B1 findings, the amino terminal region was found to be important for UGT1A1 dimerization (Ghosh et al., 2001).

The focus of the current study is to explore the intermolecular interactions of the UGTs in living cells using fluorescence resonance energy transfer (FRET). FRET is a non-invasive spectroscopic method that can be used in live cells to monitor spatial and temporal intermolecular interactions of chimeric proteins that have acceptor and donor fluorophores attached (Clegg, 1996). FRET involves the transfer of energy from a donor fluorophore in its excited state to an acceptor fluorophore by a nonradiative dipole-dipole interaction (Lakowicz, 1983), and is only able to occur if the proteins reside within angstroms from each other. To further compliment the in vivo analysis of UGT protein-protein interactions by FRET, co-immunoprecipitation experiments provided additional biochemical evidence to support the existence of the UGT1A as either homodimeric or heterodimeric aggregates in the membrane.

MATERIALS AND METHODS

Generation of the pUGT1A-CFP, pUGT1A-YFP, and pUGT1A-HA Plasmids. For the following study monomeric CFP (mCFP) and monomeric YFP (mYFP) variants were chosen as the donor and acceptor fluorophores, respectively. Due to the intrinsic property of the wild type CFP and YFP proteins to spontaneously aggregate at high concentrations, we elected to use the monomeric forms of the fluorophores, which would prevent spontaneous aggregation of the fluorophores in the membrane (Zacharias et al., 2002). mCFP and mYFP plasmids were kindly provided by Dr. Roger Tsien (University of California, San Diego). Both mCFP and mYFP were amplified by PCR with the sense primer (5'-ggatccaatggtgagcaagggcgaggag-3') containing a BamHI site (underlined) and the antisense primer (5'-gcggccgctttacttgtacagctcgtccatgcc-3') containing a NotI site (underlined). The mCFP and mYFP PCR products were subcloned into pCR 2.1-TOPO vector (Invitrogen). The amplified TOPO clones containing mCFP and mYFP were digested with BamHI and NotI restriction enzymes and each insert purified. The pEGFP-N1 expression vector (Clontech), which contains the GFP gene flanked by a multi-cloning site, was digested with BamHI and NotI to remove the GFP portion. The mCFP and mYFP inserts were ligated into the linearized pEGFP-N1 expression vector, and the resulting plasmids identified as mCFP-N1 and mYFP-N1. To make the chimeric UGT1A1-CFP and UGT1A1-YFP proteins, UGT1A1 was amplified by PCR with a sense primer (5'-ctcgagATGgctgtggagtcccag-3') containing an XhoI site (underlined) followed by an initiation ATG codon, and an antisense primer (5'-ggatcc**cca**atgggtcttggatttg-3') with a BamHI site (underlined) followed by a mutated stop codon shown in bold. After the

cloning of UGT1A1 PCR product into the pCR 2.1-TOPO vector, the insert was removed and purified by digestion with XhoI and BamHI and subcloned into the XhoI and BamHI sites in the mCFP-N1 and mYFP-N1 plasmids, creating the pUGT1A1-CFP and pUGT1A1-YFP plasmids. To generate the hemagglutinin (HA) recognition sequence fused to the UGT1A1 protein, a UGT1A1-HA fragment was generated by PCR with a sense primer (5'-ctcgagatggctgtggagtcccag-3') containing an XhoI site (underlined) and antisense primer (5'-ggatcctca**ggcataatctggcacatcataagggtattccat**ccaatgggtcttgggattt-3') containing a BamHI site (underlined) and the HA sequence in bold. The UGT1A1-HA PCR product was subcloned into pCR 2.1-TOPO vector (Invitrogen) and digested with XhoI and BamHI restriction enzymes to remove the insert. The UGT1A1-HA fragment was subcloned into the XhoI and BamHI multiple cloning site of the pcDNA 3.1(-) expression vector to produce the pUGT1A1-HA plasmid.

Construction of UGT1A-CFP, -YFP and HA tagged expression plasmids. In order to generate a library of the UGT1A -CFP, -YFP, and HA-tagged constructs, we took advantage of the feature that all of the UGT1A proteins have a unique exon 1 region and a conserved 2-5 exon region. The pUGT1A1-CFP, pUGT1A1-YFP, and pUGT1A1-HA expression vectors were used to generate all subsequent constructs. This was done by removing the exon 1, exon 2, exon 3 and a portion of the exon 4 region of UGT1A1 from the CFP, YFP, and HA expression vectors, and inserting in their place the accompanying regions of the other UGT1A cDNAs. The following procedures were performed for each UGT1A isoform. pUGT1A1-CFP, pUGT1A1-YFP and pUGT1A1-HA plasmids were each digested with the restriction enzymes NheI (located in the multiple cloning site of

each expression vector) and BstEII (located in exon 4 of each UGT1A isoform). Having constructed previously in our laboratory pcDNA 3.1 plasmids expressing UGT1A3, UGT1A4, UGT1A6, UGT1A7, UGT1A8, UGT1A9, and UGT1A10, each of the UGT1A inserts encoding these regions were isolated by digestion with NheI and BstEII. Each of the UGT1A fragments was subcloned into the linearized pUGT1A1-CFP, pUGT1A1-YFP and pUGT1A1-HA expression vectors that had the NheI and BstEII fragment removed. In all, 24 UGT1A constructs were made with each expressing a fusion protein with either -CFP, -YFP, or -HA C-terminal tags. A list of the plasmid constructs is shown in Table 3-1.

Microscopy and FRET Analysis. COS cells were plated at a density of 3.5×10^5 cells per well in 6-well plates and co-transfected with 5 µg of pUGT1A1-CFP and 5 µg of pUGT1A1-YFP plasmids using Lipofectamine 2000 (Invitrogen) according to manufacturer's protocol. After 24 h the live cells were imaged using a Zeiss Axiovert 200M inverted microscope. Donor (CFP) was excited at 455 nm and fluorescence emission detected in a bandwidth of 440-480 nm (CFP channel). Acceptor (YFP) was excited at 515 nm and fluorescence emission detected in a bandwidth of 530-535 nm (YFP channel). FRET excitation was conducted at 455 nm and fluorescence emission detected in a bandwidth of 530-535 nm (FRET channel). To correct for fluorescence bleed through into the FRET channel, cells transfected with only pUGT1A1-CFP were used to determine the donor correction factor and cells transfected with only pUGT1A1-YFP were used to determine the acceptor correction factor. Images of $UGT1A1^{CFP}$ and $UGT1A1^{YFP}$ expression in co-transfected cells were sequentially acquired with the donor

(CFP) channel, acceptor (YFP) channel, and FRET channel under identical conditions. The image obtained with the FRET channel was evaluated using Carl Zeiss AxioVision FRET software and FRET calculated using the Acceptor Ratio correction method (Youvan et al., 1997). The Acceptor ratio method corrects for the cross talk from the Donor alone, the Acceptor alone, and background intensity using the following equation: Ac= Fc/ (accgv-bgacc), where Ac= FRET concentration as Acceptor ratio; Fc= FRET concentration according to Youvan et al (Youvan et al., 1997) calculated by the equation: Fc= (fretgv-bgfret) – cfdon*(dongv-bgdon) – cfacc* (accgc-bgacc), with gv= intensity as gray value; bg= background intensity; cf= correction factor; fret= FRET image; don= Donor image; acc= Acceptor image.

FRET efficiency was also analyzed by photobleaching the Acceptor (YFP) and measuring the increase in Donor signal (CFP). Cells co-transfected with pUGT1A1-CFP and pUGT1A1-YFP were initially imaged using the CFP and YFP channels. The same cell was then illuminated using the photobleaching cube (YFP excitation 515 nm) with the laser power set to 100 % for 1 minute intervals, followed by CFP and YFP image acquisitions. This was repeated every minute over a 10 minute time course. To quantify changes in the CFP and YFP fluorescence intensity over the photobleaching time course, selected regions of interest were measured using the Carl Zeiss Axiovision FRET software and quantified using the Siegel evaluation method (Siegel et al., 2000). The evaluation method uses the following equation: BL= [1-(dongvbef-bgdon-bef)/ (dongvaft-bgdon-aft)]*100, where BL= FRET concentration by Acceptor bleaching; Don= Donor image; gv= intensity as gray value; bef= before bleaching; aft= after bleaching.

Co-Immunoprecipitation of Expressed UGT1A proteins. COS cells were plated at a density of 3.5 x 10^5 cells per well in 6-well plates and co-transfected with 5 µg of pUGT1A1-HA and 5 µg pUGT1A1-CFP plasmids using Lipofectamine 2000 (Invitrogen). After 24 h, cells were washed twice with PBS and lysed for 1 h on ice with 1 ml 1X RIPA buffer (0.05 M Tris-HCl, pH 7.4, 0.15M NaCl, 0.25% Deoxycholic acid, 1% NP-40, 1 mM EDTA) supplemented with 1 % protease cocktail inhibitor (Sigma). The lysed cells were centrifuged for 10 min at 13,000 x g and the supernatant collected. The entire supernatant from one transfected well was mixed with 30 µl of anti-HA beads (Roche) and incubated at 4 °C on a rocker platform overnight. The anti-HA beads were centrifuged for 1 minute at 1000 x g and the supernatant discarded. The anti-HA beads were washed 3 times with 1 ml of cold lysis buffer. The anti-HA beads were then resuspended in 60 µl of electrophoresis sample buffer and heated to 95 °C for 10 min. The beads were centrifuged for 1 min at 1,000 x g and the supernatant collected and used for Western blot analysis.

Western Blot Analysis. All Western blots were performed using 4-12 % NuPAGE Bis Tris polyacrylamide gels as outlined by the supplier (Invitrogen) and resolved under denaturing conditions (50 mM MOPS, 50 mM Tris-base, pH 7.7, 0.1 % SDS, 1mM EDTA). The resolved protein was transferred onto nitrocellulose membrane using a semi-dry transfer system (Norvex). The membrane was blocked with 5 % nonfat dry milk in 10 mM Tris-HCl, pH 8, 0.15 M NaCl, and 0.05 % Tween 20 (Tris-buffered saline) for 1 h at room temperature. Each membrane was washed in Tris-buffered saline

solution and incubated with an anti-UGT1A antibody, kindly provided by Dr. Alain Belanger (Laval University, Quebec, Canada), in Tris-buffered saline containing 0.02 % sodium azide at 4 °C overnight. Membranes were then washed five times with Tris-buffered saline solution and incubated with horseradish peroxidase-conjugated rabbit secondary antibody at a 1:5000 dilution in Tris-buffered saline solution containing 2 % nonfat milk for 1 h shaking at room temperature. Membranes were then washed five times with Tris-buffered saline solution and visualized using Western Lightning Chemiluminescence reagents according to the manufacturer's instructions (PerkinElmer Life Sciences) followed by exposure to X-ray film (Kodak).

UDP-Glucuronosyltransferase Activity Analysis. COS cells were plated at a density of 3.5 x 10^5 cells per well in 6-well plates and transfected with either 2 µg of each plasmid (co-transfection) or 5 µg of plasmid (single transfection) using Lipofectamine 2000 (Invitrogen). Whole cell lysates were prepared by re-suspending cells in 50 mM Tris-HCl (pH 7.6), 10 mM $MgCl_2$ followed by homogenization and sonication. Each catalytic assay was conducted in a 100 µl reaction that contained 350 µg of cellular protein, 50 mM Tris-HCl (pH 7.6), 10 mM $MgCl_2$, 0.04 µCi ^{14}-C-UDPGA (255.6 pmol/reaction), 8.5 mM saccharolactone, 100 µg of phosphatidylcholine, 0.5 mM UDP-glucuronic acid, and a final concentration of 500 µM for each substrate. The substrate octylgallate was used to determine UGT activity for UGT1A1 and UGT1A3 isoforms, while 2-napthol was used for UGT1A7. Each reaction was incubated in a 37 °C water bath for 60 min, and then terminated with the addition of 100 µl cold methanol. The protein was spun down by centrifugation at 13,000 g for 20 min, and 100 µl of the

supernatant spotted onto a Whatman glass-backed thin layer chromatography (TLC) plate (Whatman, Hillsoboro, Oregon). Chromatography was performed in a mixture (35:35:10:20 v/v) of n-butanol: acetone: acetic acid: water. Once the solvent front reached 2 cm from the top of the TLC plate, the plate was removed from the tank, dried, and exposed to a phosphor screen (Molecular Dynamics, Sunnyvale, CA) overnight. The location of the glucuronides on the plate was identified and that region of the TLC plate was scraped and placed in scintillation fluid for quantification with a liquid scintillation counter (Beckman Coulter LS6500, Fullerton, CA).

RESULTS

Determination of FRET Analysis with Expressed UGT1A^{CFP} and UGT1A^{YFP}. In order to explore intermolecular protein-protein interactions between UGT1A1 proteins in vivo, UGT1A1-CFP tagged and UGT1A1-YFP tagged fusion constructs were made. Expression patterns of the UGT1A1^{CFP} and UGT1A1^{YFP} proteins were evaluated by transfecting pUGT1A1-CFP and pUGT1A1-YFP plasmids into COS cells, respectively, followed by fluorescence microscopy analysis. In **Figure 3-1**, the top panel of cells (1A1-CFP) and lower panel of cells (1A1-YFP) illustrate that both UGT1A1^{CFP} and UGT1A1^{YFP} fusion proteins exhibit fluorescence. Protein expression of each construct was excluded from the nucleus and resembles an ER localization expression pattern.

The application of FRET has been used to monitor a vast array of protein interactions (Tsien, 1998; Miyawaki and Tsien, 2000), such as oligomerization and multimeric complex formation (Szczesna-Skorupa et al., 2003; Schmid et al., 2001; Overton and Blumer, 2000; Latif et al., 2002; van Kuppeveld et al., 2002; Scholze et al., 2002). In order to determine homodimerization of UGT1A1 in vivo, COS cells were co-transfected with pUGT1A1-CFP and pUGT1A1-YFP plasmids and the live cells evaluated for FRET. In **Figure 3-2A**, co-expression of both UGT1A1^{CFP} and UGT1A1^{YFP} is indicated in the CFP and YFP channels, respectively. Analysis with the FRET channel after correction for donor and acceptor bleed through illustrates increased fluorescence, indicating that the two proteins reside in close proximity to each other within the ER membrane. Evaluation of FRET using Acceptor Ratio analysis depicted distinct color-coded regions, illustrating FRET efficiency ranging from 40 % (green) up to 80 % (red) throughout the cell.

FIGURE 3-1

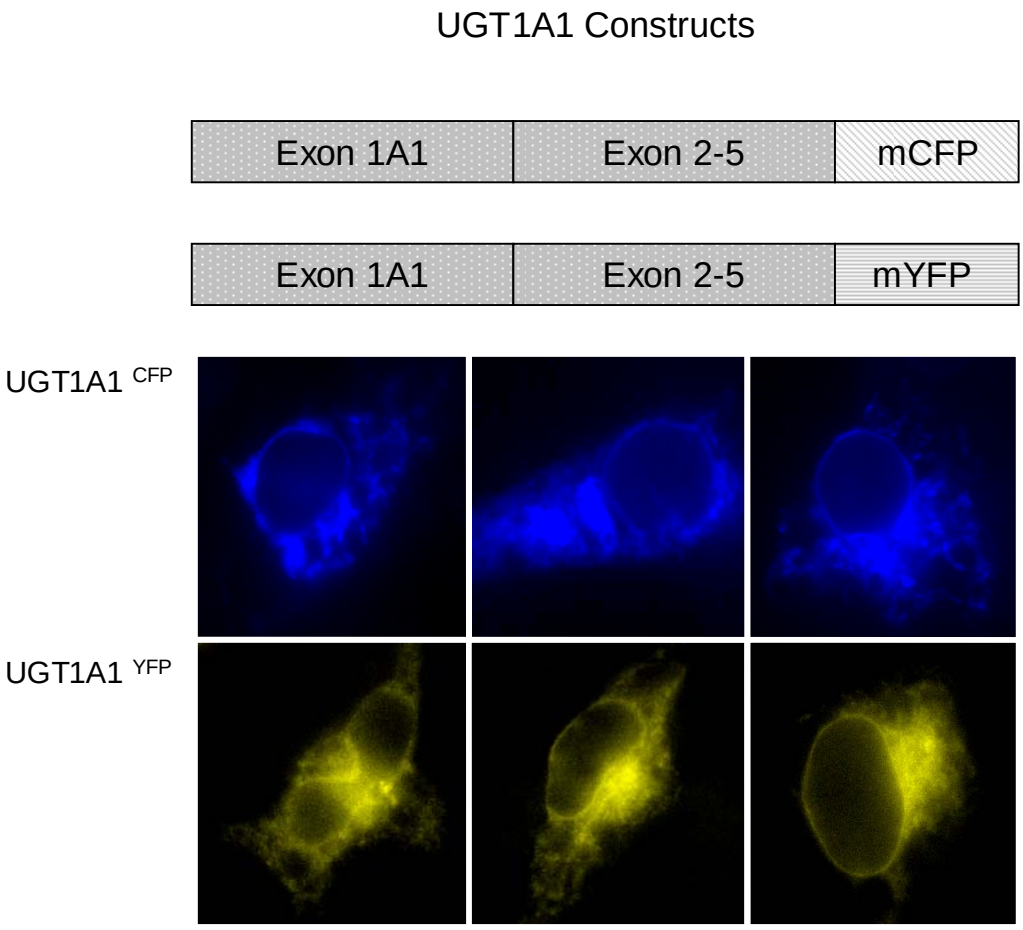


FIGURE 3-1. Detection of fluorescence following pUGT1A1-CFP and pUGT1A1-YFP transfection into COS cells. COS cells were transiently transfected with 5 µg of pUGT1A1-CFP (top panel) or 5 µg pUGT1A1-YFP (lower panel). After 24 h, the live cells were imaged with a Zeiss Axiovert 200M microscope. CFP constructs excited at 455 nm and fluorescence was detected in a bandwidth of 440-480 nm, while YFP constructs excited at 515 nm and fluorescence detected at bandwidth of 530-535 nm. Shown are three different cells with each transfection.

FIGURE 3-2

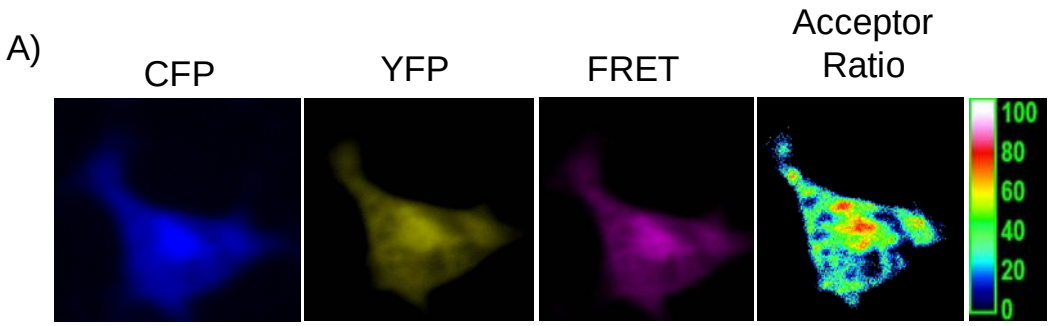


FIGURE 3-2. Detection of FRET in COS cells co-transfected with pUGT1A1-CFP and pUGT1A1-YFP. A) COS cells were co-transfected with 5 µg of pUGT1A1-CFP and pUGT1A1-YFP for 24 h. Co-expression of both UGT1A1^{CFP} and UGT1A1^{YFP} is indicated by fluorescence in both the CFP channel and YFP channel. Correction for donor and acceptor bleed through was performed and FRET signal was analyzed with the FRET channel. FRET efficiency was evaluated with the Carl Zeiss AxioVision FRET software using the Acceptor Ratio analysis and depicted as a color-coded scale ranging from 0-100 % FRET efficiency.

FIGURE 3-2

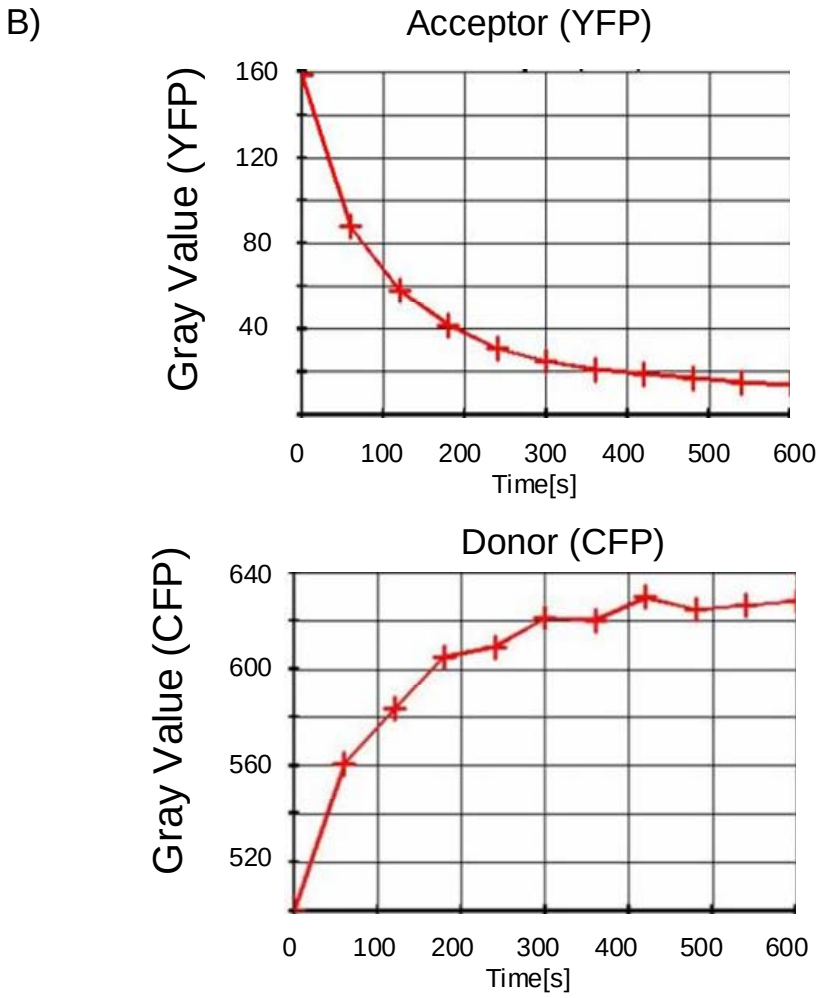


FIGURE 3-2. Detection of FRET in COS cells co-transfected with pUGT1A1-CFP and pUGT1A1-YFP. B) COS cells were co-transfected with 5 µg of pUGT1A1-CFP and pUGT1A1-YFP and initially imaged with the CFP and YFP channel. The same cell was then photobleached by excitation at 515 nm wavelength for 60 second intervals followed by CFP and YFP image acquisitions. This was repeated every minute over a 10 minute time course. Changes in the CFP and YFP fluorescence intensity over the photobleaching time course was quantified using the Siegel evaluation method in the Carl Zeiss AxioVision FRET software.

The acceptor photobleaching method was also implemented as an alternative method to quantify the absolute efficiency of FRET between the Donor (CFP) and Acceptor (YFP) fluorophores. For this experiment COS cells were co-transfected with pUGT1A1-CFP and pUGT1A1-YFP and the cells illuminated at 515 nm wavelength for 60 seconds, followed by CFP and YFP image acquisitions. This was repeated every minute over a 10 minute time course. Using the acceptor photobleaching method, FRET is manifested by the dequenching of the donor CFP signal by selective photobleaching of the acceptor YFP over time, resulting in increased CFP signal. In **Figure 3-2B** the Acceptor graph showed a sharp decrease in YFP fluorescence after each photobleaching exposure, while the Donor graph depicted a concomitant increase in CFP fluorescence throughout the photo-bleaching time course, indicating FRET between $UGT1A1^{CFP}$ and $UGT1A1^{YFP}$. Moreover, the decrease in fluorescence gray value of the Acceptor (YFP) was directly proportional to the fluorescence gray value gained by the Donor (CFP), further confirming the high FRET efficiency observed in the Acceptor Ratio analysis in **Figure** 3-**2A**. Since FRET can elucidate protein-protein interactions within angstrom distances, these results infer that the $UGT1A1^{CFP}$ and $UGT1A1^{YFP}$ fusion proteins are in physical contact within the membrane.

FRET analysis suggests that UGT1A1 forms a homodimer complex. The UGT1A proteins share 100 % amino acid identity in 244 amino acids at the carboxyl end with varying degrees of sequence divergence in the amino terminal region. Hydropothy profiles indicate that each of the UGT1A proteins show a conserved pattern of hydrophobicity with UGT1A1, allowing us to speculate that the other UGT1A proteins may behave in a similar pattern as UGT1A1 in the membrane. To examine this

possibility, homodimerization among the other UGT1A proteins was explored. COS cells were co-transfected with the corresponding pUGT1A-CFP and pUGT1A-YFP plasmids to examine homodimerization potential as measured by FRET analysis (**Figure 3-3**). As a negative control, COS cells were co-transfected with the pCFP and pYFP vectors. FRET analysis using Acceptor Ratio evaluation from pCFP/pYFP co-transfected cells showed no FRET signal as indicated by the dark blue color-coded region throughout the cell. However, Acceptor Ratio evaluations of cells co-transfected with the pUGT1A3-, pUGT1A4-, pUGT1A6-, pUGT1A7-, pUGT1A8-, pUGT1A9- or pUGT1A10-CFP and -YFP pairs showed high FRET signals ranging from 40 % (green) to 90 % (red-white) FRET efficiency. It can be seen in each of the FRET channels that all of the UGT1A-CFP/YFP combinations produced a FRET signal. No FRET was identified in select regions of the cell, as indicated by the black and dark blue regions, particularly the nucleus.

To examine the potential of UGT1A1 to dimerize with the other UGT1A proteins, co-transfection of COS cells with pUGT1A1-CFP and either pUGT1A3-YFP, pUGT1A4-YFP, pUGT1A6-YFP, pUGT1A7-YFP, pUGT1A8-YFP, pUGT1A9-YFP or pUGT1A10-YFP was performed and evaluated for FRET. In **Figure 3-4**, it is shown that Acceptor Ratio evaluation for each $UGT1A1^{CFP}/UGT1A^{YFP}$ pair resulted in a high FRET signal ranging from 40 % (green) to 100 % (white) FRET efficiency among the cells. This evidence suggests that UGT1A1 is able to heterodimerize with either UGT1A3, UGT1A4, UGT1A6, UGT1A7, UGT1A8, UGT1A9 or UGT1A10. Combined, these results suggest that each of the UGT1A proteins is capable of forming homodimers and heterodimers in the ER.

FIGURE 3-3

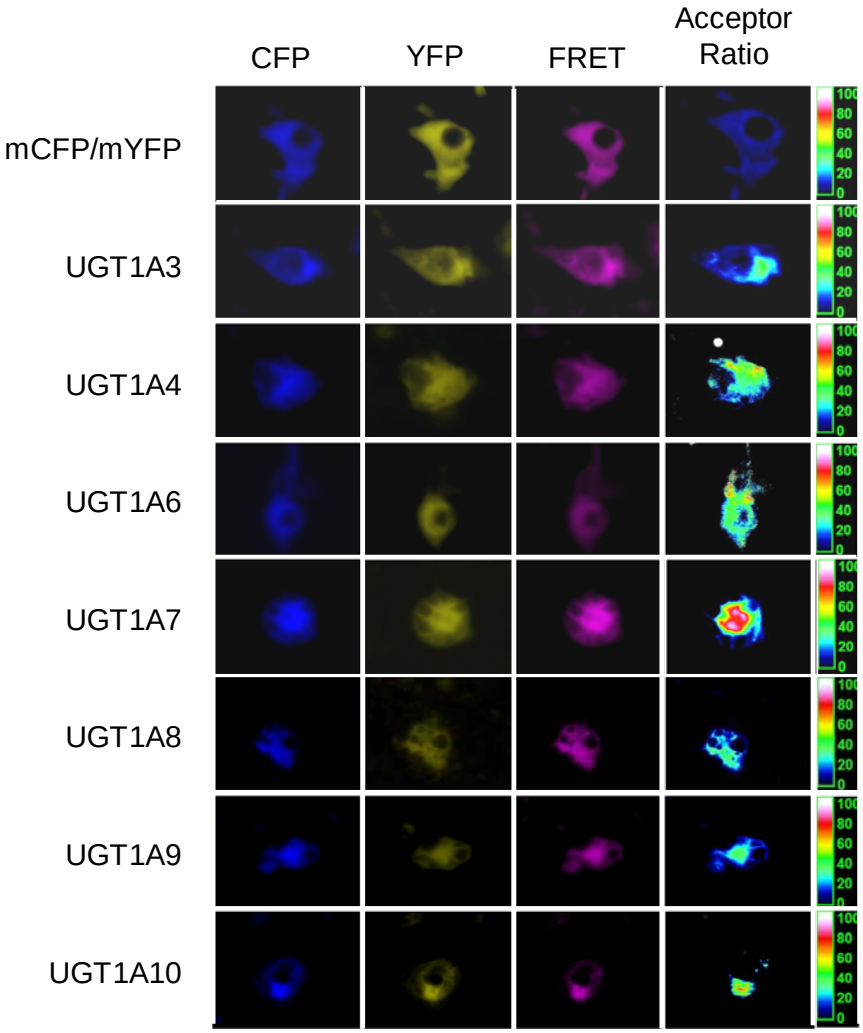


FIGURE 3-3. Homodimerization analysis of UGT1A proteins by FRET analysis. COS cells were co-transfected with 5 µg of pUGT1A-CFP and 5 µg of the corresponding pUGT1A-YFP plasmid for 24 h. Co-expression of both $UGT1A^{CFP}$ and $UGT1A^{YFP}$ is indicated by fluorescence in both the CFP channel and YFP channel. Correction for donor and acceptor bleed through was performed and FRET signal was analyzed. FRET efficiency was evaluated with the Carl Zeiss AxioVision FRET software using the Acceptor Ratio analysis and depicted as a color-coded scale ranging from 0-100 % FRET efficiency.

FIGURE 3-4

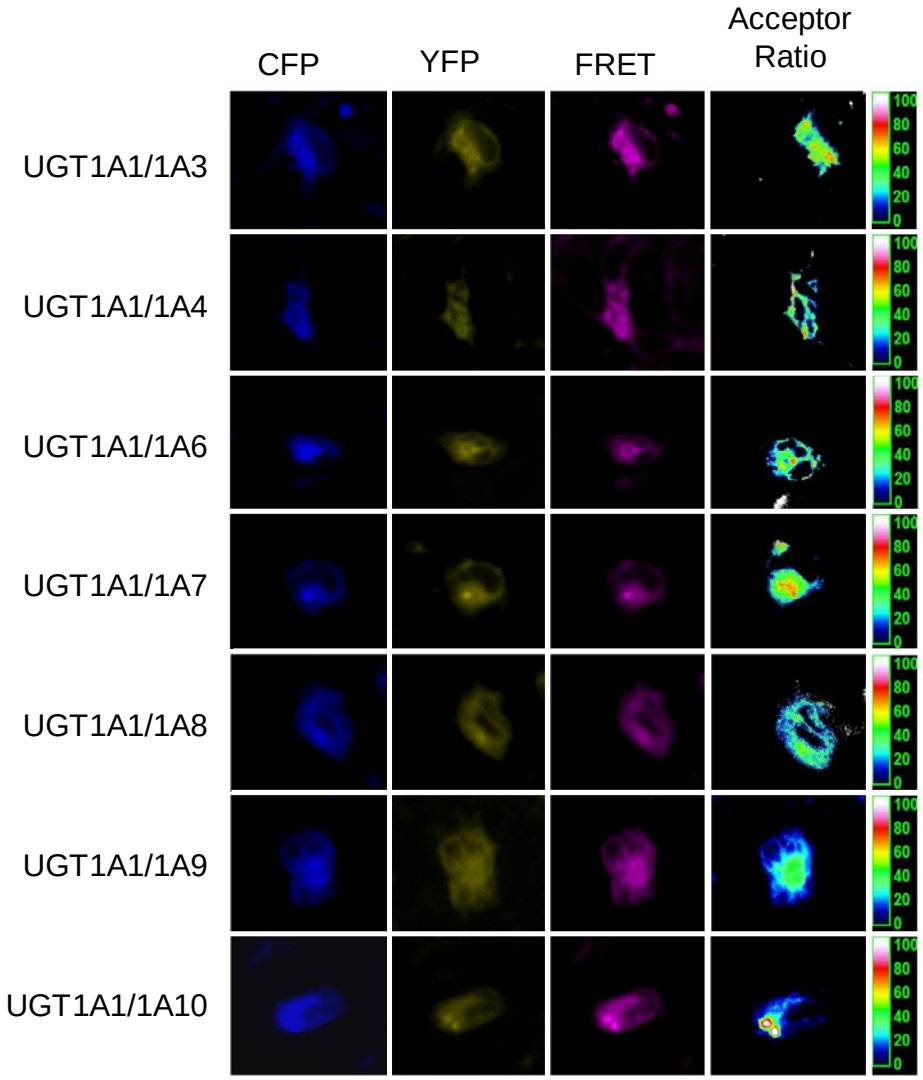


FIGURE 3-4. Heterodimerization analysis of UGT1A1 with other UGT1A proteins by FRET analysis. COS cells were co-transfected with 5 µg of pUGT1A1-CFP and 5 µg of the corresponding pUGT1A-YFP plasmid for 24 h. Co-expression of both $UGT1A1^{CFP}$ and $UGT1A^{YFP}$ is indicated by fluorescence in both the CFP channel and YFP channel. Correction for donor and acceptor bleed through was performed and FRET signal was analyzed. FRET efficiency was evaluated with the Carl Zeiss AxioVision FRET software using the Acceptor Ratio analysis and depicted as a color-coded scale ranging from 0-100 % FRET efficiency.

Co-immunoprecipitation Confirms the Existence of Homo- and Heterodimerization of the UGT1A Proteins. In addition to the in vivo analysis of protein-protein interactions using FRET, co-immunoprecipitation experiments were conducted to examine the potential of the UGT1A proteins to form heterodimer complexes. To carry out these experiments, we first constructed expression plasmids of each of the UGT1A cDNAs fused with a hemagglutinin (HA) sequence. The HA-tagged expressed proteins can be recognized with mono-specific HA antibodies, and when these plasmids are expressed in COS cells their expressed $UGT1A^{HA}$ fusion products can be immunoprecipitated with anti-HA beads. The addition of the HA sequence tag (11 amino acids) at the carboxyl-end of each of the UGT1A proteins does not add significantly to the molecular mass of the protein, and they can be resolved on SDS-polyacrylamide gels as approximately 56 kD proteins. We rationalized that if the $UGT1A^{HA}$ proteins could be expressed in conjunction with $UGT1A^{CFP}$ proteins, dimerization of the proteins following immunoprecipitation could be identified by the resolution of the 86 kDa $UGT1A^{CFP}$ proteins and the 56 kDa $UGT1A^{HA}$ proteins.

To confirm homodimerization of UGT1A1, both pUGT1A1-HA and pUGT1A1-CFP were expressed individually (**Figure 3-5**, lanes 1 & 2) or co-expressed (**Figure 3- 5**, lane 3) and whole cell lysates immunoprecipitated with the anti-HA beads. Lane 1 illustrates that $UGT1A1^{HA}$ was immunoprecipitated with the anti-HA beads, while $UGT1A1^{CFP}$ was not immunoprecipitated (lane 2), demonstrating the specificity of the anti-HA beads for the HA-tagged protein. In lane 3, COS cells were co-transfected with pUGT1A1-HA and pUGT1A1-CFP followed by immunoprecipitation with anti-HA beads. Western blot analysis with the anti-UGT1A antibody illustrated the presence of

two bands, one at ~ 56 kDa ($UGT1A1^{HA}$) and the other at ~ 86 kDa ($UGT1A1^{CFP}$), indicating that $UGT1A1^{CFP}$ was co-immunoprecipitated with the anti-HA beads only in the presence of expressed $UGT1A1^{HA}$ protein. In lane 4, individual transfections with pUGT1A1-HA and pUGT1A1-CFP constructs, followed by mixing the whole cell lysates prior to immunoprecipitation with anti-HA beads did not result in the co-immunoprecipitation of $UGT1A1^{CFP}$. This result suggests that protein-protein interactions leading to dimerization may require coordinated synthesis of the UGTs in the cell.

Homodimerization of all the UGT1A proteins and heterodimerization of the UGT1A proteins with UGT1A1 were also evaluated by the co-immunoprecipitation technique. When each of the pUGT1A-HA and UGT1A-CFP plasmids were transfected individually, expressed $UGT1A^{HA}$ proteins were identified from whole cell lysates following immunoprecipitation with anti-HA beads, while the anti-HA beads did not immunoprecipitate any of the expressed $UGT1A^{CFP}$ proteins (**Figure 3-6**). This result confirms that the anti-HA beads will identify only $UGT1A^{HA}$ expressed proteins.

FIGURE 3-5

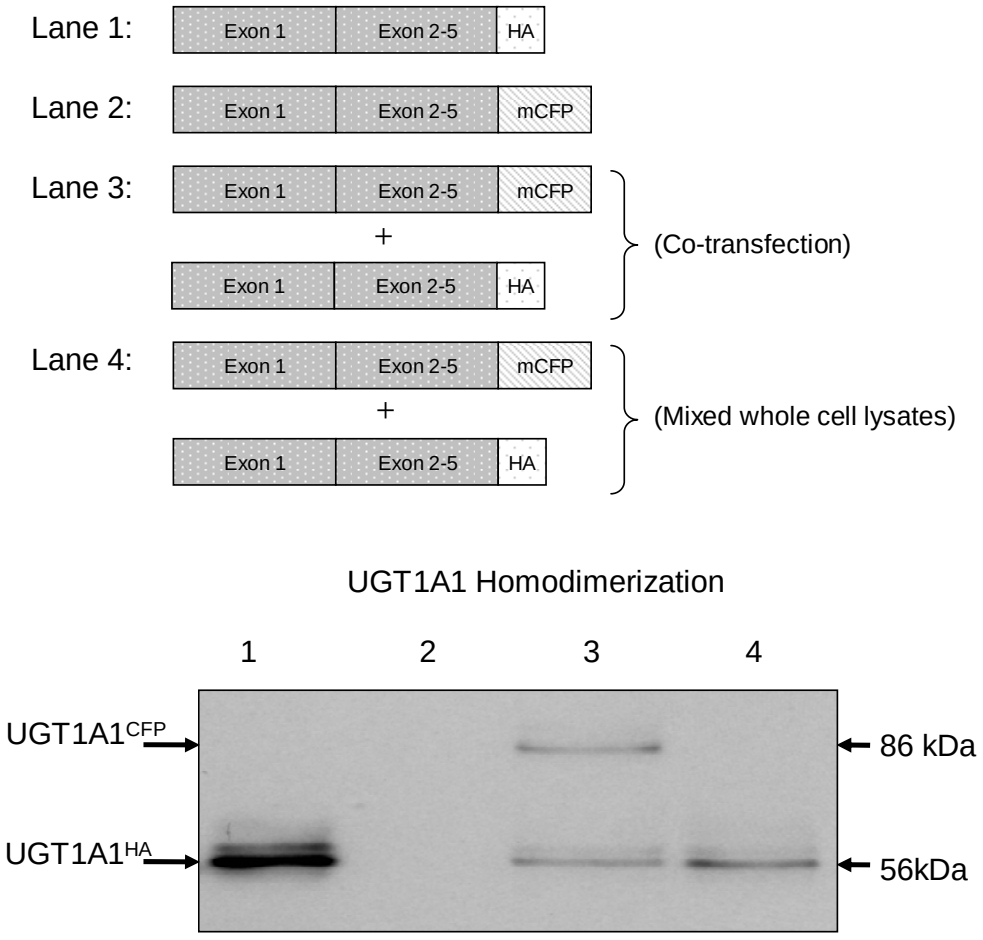


FIGURE 3-5. Co-immunoprecipitation analysis of UGT1A1 homodimerization. The line drawings indicate the plasmids used for each lane shown in the Western blot. For these experiments, COS cells were transfected with 5 µg of pUGT1A1-HA (Lane 1) or 5 µg of pUGT1A1-CFP (Lane 2). Lane 3 represents co-transfection with both pUGT1A1-CFP and pUGT1A1-HA. After 24 h following each transfection, the cells were lysed in 1 ml RIPA buffer supplemented with 1 % protease inhibitor cocktail and the expressed proteins immunoprecipitated with anti-HA beads overnight. In lane 4, solubilized lysates from COS cells transfected with 5 µg of pUGT1A1-HA and COS cells transfected 5 µg of pUGT1A1-CFP were mixed prior to immunoprecipitation. Detection of the expressed proteins was conducted by Western blot analysis using an anti-UGT1A antibody.

FIGURE 3-6

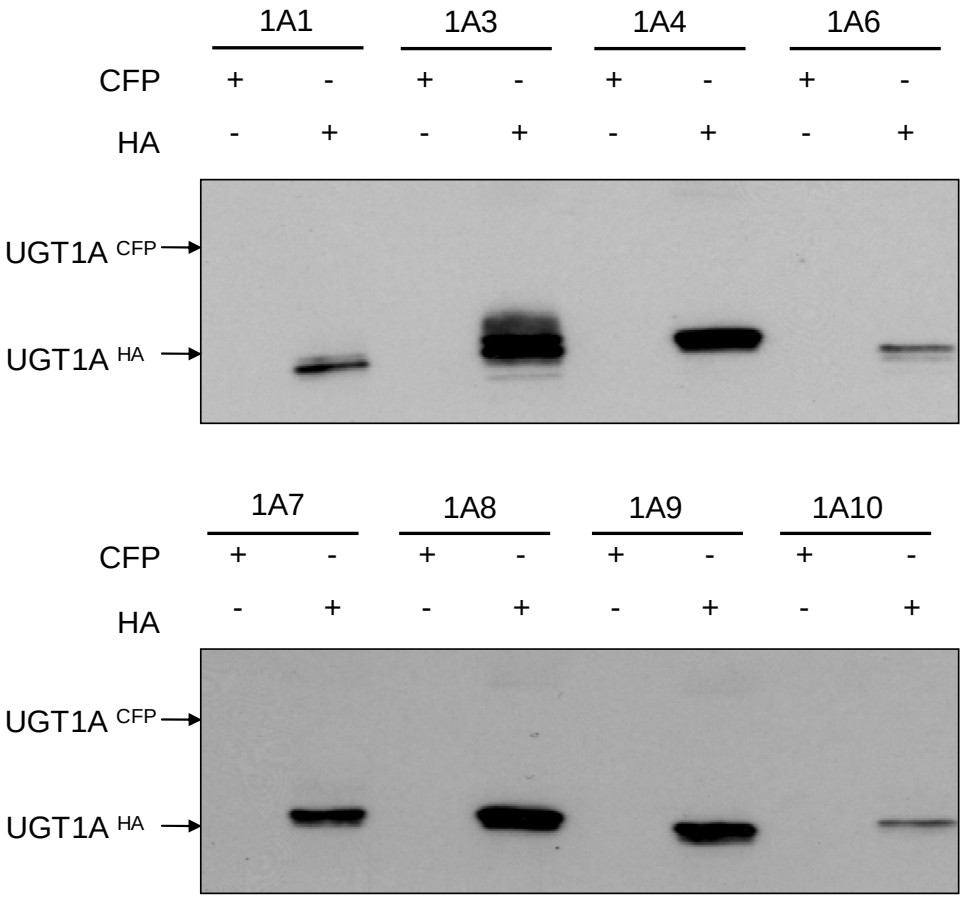


FIGURE 3-6. The anti-HA beads immunoprecipitate UGT1A^{HA} expressed proteins. To monitor the specificity of the proteins immunoprecipitated with the anti-HA beads, COS cells were transfected with either 5 µg of pUGT1A-HA or pUGT1A-CFP for 24 h. The cells were lysed in 1 ml RIPA buffer supplemented with 1 % protease inhibitor cocktail and immunoprecipitated with anti-HA beads overnight. Western blot analysis was performed using an anti-UGT1A antibody.

Homodimerization of the UGT1A proteins was tested by co-transfecting pUGT1A-CFP with the corresponding pUGT1A-HA constructs followed by co-immunoprecipitation with anti-HA beads. As shown in **Figure 3-7A**, Western blot analysis revealed two distinct bands indicating the presence of the individual $UGT1A^{HA}$ fusion proteins (lower band) as well as the $UGT1A^{CFP}$ fusion proteins (upper band). This data indicates that each of the UGT1A proteins is able to homodimerize. Heterodimerization analysis between UGT1A1 and each of the UGT1A proteins was evaluated by co-transfecting COS cells with pUGT1A1-HA and each pUGT1A-CFP plasmid, followed by co-immunoprecipitation with anti-HA beads (**Figure 3-7B**). Western blot analysis with the anti-UGT1A antibody revealed two distinct bands, the lower band representing $UGT1A1^{HA}$ and the upper band in each lane representing expression of each $UGT1A^{CFP}$ protein. This data confirms FRET analysis and leads us to conclude that UGT1A1 is able to heterodimerize with each of the UGT1A proteins.

FIGURE 3-7

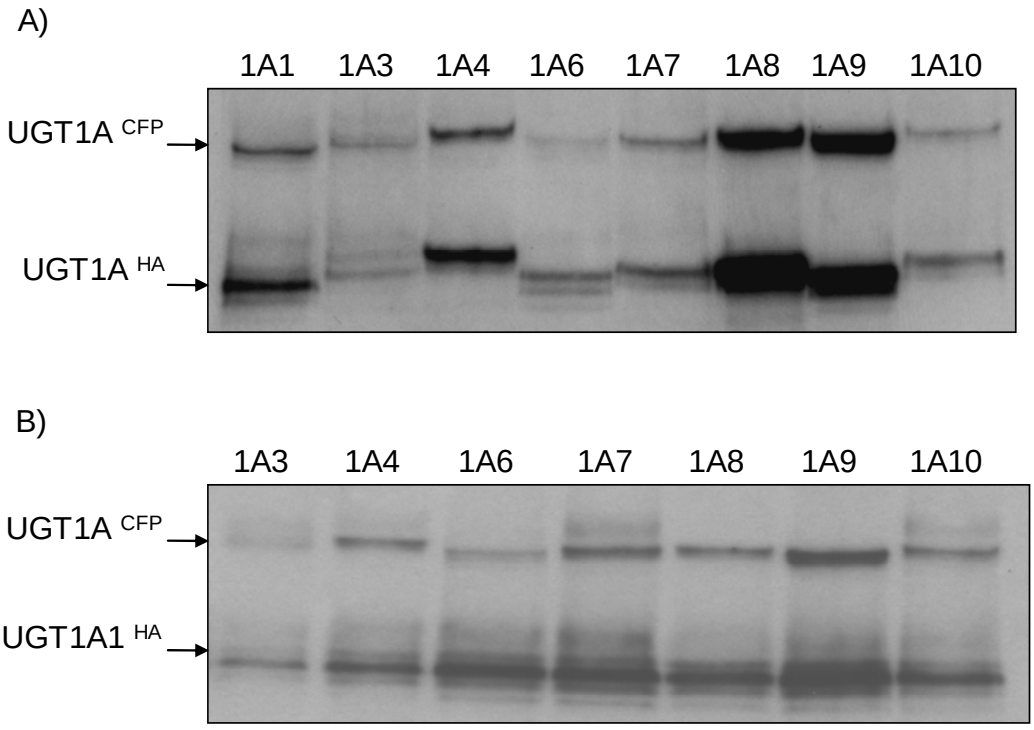


FIGURE 3-7. Oligomerization of UGT1A Proteins. A) COS cells were co-transfected with 5 µg of pUGT1A-HA and 5 µg of the corresponding pUGT1A-CFP. After 24 h, the cells were lysed in 1 ml RIPA buffer supplemented with 1 % protease inhibitor cocktail and immunoprecipitated with anti-HA beads overnight. Western blot analysis was performed using an anti-UGT1A antibody. **B)** COS cells were co-transfected with 5 µg of pUGT1A1-HA and 5 µg of either pUGT1A3-CFP, pUGT1A4-CFP, pUGT1A6-CFP, pUGT1A7-CFP, pUGT1A8-CFP, pUGT1A9-CFP or pUGT1A10-CFP. After 24 h, the cells were lysed in 1 ml RIPA buffer supplemented with 1 % protease inhibitor cocktail and immunoprecipitated with anti-HA beads overnight. Western blot analysis was performed using an anti-UGT1A antibody.

Functional Analysis of Oligomeric UGT Isoforms. Functional analysis of several chimeric UGT isoforms was performed to ensure that the large fluorescent tags at the C-terminus did not alter UGT activity. Three chimeras were chosen as representatives for functional analysis. Expressed UGT1A1^{CFP} and UGT1A3^{CFP} fusion proteins displayed similar levels of UGT activity for the substrate octylgallate as compared to the untagged UGT1A1 and UGT1A3 proteins, illustrated by similar intensities of bands representing the glucuronides in TLC analysis (**Figure 3-8A**). Expressed UGT1A7^{CFP} also had equal levels of UGT activity for the substrate 2-napthol as compared to untagged UGT1A7 protein (**Figure 3-8A**). This data indicates that the addition of the C-terminal tags did not affect the functionality of the UGTs.

The functional importance of UGT protein-protein interactions was also explored by co-transfecting two UGT isoforms and measuring the effect on specific activity. In **Figure 3-8B** the co-transfection of pUGT1A1 and pUGT1A7 yielded approximately equivalent protein concentrations of each UGT isoform as compared to the single transfections of pUGT1A1 and pUGT1A7. Specific activity for 2-napthol was measured and it was observed that UGT1A7 had 3-fold higher specific activity as compared to UGT1A1 (**Figure 3-8C**). Co-transfection of pUGT1A1/pUGT1A7 resulted in a slightly increased specific activity for 2-napthol as compared to UGT1A7, potentially indicating an additive effect of specific activities (**Figure 3-8C**).

FIGURE 3-8

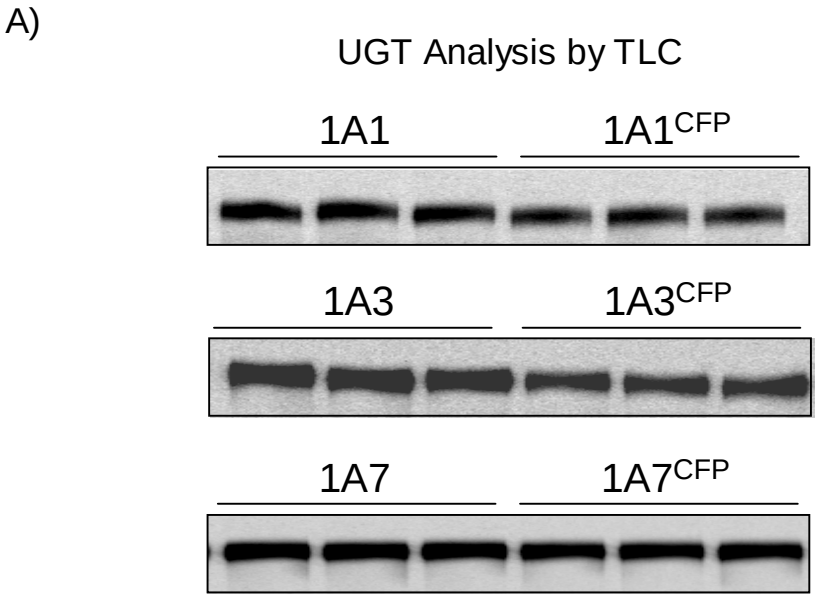


FIGURE 3-8. Functional analysis of chimeric and oligomeric UGT1A proteins. A) COS cells were transfected with 5 µg of untagged pUGT1A1, pUGT1A3, pUGT1A7 or 5 µg of pUGT1A1-CFP, pUGT1A3-CFP, pUGT1A7-CFP plasmids. Whole cell lysates were prepared and each catalytic assay was conducted in a 100 µl UGT reaction mix that contained 350 µg of cellular protein and a final concentration of 500 µM substrate (octylgallate for UGT1A1 and UGT1A3 isoforms, and 2-napthol for UGT1A7). 100 µl of the supernatant was spotted onto a TLC plate and chromatography was performed in a mixture (35:35:10:20 v/v) of n-butanol: acetone: acetic acid: water. The dried TLC plate was then exposed to a phosphor screen overnight.

FIGURE 3-8

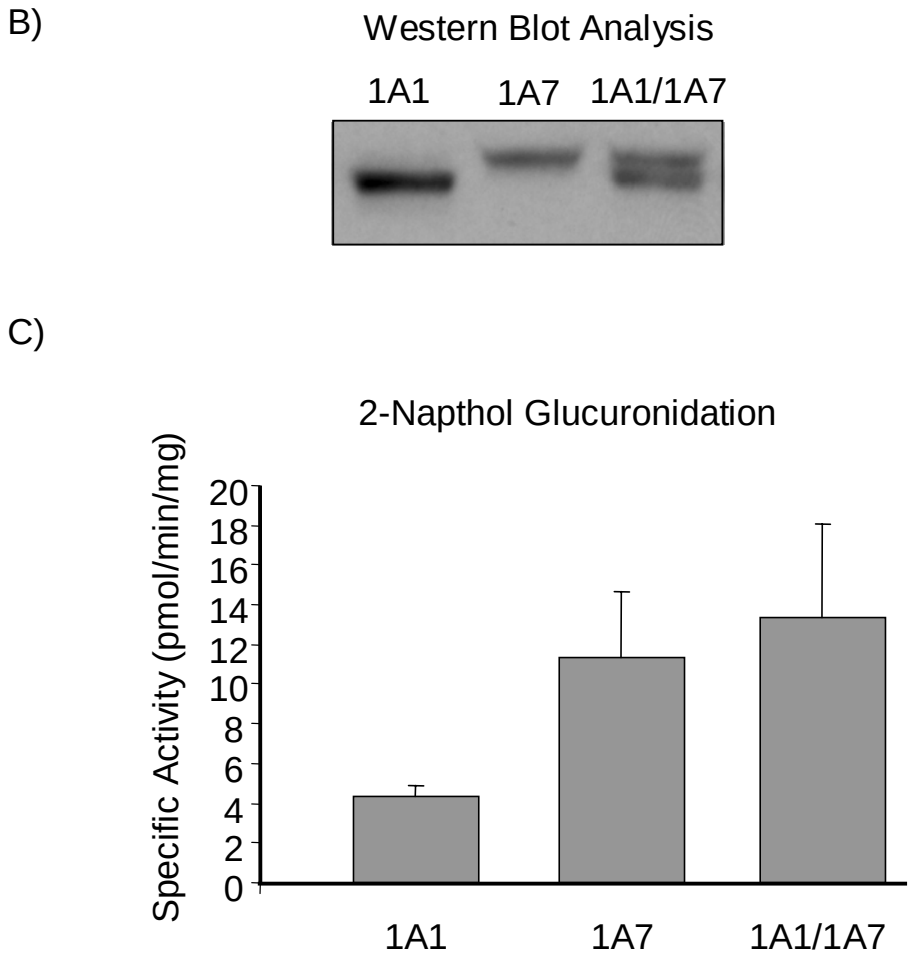


FIGURE 3-8. Functional analysis of chimeric and oligomeric UGT1A proteins. B) COS cells were transfected with either 2 µg pUGT1A1, 2 µg pUGT1A7, or co-transfected with 2 µg of each plasmid. Whole cell lysates were prepared and Western blot analysis was performed using an anti-UGT1A antibody. **C)** COS cells were transfected with either 2 µg pUGT1A1, 2 µg pUGT1A7, or co-transfected with 2 µg of each plasmid. UGT assays were performed with 500 µM 2-napthol as the substrate. The location of the glucuronides on the plate was identified and that region of the TLC plate was scraped and quantified.

DISCUSSION

In the present study, we have utilized FRET to determine quaternary structure and intermolecular interactions among UGT1A proteins in live cells. In addition, we have provided complimentary biochemical evidence for homo- and hetero-dimerization of these proteins by co-immunoprecipitation analysis. In this study, we have designed a collection of plasmids that express fluorescently tagged UGT1A proteins, allowing us to explore the intermolecular interactions among the UGT1A proteins in vivo. This technique is highly sensitive and allows for the detection of molecular interactions occurring within 1-10 nm distance and does not require the proteins to be cross-linked to detect this interaction.

Analysis of FRET between membrane-bound associated UGTs illustrate that expressed UGT1A1^{CFP} was able to homodimerize with UGT1A1^{YFP}. Association of UGT1A1 as a homodimer supports previous findings where nearest neighbor cross-linking studies followed by gel filtration have suggested the close proximity of the UGT1A1 proteins within the ER (Ghosh et al., 2001). Homodimerization analysis of other UGT1A isoforms by FRET also revealed that UGT1A3, UGT1A4, UGT1A6, UGT1A7, UGT1A8, UGT1A9, and UGT1A10 all have the capacity to homodimerize. Homodimerization of UGT1A9 by FRET supports previously published biochemical data that UGT1A9 forms a stable homodimer (Kurkela et al., 2003). The evaluation of UGT1A1 protein-protein interactions with other UGT1A proteins by FRET analysis also revealed the promiscuous nature of UGT1A1 to heterodimerize with UGT1A3, UGT1A4, UGT1A6, UGT1A7, UGT1A8, UGT1A9, and UGT1A10. Although it has been suggested from two-hybrid mammalian studies that UGT1A1 and UGT1A6 are unable to

oligomerize (Ghosh et al., 2001), both FRET analysis in conjunction with co-immunoprecipitation data indicate that these two proteins are able to oligomerize in vivo. Two-hybrid systems require the bait and prey constructs to translocate to the nucleus and initiate transcriptional activation of the reporter genes. It is possible that the membrane-bound localization of the UGT proteins within the ER may have prevented translocation of the UGT bait and prey constructs from entering the nucleus. Our studies support other findings where interactions between UGT1A and UGT2B1 proteins have been suggested by co-immunoprecipitation experiments (Ikushiro et al., 1997) and heterodimerization between UGT1A4 and UGT1A9 have also been observed (Kurkela et al., 2004).

In addition to the in vivo FRET technique, the homodimerization and heterodimerization of the UGT1A proteins were also evaluated by co-immunoprecipitation analysis. For this experiment each UGT1A protein was fused with a hemagglutinin (HA) epitope at the C-terminus. These co-immunoprecipitation experiments, conducted with anti-HA beads, provided an alternative and complimentary technique to the in vivo FRET analysis. The co-immunoprecipitation data indicated homodimerization of UGT1A proteins with their respective isoform, clearly illustrated by the presence of $UGT1A^{HA}$ (~ 56 kDa) and $UGT1A^{CFP}$ (~ 86 kDa) proteins. This technique also confirmed the FRET results that UGT1A1 heterodimerized with all of the UGT1A plasmids. The generation of the library of UGT1A plasmids containing the CFP/YFP/HA epitopes provides a useful molecular tool to evaluate any combination of UGT interactions.

The functional implications of homo- or hetero-oligomerization of UGT1A proteins is of interest since several studies have suggested the importance of

oligomerization for function. UGT2B1 has been suggested to form oligomers, and the functional relevance of this oligomer interaction became apparent when two different inactive mutant forms of UGT2B1 were co-expressed in COS cells and activity was restored (Meech and Mackenzie, 1997). Another study suggests that dimerization may facilitate a dominant negative effect. Crigler-Najjar syndrome type II shows dominant-negative inheritance for bilirubin glucuronidation. When the mutated form of UGT1A1 found in Crigler-Najjar type II patients was co-expressed in COS cells with wild type UGT1A1, activity was found to be 6 % that of the wild type (Koiwai et al., 1996). This result suggests that the oligomerization of mutant UGT1A1 with wild type UGT1A1 leads to an inactive aggregate, while expression of the wild type UGT1A1 is completely functional. The effects of dimerization on function were explored in this study by co-expression of UGT1A1 with UGT1A7 in COS cells. The data indicated that there was no significant difference in specific activities between cells co-expressing UGT1A1/UGT1A7 as compared to cells expressing only UGT1A7, while cells expressing only UGT1A1 had a much lower specific activity for 2-napthol. The FRET data and co-immunoprecipitation data suggest that UGT1A1 and UGT1A7 are capable of forming heterodimers, and therefore one can speculate that potentially 50 % of the proteins in the co-expressing cells would be UGT1A1/UGT1A7 heterodimers, while only 25 % would be UGT1A7 homodimers. Since there was no significant difference in specific activities between cells expressing only UGT1A7 and cells co-expressing UGT1A1/1A7, this would suggest that the UGT1A1/UGT1A7 heterodimer has equal specific activity for 2-napthol as UGT1A7 homodimer. Although UGT1A1 was found to have a much lower specific activity for 2-napthol than UGT1A7, the presence of

UGT1A1 in the heterodimer complex did not seem to inhibit UGT1A7 activity. Unlike the oligomerization studies performed with UGT2B1 mutants (Meech and Mackenzie, 1997) and UGT1A1 mutants (Koiwai et al., 1996), the UGTs used in these experiments were wild type and fully functional, and revealed that the heterodimer complex had similar functional activity as the homodimer.

Recent findings have also implicated protein-protein interactions between drug metabolizing enzymes (Ishii et al., 2005). Phase I enzymes, such as cytochrome P450 (CYP), and phase II enzymes, such as the UGTs, play important roles in detoxification of endogenous and exogenous compounds. During drug metabolism it is not uncommon for a metabolite produced by a cytochrome P450 to be sequentially metabolized by other enzymes to further facilitate elimination. The efficiency of concerted metabolism of compounds may be enhanced if enzymes physically interacted with one another (Srivastava and Bernhard, 1987), implicating the significance of observed interactions between phase I and phase II proteins. CYP1A1 has been found to associate with microsomal epoxide hydrolase, UGTs, and NADPH cytochrome P450-reductase (Taura et al., 2000). Immunoprecipitation of CYP3A4 from human liver microsomes resulted in co-immunoprecipitation of UGT2B7, UGT1A1, and UGT1A6 (Fremont et al., 2005). The functional relevance of CYP-UGT interaction was tested by co-expressing CYP3A4 and UGT2B7 in COS cells and it was found that UGT2B7-catalyzed glucuronidation of morphine was altered by the presence of CYP3A4 (Takeda et al., 2006). Studies have also indicated that baculovirus expressed cytochrome P450 catalytic activity may be altered by the co-expression of different cytochrome P450s (Cawley et al., 1995; Yamazaki et al., 1997; Tan et al., 1997; Backes et al., 1998). In summary, these studies

indicate protein-protein interactions between drug metabolizing enzymes in the ER, and suggest the importance of such cooperative interactions in potentially modulating function.

Evidence provided in this work, as well as in the current literature, supports the hypothesis that UGTs form homo/hetero dimer complexes. Under the stringent conditions of the whole cell lysis buffer, which contained 1% NP 40 and 0.25% deoxycholic acid as solubilizing agents, it might be anticipated that the protein-protein interactions are highly specific. Since all of the UGT1A proteins were found to homodimerize with their respective isoforms and heterodimerize with UGT1A1, we hypothesize that the dimerization domain may exist in the conserved carboxyl region (exons 2-5). Although it has been suggested that the amino terminus of UGT2B1 mediates dimerization (Meech and Mackenzie, 1997). The simultaneous insertion of the UGTs into the membrane also appears to be a requirement for oligomerization since dimerization was not observed when $UGT1A1^{HA}$ and $UGT1A1^{CFP}$ whole cell lysates were mixed and immunoprecipitated with anti-HA beads, which supports a previous observation by Kurkela *et al* (Kurkela et al., 2003). This study provides evidence for biochemical and in vivo data for UGT1A protein-protein interactions, but it is unclear whether the protein-protein interactions observed are important for function. Further studies are required to isolate the region(s) responsible for the protein interactions. Therefore, the focus of our future work will be to determine the structural domains involved in facilitating oligomerization of the UGT1A proteins, and investigate the functional importance of the protein interactions among the UGTs.

Chapter 3, in full, is a reprint of the material as it appears in Operaña TN, and Tukey RH. "Oligomerization of the UDP-glucuronosyltransferase 1A proteins: homo- and heterodimerization analysis by fluorescence resonance energy transfer and co-immunoprecipitation" *Journal of Biological Chemistry* (2007) Feb 16;282(7):4821-9. I was the primary investigator and author of this article.

ACKNOWLEDGEMENTS

This work was supported in part by United States Public Health Service Grant GM49135.

	pUGT1A-HA Plasmids	***pUGT1A-CFP Plasmids***	***pUGT1A-YFP Plasmids***
1	pUGT1A1-HA	pUGT1A1-CFP	pUGT1A1-YFP
2	pUGT1A3-HA	pUGT1A3-CFP	pUGT1A3-YFP
3	pUGT1A4-HA	pUGT1A4-CFP	pUGT1A4-YFP
4	pUGT1A6-HA	pUGT1A6-CFP	pUGT1A6-YFP
5	pUGT1A7-HA	pUGT1A7-CFP	pUGT1A7-YFP
6	pUGT1A8-HA	pUGT1A8-CFP	pUGT1A8-YFP
7	pUGT1A9-HA	pUGT1A9-CFP	pUGT1A9-YFP
8	pUGT1A10-HA	pUGT1A10-CFP	pUGT1A10-YFP

Table 3-1. Plasmid constructs used in FRET analysis and co-immunoprecipitation studies.

REFERENCES

Backes,W.L., Batie,C.J., and Cawley,G.F. (1998). Interactions among P450 enzymes when combined in reconstituted systems: formation of a 2B4-1A2 complex with a high affinity for NADPH-cytochrome P450 reductase. Biochemistry. *37*, 12852-12859.

Beaulieu,M., Levesque,E., Tchernof,A., Beatty,B.G., Belanger,A., and Hum,D.W. (1997). Chromosomal localization, structure, and regulation of the *UGT2B17* gene, encoding a C19 steroid metabolizing enzyme. DNA Cell Biol *16*, 1143-1154.

Bosma,P.J., Seppen,J., Goldhoorn,B., Bakker,C., Oude,E.R., Chowdhury,J.R., Chowdhury,N.R., and Jansen,P.L. (1994). Bilirubin UDP-glucuronosyltransferase 1 is the only relevant bilirubin glucuronidating isoform in man. J. Biol. Chem. *269*, 17960-17964.

Cawley,G.F., Batie,C.J., and Backes,W.L. (1995). Substrate-dependent competition of different P450 isozymes for limiting NADPH-cytochrome P450 reductase. Biochemistry. *34*, 1244-1247.

Chen,F., Ritter,J.K., Wang,M.G., McBride,O.W., Lubet,R.A., and Owens,I.S. (1993). Characterization of a cloned human dihydrotestosterone/androstanediol UDP-glucuronosyltransferase and its comparison to other steroid isoforms. Biochemistry *32*, 10648-10657.

Chouinard,S., Tessier,M., Vernouillet,G., Gauthier,S., Labrie,F., Barbier,O., and Belanger,A. (2006). Inactivation of the Pure Antiestrogen Fulvestrant and Other Synthetic Estrogen Molecules by UDP-Glucuronosyltransferase 1A Enzymes Expressed in Breast Tissue. Mol. Pharmacol. *69*, 908-920.

Clegg,R.M. (1996). Fluorescence resonance energy transfer (FRET). In Fluorescence Imaging Spectroscopy and Microscopy, X.F.Wang and B.Herman, eds. (New York: Wiley, John & Sons, Inc.), pp. 179-251.

Dutton,G.J. (1980). Glucuronidation of drugs and other compounds., G.J.Dutton, ed. (Boca Raton: CRC Press, Inc.), pp. 1-268.

Fremont,J.J., Wang,R.W., and King,C.D. (2005). Coimmunoprecipitation of UDP-glucuronosyltransferase isoforms and cytochrome P450 3A4. Mol. Pharmacol. *67*, 260-262.

Ghosh,S.S., Sappal,B.S., Kalpana,G.V., Lee,S.W., Chowdhury,J.R., and Chowdhury,N.R. (2001). Homodimerization of human bilirubin-uridine-diphosphoglucuronate glucuronosyltransferase-1 (UGT1A1) and its functional implications. J. Biol. Chem. *276*, 42108-42115.

Harding,D., Jeremiah,S.J., Povey,S., and Burchell,B. (1990). Chromosomal mapping of a human phenol UDP-glucuronosyltransferase, *GNT1*. Ann. Hum. Genet. *54*, 17-21.

Heydel,J., LeClerc,S., Bernard,P., Pelczar,H., Gradinaru,D., Magdalou,J., Minn,A., Artur,Y., and Goudonnet,H. (2001). Rat olfactory bulb and epithelium UDP-glucuronosyltransferase 2A1 (UGT2A1) expression: in situ mRNA localization and quantitative analysis. Brain Res. Mol. Brain Res. *90*, 83-92.

Hum,D.W., Belanger,A., Levesque,E., Barbier,O., Beaulieu,M., Albert,C., Vallee,M., Guillemette,C., Tchernof,A., Turgeon,D., and Dubois,S. (1999). Characterization of UDP-glucuronosyltransferases active on steroid hormones. J Steroid Biochem Mol Biol *69*, 413-423.

Ikushiro,S., Emi,Y., and Iyanagi,T. (1997). Protein-protein interactions between UDP-glucuronosyltransferase isozymes in rat hepatic microsomes. Biochemistry. *36*, 7154-7161.

Ishii,Y., Takeda,S., Yamada,H., and Oguri,K. (2005). Functional protein-protein interaction of drug metabolizing enzymes. Front Biosci. *10*, 887-895.

Koiwai,O., Aono,S., Adachi,Y., Kamisako,T., Yasui,Y., Nishizawa,M., and Sato,H. (1996). Crigler-Najjar syndrome type II is inherited both as a dominant and as a recessive trait. Hum. Mol. Genet. *5*, 645-647.

Kurkela,M., Garcia-Horsman,J.A., Luukkanen,L., Morsky,S., Taskinen,J., Baumann,M., Kostiainen,R., Hirvonen,J., and Finel,M. (2003). Expression and characterization of recombinant human UDP-glucuronosyltransferases (UGTs). UGT1A9 is more resistant to detergent inhibition than other UGTs and was purified as an active dimeric enzyme. J. Biol. Chem. *278*, 3536-3544.

Kurkela,M., Hirvonen,J., Kostiainen,R., and Finel,M. (2004). The interactions between the N-terminal and C-terminal domains of the human UDP-glucuronosyltransferases are partly isoform-specific, and may involve both monomers. Biochem. Pharmacol. *68*, 2443-2450.

Lakowicz,J.R. (1983). In Principles of Fluorescence Spectroscopy, (New York: Plenum Press).

Latif,R., Graves,P., and Davies,T.F. (2002). Ligand-dependent inhibition of oligomerization at the human thyrotropin receptor. J. Biol. Chem. *277*, 45059-45067.

Li,Q., Lou,X., Peyronneau,M.-A., Straub,P.O., and Tukey,R.H. (1997). Expression and functional domains of rabbit liver UDP-glucuronosyltranferase 2B16 and 2B13. J. Biol. Chem. *272*, 3272-3279.

Mackenzie,P.I. (1990). Expression of chimeric cDNAs in cell culture defines a region of UDP glucuronosyltransferase involved in substrate selection. J. Biol. Chem. *265*, 3432-3435.

Mackenzie,P.I., Owens,I.S., Burchell,B., Bock,K.W., Bairoch,A., Belanger,A., Fournel-Gigleux,S., Green,M., Hum,D.W., Iyanagi,T., Lancet,D., Louisot,P., Magdalou,J., Chowdhury,Jr., Ritter,J.K., Schachter,H., Tephly,T.R., Tipton,K.F., and Nebert,D.W. (1997). The UDP glycosyltransferase gene superfamily: recommended nomenclature update based on evolutionary divergence. Pharmacogenetics *7*, 255-69.

Meech,R. and Mackenzie,P.I. (1997). UDP-glucuronosyltransferase, the role of the amino terminus in dimerization. J. Biol. Chem. *272*, 26913-26917.

Miyawaki,A. and Tsien,R.Y. (2000). Monitoring protein conformations and interactions by fluorescence resonance energy transfer between mutants of green fluorescent protein. Methods Enzymol. *327*, 472-500.

Monaghan,G., Burchell,B., and Boxer,M. (1997). Structure of the human *UGT2B4* gene encoding a bile acid UDP-glucuronosyltransferase. Mammalian Genome *9*, 692-694.

Monaghan,G., Clarke,D.J., Povey,S., See,C.G., Boxer,M., and Burchell,B. (1994). Isolation of a human YAC contig encompassing a cluster of *UGT2* genes and its regional localization to chromosome 4q13. Genomics *23*, 496-499.

Overton,M.C. and Blumer,K.J. (2000). G-protein-coupled receptors function as oligomers in vivo. Curr. Biol. *10*, 341-344.

Ritter,J.K., Chen,F., Sheen,Y.Y., Tran,H.M., Kimura,S., Yeatman,M.T., and Owens,I.S. (1992). A novel complex locus *UGT1* encodes human bilirubin, phenol, and other UDP-glucuronosyltransferase isozymes with identical carboxyl termini. J. Biol. Chem. *267*, 3257-3261.

Schmid,J.A., Just,H., and Sitte,H.H. (2001). Impact of oligomerization on the function of the human serotonin transporter. Biochem. Soc. Trans. *29*, 732-736.

Scholze,P., Freissmuth,M., and Sitte,H.H. (2002). Mutations within an intramembrane leucine heptad repeat disrupt oligomer formation of the rat GABA transporter 1. J. Biol. Chem. *277*, 43682-43690.

Siegel,R.M., Chan,F.K., Zacharias,D.A., Swofford,R., Holmes,K.L., Tsien,R.Y., and Lenardo,M.J. (2000). Measurement of molecular interactions in living cells by fluorescence resonance energy transfer between variants of the green fluorescent protein. Sci. STKE. *2000*, L1.

Srivastava,D.K. and Bernhard,S.A. (1987). Mechanism of transfer of reduced nicotinamide adenine dinucleotide among dehydrogenases. Transfer rates and equilibria with enzyme-enzyme complexes. Biochemistry. *26*, 1240-1246.

Szczesna-Skorupa,E., Mallah,B., and Kemper,B. (2003). Fluorescence resonance energy transfer analysis of cytochromes P450 2C2 and 2E1 molecular interactions in living cells. J. Biol. Chem. *278*, 31269-31276.

Takeda,S., Kitajima,Y., Ishii,Y., Nishimura,Y., Mackenzie,P.I., Oguri,K., and Yamada,H. (2006). Inhibition of UDP-glucuronosyltransferase 2b7-catalyzed morphine glucuronidation by ketoconazole: dual mechanisms involving a novel noncompetitive mode. Drug Metab Dispos. *34*, 1277-1282.

Tan,Y., Patten,C.J., Smith,T., and Yang,C.S. (1997). Competitive interactions between cytochromes P450 2A6 and 2E1 for NADPH-cytochrome P450 oxidoreductase in the microsomal membranes produced by a baculovirus expression system. Arch. Biochem. Biophys. *342*, 82-91.

Taura,K.I., Yamada,H., Hagino,Y., Ishii,Y., Mori,M.A., and Oguri,K. (2000). Interaction between cytochrome P450 and other drug-metabolizing enzymes: evidence for an association of CYP1A1 with microsomal epoxide hydrolase and UDP-glucuronosyltransferase. Biochem. Biophys. Res. Commun. *273*, 1048-1052.

Thibaudeau,J., Lepine,J., Tojcic,J., Duguay,Y., Pelletier,G., Plante,M., Brisson,J., Tetu,B., Jacob,S., Perusse,L., Belanger,A., and Guillemette,C. (2006). Characterization of common UGT1A8, UGT1A9, and UGT2B7 variants with different capacities to inactivate mutagenic 4-hydroxylated metabolites of estradiol and estrone. Cancer Res. *66*, 125-133.

Tsien,R.Y. (1998). The green fluorescent protein. Annu. Rev. Biochem. *67*, 509-544.

Tukey,R.H. and Strassburg,C.P. (2001). Genetic multiplicity of the human UDP-glucuronosyltransferases and regulation in the gastrointestinal tract. Molecular Pharmacology *59*, 405-414.

van Kuppeveld,F.J., Melchers,W.J., Willems,P.H., and Gadella,T.W., Jr. (2002). Homomultimerization of the coxsackievirus 2B protein in living cells visualized by fluorescence resonance energy transfer microscopy. J. Virol. *76*, 9446-9456.

Wooster,R., Sutherland,L., Ebner,T., Clarke,D., Da Cruz e Silva,O., and Burchell,B. (1991). Cloning and stable expression of a new member of the human liver phenol/bilirubin: UDP-glucuronosyltransferase cDNA family. Biochem. J. *278*, 465-469.

Yamazaki,H., Gillam,E.M., Dong,M.S., Johnson,W.W., Guengerich,F.P., and Shimada,T. (1997). Reconstitution of recombinant cytochrome P450 2C10(2C9) and comparison with cytochrome P450 3A4 and other forms: effects of cytochrome P450-P450 and cytochrome P450-b5 interactions. Arch. Biochem. Biophys. *342*, 329-337.

Youvan,D.C., Silva,C.M., Bylina,J., Coleman,W.J., Dilworth,M.R., and Yang,M.M. (1997). Calibration of fluorescence resonance energy transfer in microscopy using genetically engineered GFP derivatives on nickel chelating beads. Biotechnology *3*, 1-18.

Zacharias,D.A., Violin,J.D., Newton,A.C., and Tsien,R.Y. (2002). Partitioning of lipid-modified monomeric GFPs into membrane microdomains of live cells. Science. *296*, 913-916.

CHAPTER 4

Dimerization Domains of UGTs

INTRODUCTION

UDP-glucuronosyltransferases (UGTs) are phase II conjugating enzymes that catalyze the transfer of glucuronic acid to a wide variety of lipophilic substrates such as steroids, bile acids, bilirubin, dietary constituents, and drugs (Dutton, 1980). The addition of the large polar sugar moiety to the lipophilic substrate increases its water solubility, thereby facilitating excretion into the urine and bile. UGTs are abundantly expressed in the liver, and it is widely accepted that the liver is the most important site of glucuronidation. Extrahepatic expression of UGTs is also found throughout the gastrointestinal tract, kidney, skin, and reproductive organs (Strassburg *et al.,*1997; Burchell and Coughtrie, 1989; Tukey and Strassburg, 2000).

Based on evolutionary divergence, the UGTs are classified into two families, UGT1A and UGT2 (Mackenzie 1997). The UGT2 subfamily primarily conjugates endogenous compounds such as bile acids (Monaghan 1997) , steroids (Hum 1999), and hormones (Thibaudeau 2006), while the UGT1A subfamily is mainly involved in xenobiotic metabolism of pharmaceutical drugs, environmental contaminants, and dietary compounds. The UGT1A family is composed of nine functional isoforms, UGT1A1 and UGT1A3-UGT1A10 (Mackenzie *et al.,* 1997; Ritter *et al.,* 1992) that is derived from a single gene locus (Harding *et al.,* 1990). Four exons located at the 3' end of *UGT1A* (exons 2-5) encode for the carboxyl domain of all of the UGT isoforms. Upstream to the four constant exons are a series of first exons which encode the N-terminal domains of UGT1A proteins. Through a process called exon sharing, the first exon sequence is combined with the common exons 2-5, resulting in *UGT1A* gene products that have a variable amino terminus and identical C-terminal domains (Wooster *et al.,* 1991; Ritter *et*

*al.,*1992). The C-terminal domain of all of the UGTs is highly homologous which suggests an evolutionarily conserved function of binding UDP-glucuronic acid (UDPGA). The N-terminal binding domain of the UGTs is highly divergent and is believed to account for substrate specificity. Substrate specificity varies among UGT isoforms with some having strict specificity, while others accept a wide range of structurally unrelated substrates. In addition, UGTs have considerable overlap of substrate specificity among different isoforms (Meech and Mackenzie, 1997a).

UGTs are membrane bound proteins localized to the endoplasmic reticulum (ER) (Vanstapel *et al.,* 1988; Shepherd *et al.,* 1989). The majority of the protein resides in the lumen of the ER with a single transmembrane spanning domain near the C-terminus (Iyanagi *et al.,* 1986) followed by a 20 amino acid carboxyl tail that contains the ER retention signal that protrudes into the cytosol (Meech and Mackenzie, 1997a). Recent inquiry into the quaternary structure of these proteins indicates that UGTs are capable of forming oligomers within the ER (Ikushiro *et al.,* 1997; Ghosh *et al.,* 2001; Kurkela *et al.,* 2003; Operaña and Tukey, 2007). Evidence from our lab has indicated that UGT1A proteins form homodimers, as well as heterodimers with UGT1A1 (Operaña and Tukey, 2007). The importance of UGT protein-protein interactions has been implicated in certain Japanese patients with Crigler-Najjar syndrome type II that showed dominant-negative inheritance for bilirubin glucuronidation. When the truncated mutant form of UGT1A1 in Crigler-Najjar type II patients was co-expressed in COS cells with wild type UGT1A1, activity was found to be 6% of the wild type (Koiwai *et al.,* 1996). This suggests that the mutant UGT1A1 may be exerting a dominant-negative effect. The data in the literature reveals that UGT1A proteins form dimers within the ER, however, the structural domains

involved in the protein-protein interactions are unknown. Therefore, the focus of these experiments will be to determine the structural domains involved in UGT1A1 oligomerization and to investigate the functional importance of protein interactions among the UGTs.

MATERIALS AND METHODS

Generation of UGT1A1-CFP and UGT1A1-HA plasmids. To make the chimeric UGT1A1-CFP, UGT1A1 was amplified by PCR with a sense primer (5'-ctcgagATGgctgtggagtcccag-3') containing an XhoI site (underlined) followed by an initiation ATG codon, and an antisense primer (5'-ggatcc**cca**atgggtcttggatttg-3') with a BamHI site (underlined) followed by a mutated stop codon shown in bold. After the cloning of the UGT1A1 PCR product into the pCR 2.1-TOPO vector, the insert was removed and purified by digestion with XhoI and BamHI and subcloned into the XhoI and BamHI sites in the mCFP-N1 and mYFP-N1 plasmids, creating the pUGT1A1-CFP plasmid. To generate the hemagglutinin (HA) recognition sequence fused to the UGT1A1 protein, a UGT1A1-HA fragment was generated by PCR with a sense primer (5'-ctcgagatggctgtggagtcccag-3') containing an XhoI site (underlined), and antisense primer (5'-ggatcctca**ggcataatctggcacatcataagggtattccat**ccaatgggtcttgggattt-3') containing a BamHI site (underlined) and the HA sequence in bold. The UGT1A1-HA PCR product was subcloned into the pCR 2.1-TOPO vector (Invitrogen) and digested with XhoI and BamHI restriction enzymes to remove the insert. The UGT1A1-HA fragment was subcloned into the XhoI and BamHI multiple cloning site of the pcDNA 3.1(-) expression vector to produce the pUGT1A1-HA plasmid.

Generation of C-terminal Truncations of ΔUGT1A1-CFP. Truncated forms of UGT1A1 were amplified by PCR with a sense primer (5'-ctcgagATGgctgtggagtcccag-3') containing an XhoI site (underlined) followed by an initiation ATG codon, and specific antisense primers containing a BamHI with an ER retention signal sequence KSKTH, followed by the homology region of the desired truncated portion.

Antisense Primers:

Δ Ex5: *BamHI* **KSKTH**, start homology at amino acid 436 (Tyr).

5'- 3'*ggatcc*gc**atgggtcttggattt**gtaacttttgtcattgat.

Δ Ex4: *BamHI* **KSKTH**, start homology at amino acid 360 (Leu).

5'- 3'*ggatcc*gc**atgggtcttggattt**cagatcgttttggggtag.

Δ Ex3: *BamHI* **KSKTH**, start homology at amino acid 330 (Pro).

5'- 3' *ggatcc*gc**atgggtcttggattt**agggattttgcccaaagc.

Δ 286: *BamHI* **KSKTH**, start homology at amino acid 285 (Proline).

5'- 3'*ggatcc*gc**atgggtcttggattt**tggattttggtgaaggca.

Δ 190: *BamHI* **KSKTH**, start homology at amino acid 190 (Phe).

5'- 3' *ggatcc*gc**atgggtcttggattt**gaatgggttggggcactg.

Δ 98: *BamHI* **KSKTH**, start homology at amino acid 100 (Phe).

5'- 3'*ggatcc*gc**atgggtcttggattt**aaaaacattatgcccgag.

Δ 80: *BamHI* **KSKTH**, start homology at amino acid 80 (Pro).

5'- 3'*ggatcc*gc**atgggtcttggattt**agggtacgtcttcaa.

Δ 52: *BamHI* **KSKTH**, start homology at amino acid 52 (Glu).

5'- 3'*ggatcc*gc**atgggtcttggattt**ctgctgcagctgctg.

Δ 41: *BamHI* **KSKTH**, start homology at amino acid 41 (Leu).

5'- 3'*ggatcc*gc**atgggtcttggattt**cagccagtggctgcc.

After the cloning of truncated ΔUGT1A1 PCR product into the pCR 2.1-TOPO vector, the insert was removed and purified by digestion with XhoI and BamHI and subcloned into the XhoI and BamHI sites in the mCFP-N1 plasmid to create C-terminal truncated CFP plasmids.

Co-Immunoprecipitation of expressed wildtype and truncated forms of UGT1A1. COS cells were plated at a density of 3.5 x 10^5 cells per well in 6-well plates and co-transfected with 2 μg of truncated forms of ΔUGT1A1-CFP and 2 μg of UGT1A1-HA plasmids using Lipofectamine 2000 (Invitrogen). After 24 h, the cells were washed twice with PBS and lysed for 1 h on ice with 1 ml 1X RIPA buffer (0.05 M Tris-HCl, pH 7.4, 0.15M NaCl, 0.25% Deoxycholic acid, 1% NP-40, 1 mM EDTA) supplemented with 1 % protease cocktail inhibitor (Sigma). The lysed cells were centrifuged for 10 min at 13,000 x g and the supernatant collected. The entire supernatant from one transfected well was mixed with 20 μl of anti-HA beads (Roche) and incubated at 4 °C on a rocker platform overnight. The anti-HA beads were centrifuged for 1 minute at 1000 x g and the supernatant discarded. The anti-HA beads were washed 3 times with 1 ml of cold lysis buffer. The anti-HA beads were then resuspended in 60 μl of electrophoresis sample buffer and heated to 95 °C for 10 min. The beads were

centrifuged for 1 min at 1,000 x g and the supernatant collected and used for Western blot analysis.

Western Blot Analysis. All Western blots were performed using 4-12 % NuPAGE Bis Tris polyacrylamide gels as outlined by the supplier (Invitrogen) and resolved under denaturing conditions (50 mM MOPS, 50 mM Tris-base, pH 7.7, 0.1 % SDS, 1mM EDTA). The resolved proteins were transferred onto nitrocellulose membrane using a semi-dry transfer system (Norvex). The membrane was blocked with 5 % nonfat dry milk in 10 mM Tris-HCl, pH 8, 0.15 M NaCl, and 0.05 % Tween 20 (Tris-buffered saline) for 1 h at room temperature. Each membrane was washed in Tris-buffered saline solution and incubated overnight at 4 °C with an anti-CFP antibody (Cell Signaling) at a dilution of 1:3000 in Tris-buffered saline containing 0.02 % sodium azide. Membranes were then washed five times with Tris-buffered saline solution and incubated for 1 h shaking at room temperature with horseradish peroxidase-conjugated rabbit secondary antibody at a 1:5000 dilution in Tris-buffered saline solution containing 2 % nonfat milk. Membranes were then washed five times with Tris-buffered saline solution and visualized using Western Lightning Chemiluminescence reagents according to the manufacturer's instructions (PerkinElmer Life Sciences) followed by exposure to X-ray film (Kodak).

UDP-Glucuronosyltransferase Activity Analysis. COS cells were plated at a density of 3.5 x 10^5 cells per well in 6-well plates and each transfected with either 2 μg of each plasmid (co-transfection) or 4 μg of one plasmid (single transfection) using

Lipofectamine 2000 (Invitrogen). Whole cell lysates were prepared by re-suspending cells in 50 mM Tris-HCl (pH 7.6), 10 mM $MgCl_2$ followed by homogenization and sonication. Each catalytic assay was conducted in a 100 µl reaction that contained 350 µg of cellular protein, 50 mM Tris-HCl (pH 7.6), 10 mM $MgCl_2$, 0.04 µCi ^{14}-C-UDPGA (255.6 pmol/reaction), 8.5 mM saccharolactone, 100 µg of phosphatidylcholine, 0.5 mM UDP-glucuronic acid, and a final concentration of 500 µM for each substrate. The substrate octylgallate was used to determine UGT activity for UGT1A1 and its truncated forms. Each reaction was incubated in a 37 °C water bath for 60 min, then terminated with the addition of 100 µl cold methanol. The protein was spun down by centrifugation at 13,000 g for 20 min, and 100 µl of the supernatant spotted onto a Whatman glass-backed thin layer chromatography (TLC) plate (Whatman, Hillsboro, Oregon). Chromatography was performed in a mixture (35:35:10:20 v/v) of n-butanol: acetone: acetic acid: water. Once the solvent front reached 2 cm from the top of the TLC plate, the plate was removed from the tank, dried, and exposed to a phosphor screen (Molecular Dynamics, Sunnyvale, CA) overnight. The location of the glucuronides on the plate was identified and that region of the TLC plate was scraped and placed in scintillation fluid for quantification with a liquid scintillation counter (Beckman Coulter LS6500, Fullerton, CA).

Generation of the UGT1A1 Homology Model. The model of UGT1A1 was generated using Modeller8v1 (http://salilab.org/modeller/) based on the structure of flavonoid glycosyltransferase in complex with the UDPGA analogue, uridine-5-diphosphate-2-deoxy-2-fluoro-alpha-D-glucuose (pdb-code-2C1Z). The UDPGA

analogue is displayed in sticks with carbon, oxygen, nitrogen, and fluor atoms colored yellow, red, blue, orange, and light blue, respectively.

RESULTS

Determination of UGT1A1 Dimerization Domains Using Truncated Proteins.

UGT enzymes have been intensely studied throughout the last several decades particularly for their important role in drug metabolism, but few studies have examined the structural properties of the UGTs. Recent experimental evidence has indicated that UGTs form oligomer complexes in the ER. However, the region involved in the protein-protein interactions is currently unknown. The UGTs can be conceptually divided into two parts, the amino and the carboxy terminal domains. **Figure 4-1A** is a schematic of UGT1A1 that illustrates the various structural domains of the protein. The amino terminal domain consists of the exon 1 region, which is highly variable among all of the UGT proteins and is responsible for the substrate specificity observed for each isoform. It also has an N-terminal targeting sequence that facilitates insertion into the lumen of the ER that is eventually cleaved off during processing of the mature protein. The carboxy terminal region is comprised of exons 2-5, which is identical for all of the UGT1A proteins and is the binding region for the co-substrate UDPGA. The C-terminus also has a single spanning transmembrane helix followed by a short di-lysine motif that serves as the ER retention signal. In order to determine the region important for UGT protein-protein interaction, a series of truncated forms of UGT1A1 were designed by PCR. **Figure 4-1B** is a schematic of all the UGT1A1 C-terminal truncations fused to a CFP tag that were generated in order to determine the domains important for UGT1A1 dimerization.

FIGURE 4-1

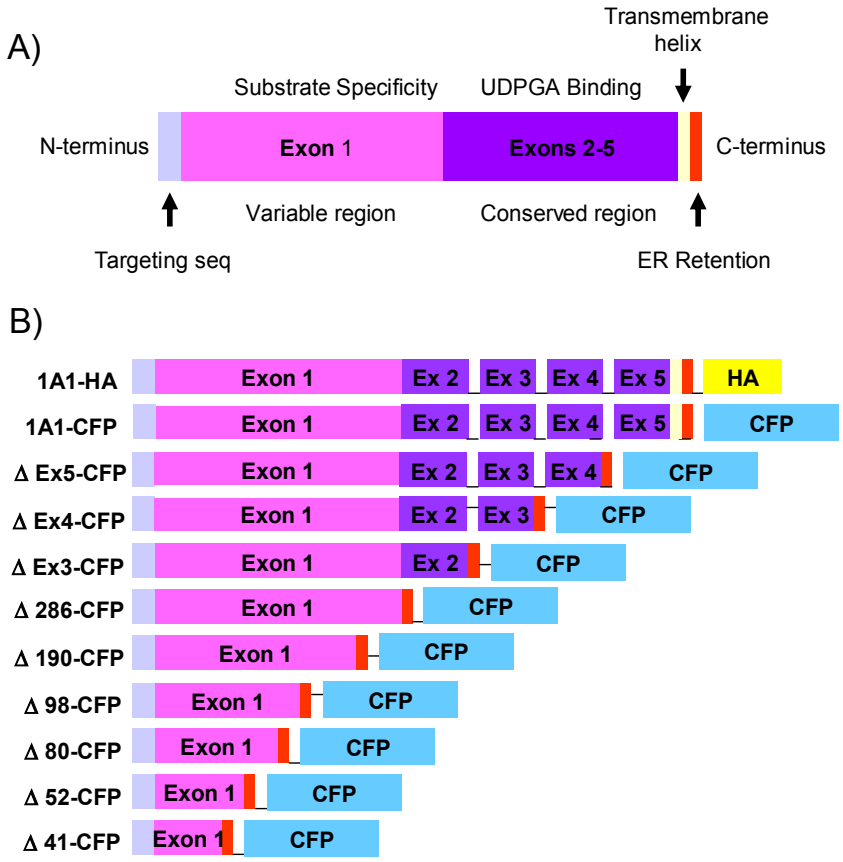


FIGURE 4-1. Schematic of UGT1A1 and the C-terminal UGT1A1 truncation constructs. A) Schematic of UGT1A1 which illustrates the various domains of the protein. It has an N-terminal targeting sequence that is cleaved off during processing of the mature protein. The exon 1 region is highly variable among all of the UGT proteins and is responsible for the substrate specificity observed for each isoform. Exons 2-5 which comprises the C-terminal domain of the protein is identical for all UGT1A proteins is the UDPGA binding region. The C-terminus also has a single spanning transmembrane helix followed by a short di-lysine motif which serves as the ER retention signal. **B)** Schematic of all the UGT1A1 C-terminal truncations fused to CFP that were generated in order to determine the domains important for UGT1A1 dimerization.

The CFP fusion tag was used as the epitope to monitor the presence of the chimeric protein since serial deletion of the UGT1A1 protein would result in loss of recognition of the truncated protein by the UGT antibody. Co-immunoprecipitation studies were performed by co-transfecting COS cells with the various truncated UGT1A1-CFP tagged constructs with the full length UGT1A1-HA plasmid to examine the potential dimer complex formation. The HA-tagged UGT1A1 fusion protein was immunoprecipitated using anti-HA beads and dimerization was examined by Western blot analysis using a GFP antibody that recognizes the CFP tag. The co-immunoprecipitation experiments in **Figure 4-2A** revealed that deletion of exon 5, exon 4, exon 3, and exon 2 did not alter the capacity of the truncated proteins to dimerize with $UGT1A1^{HA}$ protein, compared to the interaction between $UGT1A1^{CFP}$/$UGT1A1^{HA}$, as determined by the similar intensities of the CFP bands. In addition, co-expression of Δ190-CFP, a construct that is partially deleted in the exon 1 region, also dimerized with $UGT1A1^{HA}$ with similar intensity as the full length $UGT1A1^{CFP}$. Interestingly, the smaller constructs Δ98-CFP, Δ80-CFP, Δ52-CFP, and Δ41-CFP all had decreased co-immunoprecipitated CFP fusion proteins, suggesting that the binding affinity of these truncated proteins to $UGT1A1^{HA}$ was greatly reduced when compared to the interaction between $UGT1A1^{CFP}$/$UGT1A1^{HA}$. The decrease in amount of co-immunoprecipitated CFP fusion proteins was not likely due to lower expression levels of the CFP-tagged proteins because analysis of the whole cell lysate indicated that equivalent levels of CFP-tagged fusion proteins were expressed **(Figure 4-2B)**. To investigate whether the dimerization domain exists solely in the exon 1 region, a series of N-terminal deletion constructs were designed which consists of the N-terminal targeting sequence and CFP C-terminal tags.

FIGURE 4-2

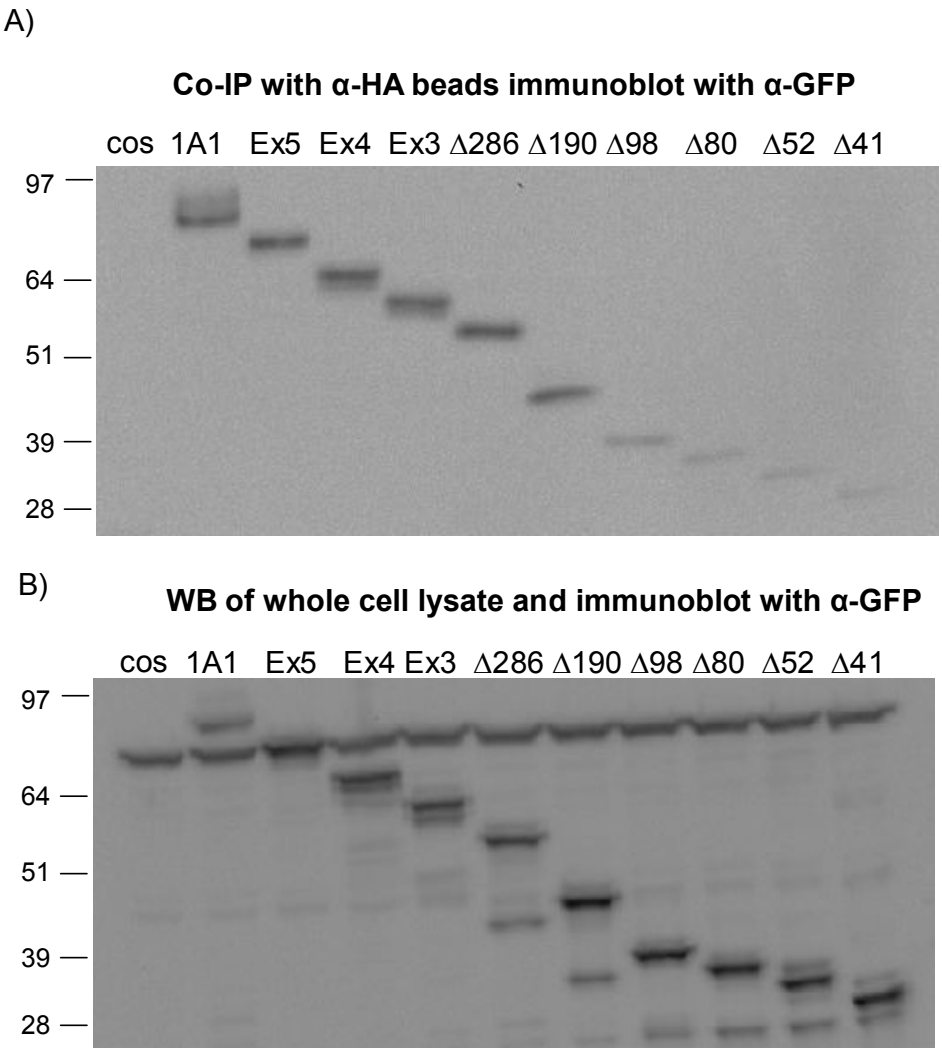


FIGURE 4-2. Co-expression of UGT1A1 with truncated constructs. A) COS cells were co-transfected with UGT1A1-HA and each of the C-terminal truncations. Whole cell lysates were collected and immunoprecipitated with anti-HA beads followed by immunoblotting with anti-GFP antibody. **B)** Western blot analysis of whole cell lysates from co-immunoprecipitation experiments using anti-GFP antibody.

Figure 4-3A is a schematic of the N-terminal serial deletion constructs used for the co-immunoprecipitation experiments. The Western blot in **Figure 4-3B** revealed that Δ280-CFP and Δ340-CFP were co-immunoprecipitated with $UGT1A1^{HA}$, while Δ450-CFP was not. The lack of co-immunoprecipitated Δ450-CFP suggests that this truncated protein could not bind to $UGT1A1^{HA}$ because Western blot analysis of the whole cell lysate indicates the presence of Δ450-CFP protein (**Figure 4-3B**).

Effects of Dimerization on UGT1A1 Function. Clinical observations in bilirubin glucuronidation deficiency in CN-2 patients have suggested that UGT dimerization may have an effect on function. The effects of homo/heterodimerization on UGT function are not well characterized. To test the potential functional consequences of dimerization, COS cells were co-transfected with the full length UGT1A1 and the various truncated forms UGT1A1. UGT activity toward the substrate octylgallate (O-gal) was measured from whole cell lysates. It is important to note that all of the truncated forms alone do not have any UGT activity. In **Figure 4-4**, UGT1A4 had no activity for O-gal, while UGT1A1 had high activity for O-gal. Co-expression of UGT1A1 and UGT1A4 had similar activity compared to UGT1A1 alone. Interestingly, co-expression of UGT1A1 with the C-terminal truncated forms of UGT1A1 all led to a reduction in UGT activity ranging from 40-80% decrease in activity.

FIGURE 4-3

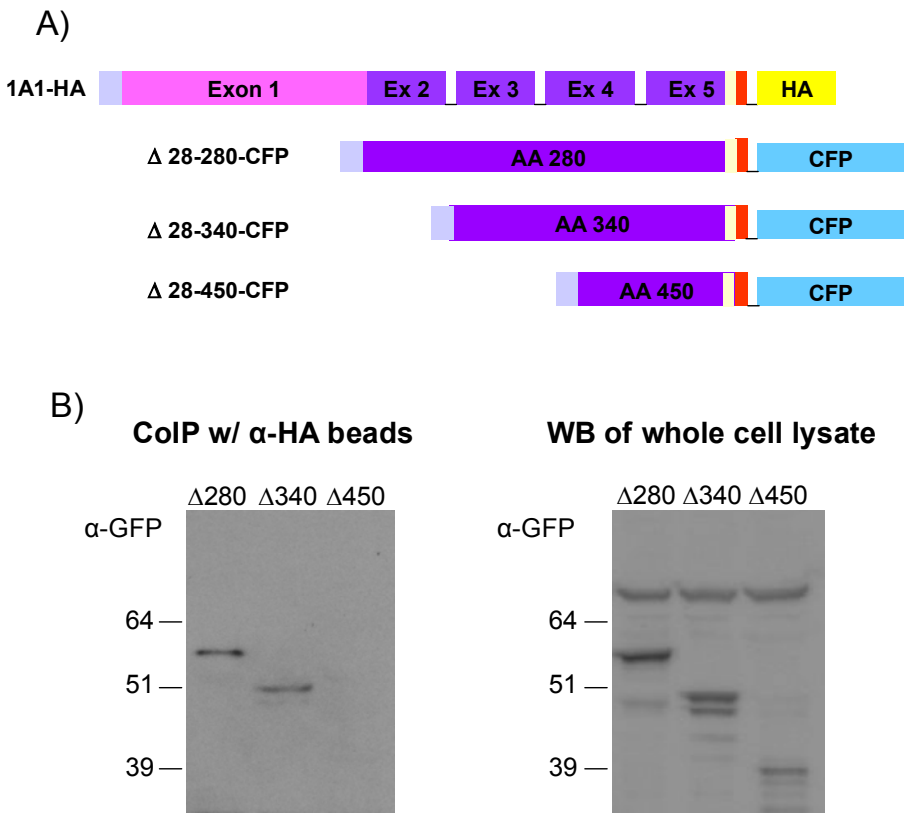


FIGURE 4-3. Co-expression of UGT1A1 with truncated constructs. A) Schematic of all the UGT1A1 N-terminal truncations fused to CFP that were generated in order to determine the domains important for UGT1A1 dimerization. **B)** COS cells were co-transfected with UGT1A1-HA and each of the N-terminal truncations. Whole cell lysates were collected and immunoprecipitated with anti-HA beads followed by immunoblotting with anti-GFP antibody.

FIGURE 4-4

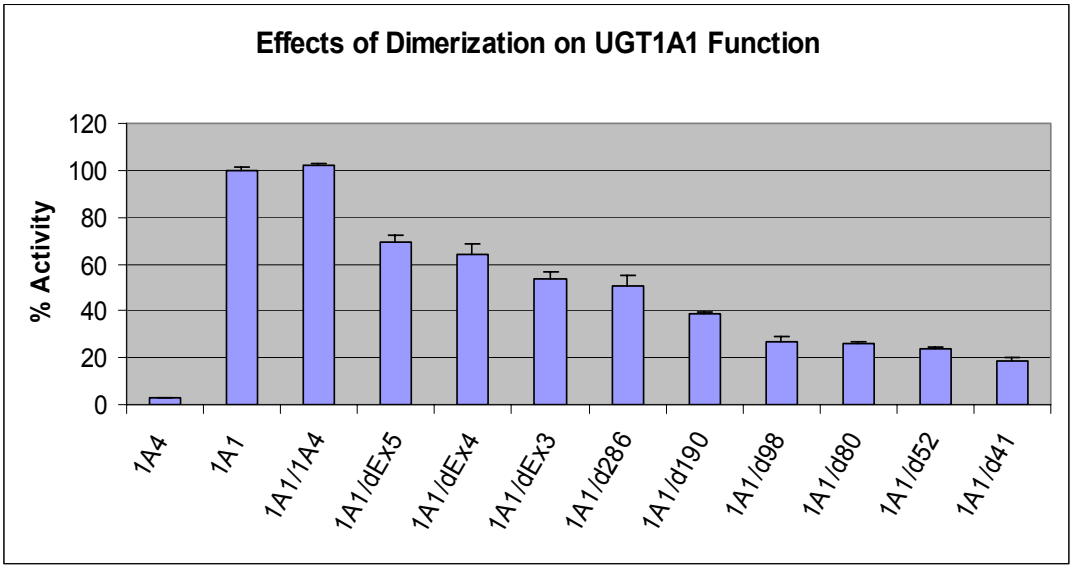


FIGURE 4-4. Effects of Dimerization on UGT1A1 function. COS cells were co-transfected with 2 µg UGT1A1 and 2 µg of each truncated plasmid or UGT1A4. Whole cell lysates were prepared. UGT assays were performed with 500 µM octylgallate as the substrate. The location of the glucuronides on the plate was identified and that region of the TLC plate was scraped and quantified.

Homology Modeling of UGT1A1. The mammalian UGTs are membrane bound proteins and have proven to be difficult to analyze by crystallography. Currently, there are no crystal structures available for the mammalian UGTs. To gain insight into the structures of UGTs, comparative structure homology modeling was implemented using crystal structures for plant glycosyltransferases as templates. The cartoon representation of the UGT1A1 model is depicted in **Figure 4-5**. The UGT1A1 model was generated using Modeller8v1 (http://salilab.org/modeller/) based on the structure of flavonoid glycosyltransferase in complex with the UDPGA analogue, uridine-5-diphosphate-2-deoxy-2-fluoro-alpha-D-glucuose (pdb-code-2C1Z). The presumed UDPGA and substrate binding sites are indicated. The C-terminal transmembrane domain of UGT1A1 was not included in the model. The UGT1A1 model illustrates that the enzyme contains two Rossmann-like folds which are often present in nucleotide binding proteins. The basic motif for each Rossmann-like domain consists of parallel beta strands that are sandwiched between alpha helices (α/ß/α), and each UGT1A1 domain was predicted to have seven parallel ß strands surrounded by eight α-helices. The C-terminal Rossmann like motif binds UDPGA while the N-terminal motif binds substrates.

FIGURE 4-5

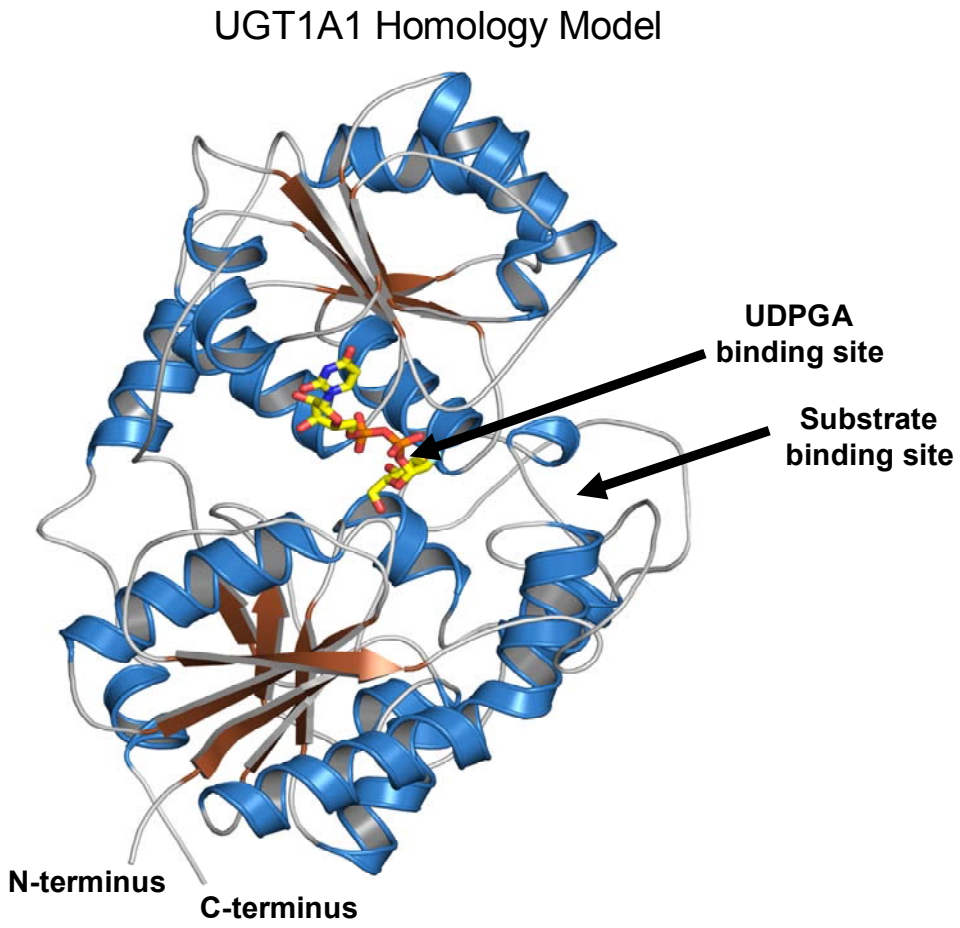


FIGURE 4-5. Homology model of UGT1A1. The UGT1A1 model was generated using Modeller8v1 (http://salilab.org/modeller/) based on the structure of flavonoid glycosyltransferase in complex with the UDPGA analogue, uridine-5-diphosphate-2-deoxy-2-fluoro-alpha-D-glucuose (pdb-code-2C1Z). The alpha-helices are colored in blue, beta-strands are colored brown, and connecting loops displayed in grey. The UDPGA analogue is displayed in sticks with carbon, oxygen, nitrogen, and fluor atoms colored yellow, red, blue, orange, and light blue, respectively. The presumed UDPGA and substrate binding sites are indicated.

The homology model of UGT1A1 was used as a scaffold to depict potential dimerization domains. In **Figure 4-6A** the homology model of UGT1A1 is shown with amino acid region 340-450 highlighted in blue in the carboxy terminus and amino acid region 98-190 highlighted in blue in the amino terminus. Based on the co-immunoprecipitation experiments a dramatic decrease in binding to $UGT1A1^{HA}$ was observed when Δ98-CFP was co-expressed. In addition Δ450-CFP lost complete binding affinity for $UGT1A1^{HA}$, suggesting that residues present between amino acids 98-190 and 340-450 may play critical roles in dimerization. **Figure 4-6B** is a space filling model of two UGT1A1 proteins with their binding clefts facing each other. The orange residues represent the amino acid region 340-450 and the blue residues depict the amino acid region 98-190. This pac-man like orientation is a hypothesized model of how two UGT1A1 proteins could come together and dimerize with the arrows indicating potential points of contact between the proteins.

FIGURE 4-6

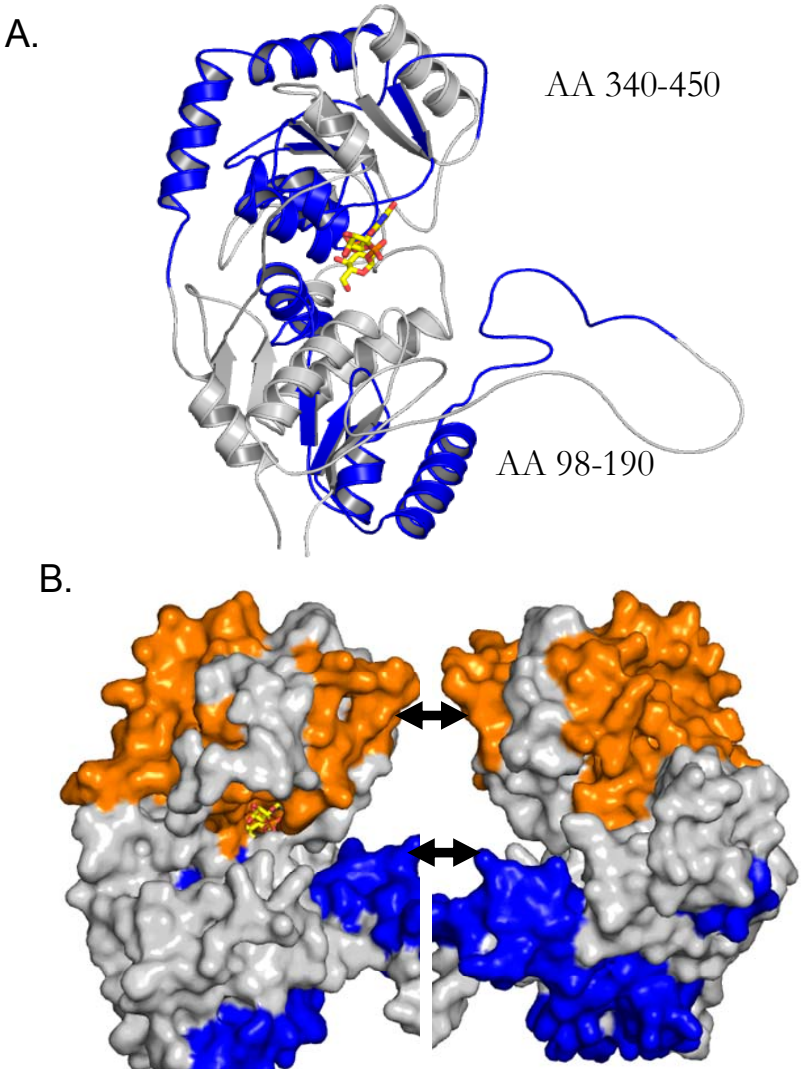


FIGURE 4-6. Potential dimerization domains and dimer orientation of UGT1A1. **A)** Amino acids 98-190 are depicted in blue in the N-terminal region and amino acids 340-450 are depicted in blue in the C-terminal region of the UGT1A1 model. **B)** A hypothetical orientation of the UGT1A1 dimer with the catalytic clefts facing each other. Amino acids 98-190 are depicted in orange and amino acids 340-450 are depicted in blue with potential points of contact between the proteins indicated by the arrows.

DISCUSSION

UGT isoforms are expressed ubiquitously in various tissues (Tukey and Strassburg, 2000), and recent data suggests that these proteins exist as homo/heterodimers. However, little evidence is available in the literature to describe how these proteins are forming dimer complexes in the ER. The purpose of these experiments was to dissect out the region(s) of UGT1A1 responsible for the protein-protein interaction observed and gain a better understanding on the quaternary structure of these proteins.

In attempts to define the potential region of the protein that could be facilitating the dimerization interaction, serial deletions of UGT1A1 were designed by PCR and the various plasmids were used in co-transfection experiments with the full length UGT1A1-HA construct. C-terminal truncations were constructed because we initially hypothesized that the dimerization domain may be located in the highly conserved region of the proteins since previous findings in the lab indicated that UGT1A proteins homo and heterodimerized (Operaña and Tukey, 2007). Co-expression of the truncated forms of UGT1A1 with UGT1A1^{HA}, followed by co-immunoprecipitation experiments using anti-HA beads revealed that deletion of exons 2-5 did not significantly alter the ability of the truncated protein to dimerize with UGT1A1^{HA}. This suggests that the domain pertinent for the protein-protein interaction most likely exists in the N-terminal portion of the protein that encodes for exon 1. Deletion of the protein after amino acid 190 in the exon 1 region also had no effect on dimerization. However, co-immunoprecipitation analysis with the smaller truncations of the UGT1A1 constructs that deleted into the exon 1 region (Δ98-CFP, Δ80-CFP, Δ52-CFP, Δ41-CFP) showed a significant loss of binding affinity to UGT1A1^{HA}. This suggests that the exon 1 region between amino acids 98-190 may play a

role in dimerization. To test this hypothesis, a series of N-terminal truncations were designed. Interestingly, the co-immunoprecipitation data illustrates that the Δ28-280-CFP construct, which lacks the entire exon 1 region of UGT1A1, was still able to dimerize with UGT1A1^{HA}. But significant loss of binding affinity was observed with the Δ28-450-CFP construct. This suggests that there could be multiple domains involved in facilitating dimerization, one in the carboxyl region and one in the amino terminal region, as deletion of a single region was not sufficient to abolish this interaction. These results partly support data implicating the potential role of the amino terminus of UGT2B1 in forming catalytically active dimers (Meech and Mackenzie, 1997b). A major difference in our findings indicates a region in the carboxyl terminus that may also be important for dimerization. The previous study utilized catalytic function as a means to gauge dimerization, however, no biochemical evidence was provided for the protein-protein interaction. This was in contrast to our co-immunoprecipitation results, which illustrated that the presence of exons 2-5 was sufficient for dimerization to occur with the full length UGT1A1 protein.

The effects of dimerization on UGT function are poorly understood. Co-expression of all the truncated forms of UGT1A1 with the full length protein resulted in significant decreases in wild type function, implicating that the inactive truncated forms may be acting as dominant negative proteins. Co-expression of UGT1A4 illustrated that heterodimerization with another UGT, which has no glucuronidation activity for the substrate octylgallate, had no effect on UGT1A1 activity. Interestingly, the decrease in catalytic function of the dimer complex seemed to be directly proportional to the size of the truncated protein. For example, co-expression of ΔEx5/UGT1A1 resulted in a 30%

reduction of UGT1A1 activity compared to the activity of UGT1A1 alone, while co-expression of Δ98/UGT1A1 resulted in 80% decrease in activity. A possible explanation for this could be that dimerization allows for greater stability of the UGT proteins, which may be important for catalytic function. The dimer complexes between the smaller UGT1A1 truncations and the full length UGT1A1 protein may be less stable and therefore less catalytically active than UGT1A1 in complex with the much longer truncations, such as ΔEx5.

The results indicating that the truncated forms of UGT1A1 potentially serve as dominant negative proteins supports the evidence in the literature that dimerization among UGTs has functional consequences. UGT2B1 has been suggested to exist as a homodimer and the relevance of this interaction became apparent when two different inactive mutant forms of UGT2B1 were co-expressed in COS cells and activity was restored (Meech 1997b). The effects of UGT dimerization on function have also been reported with UGT1As. Crigler-Najjar syndrome type II shows dominant-negative inheritance for bilirubin glucuronidation. When the mutant form of UGT1A1 in Crigler-Najjar type II patients was co-expressed in COS cells with wild type UGT1A1, activity of the wild type protein was found to be drastically reduced (Koiwai *et al.,* 1996). This result suggests that the mixed oligomer of mutant UGT1A1 with wild type UGT1A1 is inactive, while the wild type UGT1A1 homo-oligomer is active. This dominant-negative effect closely resembles the Crigler-Najjar type II phenotype observed. Other groups have also observed similar results when co-expressing UGT1A1 mutants (Levesque *et al.,* 2007; Ito *et al.,*2002) and allelic variants of UGT1A6 (Nagar *et al.,* 2004). These data

strongly indicate that the mutant UGT can act as a dominant negative regulator of the functional wild type UGT protein.

The lack of mammalian UGT crystal structures has led researchers to utilize alternative means such as comparative modeling to obtain perspective on the structure of membrane bound UGTs. Predicted secondary structure alignments of UGT1A1 and the plant glycosyltransferase indicated a good match for a template. Construction of a homology model of UGT1A1 revealed that the human UGT1A1 protein has similar folds despite its low sequence identity to the plant glycosyltransferase. The predicted UGT1A1 structure closely resembles glycosyltransferases with the GT-B fold (Coutinho *et al.,* 2003) with two distinct Rossmann-like domains each composed of seven parallel ß-strand core flanked by eight α-helices.

Although the plant glycosyltransferase template was quite useful in obtaining a global view of the structure of UGT1A1, it was also limited in providing information on various aspects of the protein. All of the available crystal structures for plant and bacterial glycosyltransferases were considerably shorter in length in the amino terminal region than the human UGTs. This posed a problem when trying to use the plant glycosyltransferase template to model these regions of UGT1A1, resulting in insertion of loop regions of the protein that were not supported by the template provided. Interestingly, this region in the amino terminus falls within amino acids 98-190, which is the region implicated as a potential dimerization domain based on the co-immunoprecipitation data. In addition, the plant glycosyltransferase proteins are monomeric proteins. This leads us to hypothesize that mammalian UGTs could have evolved to contain these inserted regions to facilitate protein-protein interaction among

UGTs. UGT proteins that exist as dimer complexes may have greater stability or increased catalytic efficiency, which could have been the evolutionary driving force for mammalian UGT proteins to interact and form homo/heterodimers.

It is unknown whether the functional units of mammalian UGTs are monomers, dimers, or both. However, based on results from this study, as well as evidence in the literature, it is evident that dimerization with an inactive/mutant form of the protein can lead to altered function of the wild type protein. We propose that the UGT dimers exist in the ER in a parallel orientation with their C-terminal transmembrane domain anchoring them in place, and that they interact via a mirror-like fashion in which the catalytic clefts of each UGT face each other and have points of contact in both the amino and the carboxyl terminus. This proposed orientation of the UGT dimer complex can be somewhat validated by a study that co-expressed two different inactive UGT2B1 mutants in which one had a mutation in the amino terminus and the other a mutation in the carboxyl terminus (Meech and Mackenzie, 1997b). The individually expressed UGT2B1 mutants were catalytically inactive, however, co-expression of both mutants resulted in partial gain of activity. This suggests that there could have been cooperative interactions between the active sites of the mutants to partially restore activity. One can imagine that the UDPGA bound in the wild type carboxyl domain of one of the UGT2B1 mutants could have transferred the glucuronic acid to the substrate bound in the cleft of the other UGT2B1 mutant lacking the mutation in the amino terminus. This promiscuity in the active site of the proteins could only occur if the catalytic clefts were in very close proximity of each other, as proposed in our dimer orientation model.

The exact structure and orientation of the UGTs within the ER is unknown. In this study we provide evidence that distinct regions exist that could be facilitating the protein-protein interactions that are observed. Although the regions we have identified are quite large we hope that this data will guide other researchers to further narrow down the regions of interest to identify these domains. In addition, our data indicates that dimerization has functional consequences on catalytic activity when heterodimer complexes are formed with inactive/truncated proteins. We have also provided a homology model of the UGT1A1 protein that could be useful in designing UGT constructs that will be amenable to crystallization.

ACKNOWLEDGMENTS

The authors would like to thank Dr. Stefaan Sansen and Dr. Eric F. Johnson from The Scripps Research Institute for their assistance with the homology modeling of UGT1A1. This work was supported in part by United States Public Health Service Grant GM49135.

REFERENCES

Burchell B, Coughtrie MW. UDP-glucuronosyltransferases. Pharmacol Ther. 1989;43(2):261-89. Review.

Coutinho PM, Deleury E, Davies GJ, Henrissat B. An evolving hierarchical family classification for glycosyltransferases. J Mol Biol. 2003 Apr 25;328(2):307-17.
Dutton, G.J. (1980) Glucuronidation of Drugs and Other Compounds. CRC Press, Boca Raton, Fla, USA.

Ghosh SS, Sappal BS, Kalpana GV, Lee SW, Chowdhury JR, Chowdhury NR. Homodimerization of human bilirubin-uridine-diphosphoglucuronate glucuronosyltransferase-1 (UGT1A1) and its functional implications. J Biol Chem. 2001 Nov 9;276(45):42108-15. Epub 2001 Aug 23.

Harding D, Jeremiah SJ, Povey S, Burchell B. Chromosomal mapping of a human phenol UDP-glucuronosyltransferase, GNT1. Ann Hum Genet. 1990 Jan;54 (Pt 1):17-21.

Hum DW, Bélanger A, Lévesque E, Barbier O, Beaulieu M, Albert C, Vallée M, Guillemette C, Tchernof A, Turgeon D, Dubois S. Characterization of UDP-glucuronosyltransferases active on steroid hormones. J Steroid Biochem Mol Biol. 1999 Apr-Jun;69(1-6):413-23. Review.

Ikushiro S, Emi Y, Iyanagi T. Protein-protein interactions between UDP-glucuronosyltransferase isozymes in rat hepatic microsomes. Biochemistry. 1997 Jun 10;36(23):7154-61.

Ito M, Yamamoto K, Maruo Y, Sato H, Fujiyama Y, Bamba T. Effect of a conserved mutation in uridine diphosphate glucuronosyltransferase 1A1 and 1A6 on glucuronidation of a metabolite of flutamide. Eur J Clin Pharmacol. 2002 Apr;58(1):11-4. Epub 2002 Feb 16.

Iyanagi T, Haniu M, Sogawa K, Fujii-Kuriyama Y, Watanabe S, Shively JE, Anan KF. Cloning and characterization of cDNA encoding 3-methylcholanthrene inducible rat mRNA for UDP-glucuronosyltransferase. J Biol Chem. 1986 Nov 25;261(33):15607-14.

Koiwai O, Aono S, Adachi Y, Kamisako T, Yasui Y, Nishizawa M, Sato H. Crigler-Najjar syndrome type II is inherited both as a dominant and as a recessive trait. Hum Mol Genet. 1996 May;5(5):645-7.

Kurkela M, Garcia-Horsman JA, Luukkanen L, Morsky S, Taskinen J, Baumann M, Kostiainen R, Hirvonen J, Finel M. Expression and characterization of recombinant human UDP-glucuronosyltransferases (UGTs). UGT1A9 is more resistant to detergent inhibition than other UGTs and was purified as an active dimeric enzyme. J Biol Chem. 2003 Feb 7;278(6):3536-44. Epub 2002 Nov 14

Lévesque E, Girard H, Journault K, Lépine J, Guillemette C. ulation of the UGT1A1 bilirubin-conjugating pathway: role of a new splicing event at the UGT1A locus. Hepatology. 2007 Jan;45(1):128-38.

Mackenzie PI, Owens IS, Burchell B, Bock KW, Bairoch A, Belanger A, Fournel-Gigleux S, Green M, Hum DW, Iyanagi T, Lancet D, Louisot P, Magdalou J, Chowdhury JR, Ritter JK, Schachter H, Tephly TR, Tipton KF, Nebert DW. The UDP glycosyltransferase gene superfamily: recommended nomenclature update based on evolutionary divergence. Pharmacogenetics. 1997 Aug;7(4):255-69. Review.

Meech R, Mackenzie PI. Structure and function of uridine diphosphate glucuronosyltransferases. Clin Exp Pharmacol Physiol. 1997a Dec;24(12):907-15. Review.

Meech R, Mackenzie PI. UDP-glucuronosyltransferase, the role of the amino terminus in dimerization. J Biol Chem. 1997b Oct 24;272(43):26913-7.
Monaghan G, Burchell B, Boxer M. Structure of the human UGT2B4 gene encoding a bile acid UDP-glucuronosyltransferase. Mamm Genome. 1997 Sep;8(9):692-4.

Nagar S, Zalatoris JJ, Blanchard RL. Human UGT1A6 pharmacogenetics: identification of a novel SNP, characterization of allele frequencies and functional analysis of recombinant allozymes in human liver tissue and in cultured cells. Pharmacogenetics. 2004 Aug;14(8):487-99.

Operaña TN, Tukey RH. Oligomerization of the UDP-glucuronosyltransferase 1A proteins: homo- and heterodimerization analysis by fluorescence resonance energy transfer and co-immunoprecipitation. J Biol Chem. 2007 Feb 16;282(7):4821-9. Epub 2006 Dec 19.

Ritter JK, Chen F, Sheen YY, Tran HM, Kimura S, Yeatman MT, Owens IS. A novel complex locus UGT1 encodes human bilirubin, phenol, and other UDP-glucuronosyltransferase isozymes with identical carboxyl termini. J Biol Chem. 1992 Feb 15;267(5):3257-61.

Shepherd SR, Baird SJ, Hallinan T, Burchell B. An investigation of the transverse topology of bilirubin UDP-glucuronosyltransferase in rat hepatic endoplasmic reticulum. Biochem J. 1989 Apr 15;259(2):617-20.

Strassburg CP, Oldhafer K, Manns MP, Tukey RH. Differential expression of the UGT1A locus in human liver, biliary, and gastric tissue: identification of UGT1A7 and UGT1A10 transcripts in extrahepatic tissue. Mol Pharmacol. 1997 Aug;52(2):212-20.
Thibaudeau J, Lépine J, Tojcic J, Duguay Y, Pelletier G, Plante M, Brisson J, Têtu B, Jacob S, Perusse L, Bélanger A, Guillemette C. Characterization of common UGT1A8, UGT1A9, and UGT2B7 variants with different capacities to inactivate mutagenic 4-hydroxylated metabolites of estradiol and estrone. Cancer Res. 2006 Jan 1;66(1):125-33.

Tukey RH, Strassburg CP. Human UDP-glucuronosyltransferases: metabolism, expression, and disease. Annu Rev Pharmacol Toxicol. 2000;40:581-616. Review.
Vanstapel F, Blanckaert N. Topology and regulation of bilirubin UDP-glucuronyltransferase in sealed native microsomes from rat liver. Arch Biochem Biophys. 1988 May 15;263(1):216-25.

Wooster R, Sutherland L, Ebner T, Clarke D, Da Cruz e Silva O, Burchell B. Cloning and stable expression of a new member of the human liver phenol/bilirubin: UDP-glucuronosyltransferase cDNA family. Biochem J. 1991 Sep 1;278 (Pt 2):465-9.

CHAPTER 5

Conclusions

Generation and Characterization of the Human CYP1A1^{GFP} Transgenic Mouse Model.

The current CYP1A1 cell based bioassays and the transgenic mouse models that are currently available are useful for studying transcriptional events that regulate *CYP1A1* gene expression but cannot provide any information about the induction of the functional CYP1A1 protein. The activation of the AhR signaling cascade results in the transcriptional activation of target genes within the Ah locus and culminates in the translation and increased protein expression of various drug metabolizing enzymes, such as CYP1A1. Since the deleterious effects of exposure to environmental contaminants, like PAHs, are due to the enzymatic function of the CYP1A1 protein to bioactivate certain compounds, it would be advantageous to be able to determine the presence and function of the human CYP1A1 protein. The CALUX assays and other transgenic mouse models are limited in this sense and the functional consequences regarding the induction of the human CYP1A1 protein cannot be addressed using these models. Moreover, several of the transgenic mouse lines that have been constructed which have limited portions of the CYP1A1 promoter region have shown discrepancies in basal levels of reporter activity, and have varied tissue specific expression patterns. Our lab has attempted to address the drawbacks of the current cell based bioassays and transgenic mouse models by constructing a transgenic mouse strain (Tg-*CYP1A1*^{GFP}) expressing a chimeric gene consisting of the entire human *CYP1A1* gene (15 kb) fused with a *GFP* reporter gene. We believe this to be an ideal transgenic mouse model to examine the regulation of human CYP1A1 in vivo.

Characterization of the CYP1A1^{GFP} transgenic mouse illustrated that the CYP1A1^{GFP} transgene was highly inducible in a tissue- and cell type- specific manner following i.p. and oral treatment with TCDD. The fluorescence microscopy revealed that CYP1A1^{GFP} expression was localized to the hepatocytes in the liver and the Clara cells in the lungs. Isolated primary hepatocytes were also inducible by various known AhR ligands, illustrating the usefulness of these cells for potential high-throughput bioassay screening. Treatment of the primary hepatocytes with TCDD led to the induction of CYP1A1^{GFP} in a time and dose dependent manner. The tissue specific expression patterns of induced CYP1A1^{GFP} were similar to that of the induced mouse Cyp1a1 and highly correlated with the expected human expression patterns. However, species specific differences were observed following oral treatment with BaP. Human CYP1A1^{GFP} was induced in the liver following oral treatment with BaP but no mouse Cyp1a1 was detected in the liver. This suggests that this CYP1A1^{GFP} transgenic model may provide insight in species specific regulation of the human *CYP1A1* locus in various tissues. This could also indicate a greater sensitivity of the human *CYP1A1* gene to be activated than the mouse *Cyp1a1* gene upon oral exposure to certain AhR ligands.

The human CYP1A1^{GFP} transgenic mouse model that we have generated is an ideal model because it encodes for the functional CYP1A1 protein and it also contains the entire *CYP1A1* promoter region with pertinent regulatory elements that have been excluded in the other transgene constructs. Our model allows for the study of transcriptional regulation of the *CYP1A1* gene and the functional protein simultaneously. In addition, we have incorporated the cost effective GFP reporter fused to the CYP1A1 protein to quickly and easily monitor CYP1A1 induction. Isolation of primary

hepatocytes from these transgenic animals could also be adapted for use in a high-throughput assay for screening of novel AhR ligands by directly measuring GFP fluorescence from the cells. The CYP1A1^{GFP} transgenic mouse model allows for the study of humoral, hormonal, and environmental factors that regulate the expression of the *CYP1A1* gene in vivo and can be used to better understand the complex series of events that can lead to diseased states upon exposure to certain classes of environmental contaminants.

Elucidation of UGT Protein-Protein Interactions

The quaternary structures of the UGT proteins in the ER were first suggested in the mid-1980s. Initial reports of UGT oligomerization were based on radiation inactivation analysis (Peters *et al.,* 1984), followed by observations that purification of UGTs by size exclusion columns resulted in dimeric aggregates (Matern *et al.,* 1982; Gschaidmeier and Bock, 1994). Heterodimerization of UGT isoforms were also implicated in purification studies in which UGTs glucuronidating testosterone and androsterone could not be separated (Matsui and Nagai, 1986). Homodimerization of UGT1A1 and UGT1A9 proteins have also been previously reported, and the methods used to establish these protein-protein interactions have mainly focused on biochemical techniques (Ghosh *et al.,* 2001; Kurkela *et al.,* 2003). Kurkela et al demonstrated homodimerization of UGT1A9 using His and HA epitope-tagging (Kurkela *et al.,* 2003). Ghosh et al conducted nearest neighbor cross-linking studies followed by gel filtration, which provided evidence for UGT1A1 homodimerization (Ghosh *et al.,* 2001). This experiment is suggestive of the close proximity of the UGT1A1 proteins, which is not

surprising since the proteins are membrane-bound within the ER in a two dimensional space. In addition, Ghosh et al used the two-hybrid mammalian system to determine UGT1A1 intermolecular protein interaction. This approach was based on the co-expression of a bait vector containing a DNA binding domain (Lex DNA binding domain) and UGT1A1, and the prey vector containing a transactivating domain (Gal4) fused to UGT1A1. UGT1A1 protein-protein interactions bring the bait and prey constructs in close proximity, resulting in translocation to the nucleus and transcriptional activation of the reporter gene (Ghosh *et al.,* 2001). This technique is problematic since the UGT1A1 proteins are membrane-bound in the ER, which prevents translocation into the nucleus and resulting in no transcriptional activation of the reporter gene. Although these studies provide a framework to investigate the potential homo/hetero-oligomerization of the UGT1A proteins, sufficient data is lacking to concretely establish UGT protein-protein interactions in vivo. For my thesis work, I proposed to address this problem by implementing the fluorescence technique FRET to determine homo/heterodimerization of UGTs in live cells.

To explore the intermolecular interactions among UGT proteins in vivo, I generated a library of CFP- and YFP-tagged UGT1A constructs and utilized FRET to measure protein-protein interactions in cells co-transfected with the CFP- and YFP-tagged UGTs. This technique revealed that UGT1A1 was able to homodimerize, supporting previous findings that used a two-hybrid system to test this interaction (Ghosh *et al.,* 2001). In addition, I also examined the ability of all other UGT1A proteins to homodimerize using FRET and showed that all of the UGT1A proteins were capable of interacting with their respective isoforms. I also tested if UGT1A1 could heterodimerize

with all of the UGT1A proteins and discovered that UGT1A1 was able to interact with all of the UGT1A proteins. The FRET data indicated high FRET signals ranging from 40 % to 90 % FRET efficiency and the signal was localized in the cytoplasm. To my knowledge, the UGT FRET data obtained is the first evidence demonstrating UGT oligomerization in vivo, which supports the biochemical data currently present in the literature. These findings were further supported using biochemical analysis through co-immunoprecipitation experiments. Co-expression of HA-tagged and CFP-tagged UGT1A proteins, followed by immunoprecipitation with anti-HA beads, illustrated the ability of each UGT1A protein to homodimerize and confirmed that UGT1A1 was capable of forming heterodimer complexes with all of the UGT1A proteins, corroborating the FRET results. These data support previous finding that His-tagged UGT1A9 was also found to homodimerize (Kurkela *et al.,* 2003).

The co-immunoprecipitation experiments offered an alternative and complementary technique to the in vivo FRET analysis. Prior to the generation of the epitope-tagged plasmid library of the UGT1A constructs, it was difficult to ascertain the dimerization interactions among the UGT1A proteins because of the lack of isoform specific antibodies available for the UGTs. This library of CFP-, YFP-, and HA-tagged constructs allows for the determination of any pair of UGT interactions without the need for isoform specific antibodies because of the of the C-terminal fusion tags that can be used as a marker for Western blot analysis. One can use a CFP-tagged and a HA-tagged UGT construct and be able to distinguish between the two isoforms simply based on the shift in the molecular weight of the protein due to the presence of the C-terminal tag. Moreover, this unique plasmid library allows for the in vivo detection of protein-protein

interaction using FRET analysis, as well as biochemical analysis of dimerization via co-immunoprecipitation experiments using the HA-tagged constructs.

There is also accumulating evidence that UGTs extend their promiscuous protein-protein interaction to phase I enzymes. Initial reports of interactions between rat CYP1A1 and UGTs were detected by affinity chromatography using CYP1A1-conjugated Sepharose 4B columns, which indicated the co-elution of UGTs, microsomal epoxide hydrolase, and NADPH P450 reductase (Taura *et al.,* 2000). Co-immunoprecipitation of human liver microsomes showed that CYP3A4 was able to immunoprecipitate UGT1A1, UGT1A6, and UGT2B7 (Fremont *et al.,* 2004). The functional consequence of such interactions were evaluated and it was revealed that the presence CYP3A4 was able to modulate UGT2B7 function, resulting in altered regioselectivity of morphine glucuronidation (Takeda *et al.,* 2005). Although another study showed that simultaneous expression of rat CYP1A1 and UGT1A6 had no affect on UGT1A6 function (Ikushiro 2004), suggesting that interactions between UGTs and CYPs could be isoform specific (Takeda *et al.,* 2005; Ishii *et al.,* 2005). Characterization of isoform specificity of CYP interaction with UGTs was assessed by co-immunoprecipitation using isoform specific antibodies for CYP1A2, 2B2, 2C11/2C13, and 3A2 (Ishii *et al.,* 2007). The data indicated significant differences in the levels of UGTs co-immunoprecipitated with each CYP isoform, supporting the notion that these interactions could be isoform dependent. In addition, the study showed that the UGTs immunoprecipitated in the CYP-UGT complex were catalytically active for the substrate 4-methylumbelliferone, although the antibody used could not differentiate which UGT isoforms were present (Ishii *et al.,* 2007). It is hypothesized that functional cooperation between UGTs and CYPs facilitates multistep

drug metabolism in which a metabolite produced by a CYP is directly transferred to a UGT for further sequential metabolism, allowing for increased efficiency of substrate detoxification (Ishii *et al.,* 2005).

Structural Domains Involved in UGT Dimerization

The results obtained by FRET analysis and co-immunoprecipitation experiments indicate that UGT1A1 dimerizes with all of the UGT1A proteins, however, the structural domains involved in the protein-protein interaction are unknown. Therefore, I began to delve into the structural aspects of UGTs to determine the pertinent domains involved in oligomerization. Since all of the UGT1A isoforms have identical C-terminal domains due to exon sharing, I hypothesized that this region may be responsible for the protein-protein interactions observed. I set out to identify the dimerization domain(s) by generating a library of C-terminal truncations of UGT1A1 constructs fused to a CFP-tag, which was conveniently used as the epitope to determine the presence of the truncated UGT. Co-immunoprecipitation studies were performed by co-expressing COS cells with the UGT1A1-CFP tagged truncations with the full length UGT1A1-HA plasmid to examine the heterodimer interaction. To my surprise, deletion of exons 2-5, which encode for the conserved UDPGA binding region of all of the UGTs, had little effect on binding capacity and still bound to UGT1A1. Co-expression using the Δ190-CFP construct, which consists of a partial deletion of the exon 1 region, also displayed similar binding affinity as the full length protein. However, significant loss of binding to $UGT1A1^{HA}$ was observed with the Δ98-CFP truncation. N-terminal truncations were also generated to determine if deletion of the entire exon 1 region could abolish dimerization with

UGT1A1. The data revealed that the deletion between amino acids 340-450 resulted in loss of binding to $UGT1A1^{HA}$. The co-immunoprecipitation results suggest that potentially two distinct regions within the UGT1A1 protein may be important in facilitating protein-protein interaction, the N-terminal region (amino acids 98-190) and the C-terminal region (amino acids 340-450).

To investigate the importance of dimerization on UGT function, truncated forms of UGT1A1 were co-expressed with the full length protein. Analysis of protein function using thin layer chromatography showed that co-expression of the truncated forms with the UGT1A1 protein caused a decrease in function of the wild type protein toward the substrate octylgallate. The decrease in UGT1A1 activity was also directly proportional to the size of the co-expressed truncated UGT1A1 protein, since the heterodimer complexes with longer truncations had greater activity than shorter truncations. This observation may indicate that dimerization is important for the stability of the complex, as well as the catalytic function. This dominant negative effect supports the previous observations that heterodimerization of UGTs with mutant forms can lead to altered glucuronidation activity (Meech and Mackenzie, 1997; Koiwai *et al.,* 1996; Levesque *et al.,* 2007; Ito *et al.,*2002; Nagar 2004).

Evidence provided in this body of work indicates that the UGT1A family of proteins forms dimer complexes within the ER membrane, a property that could influence function and substrate specificity. Based on my results, co-expression of a truncated form of UGT1A1 leads to dominant negative effect on the function of the wild type UGT1A1 protein. I have also shown that heterodimerization between UGT1A4 and UGT1A1 does not alter the glucuronidation activity of UGT1A1 towards the substrate octylgallate, even

though UGT1A4 has no activity towards the substrate. This suggests that the UGT1A1/UGT1A4 heterodimer has similar activity as the UGT1A1 homodimer. In contrast, other studies have shown that heterodimerization may alter substrate specificity. It was observed that heterodimerization of UGT2B21 and UGT2B22 altered the substrate specificity of UGT2B21, resulting in an enhanced morphine-6-glucuronide formation compared to the activity of UGT2B21 alone (Ishii *et al.,* 2001). Another study showed that the heterodimerization of wild type UGT1A6 and UGT2B7 can lead to both enhancement and decrease in specific activity depending on the substrate (Kurkela *et al.,* 2007). The effects of protein-protein interactions among UGT1A proteins were investigated using various substrates and showed that the effects of heterodimerization on the kinetics of specific activities also varied depending on the isoforms present and substrates that were used (Fujiwara *et al.,* 2007a; Fujiwara *et al.,* 2007b). Thus, the effects of heterodimerization in modulating UGT function seem to be isoform specific and most likely substrate dependent. Some studies indicate that heterodimerization between a mutant and wild type protein may have a compensatory effect on the function of the mutant protein. For example, when a truncation mutant of UGT1A9 was co-expressed with full length UGT1A4 the activity of UGTA9 for the substrate entacapone was restored (Kurkela *et al.,* 2004). It was also observed that the presence of other UGT isoforms attenuated the effect of the Y485D mutation on the activity of UGT1A6 for several substrates (Kurkela *et al.,* 2007). It has been suggested that alterations in heterodimer specific activity could be due to the formation of unique substrate binding sites that do not exist in the homodimeric state of the proteins (Meech and Mackenzie, 1997). These findings reveal that the activity of these enzymes are governed in a complex

manner and the effects on specific activities of heterodimers are dependent on which isoforms are present, as well as the substrate utilized to probe for the activity of the protein.

The recent finding that UGTs exist as dimer complexes significantly impacts our understanding of drug metabolism and potential drug-drug interactions, particularly in light of the fact that many UGTs have a high degree of allelic diversity. Some polymorphic UGTs have demonstrated a significant pharmacological impact on drug response, drug-induced toxicity, and potential susceptibility to cancer (Guillemette, 2003; Desai *et al.,* 2003; Nagar *et al.,* 2006). Previously it was assumed that the UGTs functioned as monomeric proteins and that the polymorphic UGT was functionally compromised compared to the wild type protein. However, this paradigm is complicated by the dimerization capacity of the UGTs, which could potentially overcome the impairment elicited by a single polymorphic event. The functional relevance of UGT oligomerization has broadened the complexity of our understanding of pharmacogenetics as it pertains to the polymorphic patterns of UGT expression and the outcome of drug metabolism.

Although the clinical relevance of UGT protein-protein interactions has yet to be studied, there could be potentially grave consequences regarding the effects of UGT dimerization on drug induced toxicity. It has been observed that patients affected with Gilbert's syndrome (deficiency in UGT1A1 activity) display lower glucuronidation rates for a number of therapeutic drugs including acetaminophen (Douglas *et al.,* 1978), lorazapam (Carulli *et al.,* 1976), and irinotecan (Iyer *et al.,* 1998). Irinotecan is an anticancer drug used to treat metastatic colorectal cancer (Kawato *et al.,* 1991) and it has

been suggested that individuals with Gilbert's syndrome are at a greater risk to experience irinotecan-induced toxicity, which includes severe diarrhea and neutropenia (Wasserman *et al.,* 1997). Based on the dominant negative effects of co-expression with mutant and or truncated forms of UGT1A1 on wild type function, one can extrapolate that an individual expressing a mutant form of UGT1A1 may also have greater risk of drug-induced toxicity due to lowered activity of the dimeric UGTs. This leads to the hypothesis that dimerization among UGT proteins may greatly influence the pharmacokinetics, the pharmacologic effects, and toxicity of drugs that are glucuronidated.

Homology Modeling of UGT1A1

The exact structure and orientation of the UGTs within the ER is unknown, however, I have provided preliminary results that distinct regions exist that could be facilitating dimerization among the UGTs. In order to understand the structural properties that govern protein-protein interaction, a homology model of UGT1A1 was constructed using the crystal structure of a plant glycosyltransferase as a template. The homology model of UGT1A1 indicates that it falls into the GT-B fold category of glycosyltransferases (Coutinho *et al.,* 2003), composed of two distinct Rossmann-like domains each containing a seven parallel ß-strand core flanked by eight α-helices. The interface between the N-terminal and C-terminal globular domains form the catalytic cleft where the glucuronic acid can be transferred from UDPGA to the desired substrate. I have also mapped the potential dimerization regions onto the homology model and attempted to examine potential points of contact between the UGT1A1 proteins.

Although the regions identified are quite large, I hope that this data will guide other researchers to further narrow down the regions of interest to determine the basic unit of interaction. A major drawback with homology modeling, however, was the fact that the crystal structure for the plant glycosyltransferase was much shorter than the human UGT1A1. This posed a problem when trying to model the portion containing the amino acids 98-190 of UGT1A1. Interestingly, this region was implicated as a potential dimerization domain based on the co-immunoprecipitation data, which leads me to question whether this evolutionary insertion could have evolved to facilitate protein-protein interaction in mammalian UGTs. Homology modeling of UGT1A1 also enabled the exploration of possible orientations of the UGT1A1 dimer complex, giving rise to the hypothesis that the catalytic clefts of the proteins are in very close proximity. I postulate that the UGT proteins exist in a pac-man like orientation with the catalytic clefts facing each other, which would enable a functional interaction between the N-terminal domain of a protein with the C-terminal domain of another protein. This hypothesized orientation could account for the partial compensation for each defect and restoration of UGT activity observed when two different functionally inactive mutant UGTs were co-expressed (Meech and Mackenzie, 1997).

The homology model of human UGT1A1 using the crystal structure of plant UGT71G1 as a template supports the structure predictions that were based on sequence alignments (Locuson and Tracy, 2007; Li and Wu, 2007). A recent publication on the comparative modeling of UGT1A1 by Locuson and Tracy confirmed the presence of a 44-residue consensus sequence in the C-terminal domain (Locuson and Tracy, 2007) that is believed to be important for the binding of the UDP moiety of the sugar nucleotide

(Ross *et al.,* 2001; Mackenzie *et al.,* 1997). Their extensive analysis of the UGT1A1 homology model provided insight on two catalytic residues located in the N-terminal domain: UGT1A1 H39, which is believed to serve as the general base catalyst for aglycone deprotonation, and UGT1A1 D151, which ensures deprotonation of the histidine (Locuson and Tracy, 2007; Li and Wu, 2007). Mutational analysis of the equivalent histidine (Kubota *et al.,* 2007; Li *et al.,* 2007) and aspartic residues in the UGT1A (Li *et al.,* 2007) and UGT2B7 (Miley *et al.,* 2007) proteins support the notion that these two amino acids play important roles for catalytic function. Significant efforts have been employed to characterize the UGT binding sites in order to determine critical residues for substrate specificity and catalytic function (Mackenzie, 1990; Senay *et al.,* 1997; Rodominska-Pandya *et al.,* 1999; Ouzzine *et al.,* 2000; Ghosh *et al.,* 2005; Senay *et al.,*2002; Coffman *et al.,* 2003; Barre *et al.,* 2007; Li *et al.,* 2007; Kubota *et al.,* 2007), but it has been difficult to ascertain the functional role of each residue without knowledge of the crystal structure of the UGT proteins.

To this date, there is no available crystal structure of a human UGT enzyme containing both the N-terminal and C-terminal domains intact. However, a high-resolution 1.8 Å apo crystal structure of the C-terminal domain of UGT2B7 (2B7CT) has been recently solved and it is the first structural data available for the human UGTs (Miley *et al.,* 2007). The apo crystal structure depicts a Rossmann-like fold with the presumed UDPGA binding site remarkably similar to that of the plant glycosyltransferases with only a few amino acid variances. Mutational analysis of several residues predicted to be pertinent for the interaction with the diphosphate or the glucuronic acid moiety resulted in loss of enzyme activity, while mutations disrupting the

uracil base interactions had only moderate effects. Homology modeling of the full length UGT2B7 protein revealed that it also contains the critical residues H35 and D151 in the catalytic positions and mutating these key residues abolished activity (Miley *et al.,* 2007). These data further support that the human UGTs utilize a serine hydrolase-like catalytic triad for catalysis (Shao *et al.,* 2005; Offen *et al.,* 2006). The partial crystal structure of 2B7CT, in conjunction with homology modeling of the full length UGT proteins, have provided a much needed framework to understand the roles of amino acids identified as being important for UGT function. It was initially predicted that a highly conserved His370 in UGT1A6 was involved in catalysis (Ouzzine *et al.,* 2000) but it was later re-evaluated and suggested to be important for UDPGA binding along with another conserved residue Glu379 (Patana *et al.,* 2007). In another study, the conserved DQxD motif was identified to be important for UDPGA binding in UGT1A10 and presumably for all of the UGT1A proteins (Xiong *et al.,* 2007) and UGT2B7 (Miley *et al.,* 2007). By combining the knowledge provided by homology modeling with the mutational analysis of critical amino acids in the active site of the proteins, recent advances have been made in the prototyping of ligand based in silico models capable of predicting the binding affinity and substrate specificity of UGTs (Sorich *et al.,* 2008). Pharmacophore modeling has produced accurate predictions and insight into potential substrate bias towards aromatic and aliphatic hydroxyl groups but improved structural data for the UGTs will enable greater understanding of the glucuronidation process. Current efforts are underway to determine the crystal structure for the entire N-terminal and C-terminal domains of the UGT enzymes. Unfortunately, their membrane bound nature and unstable N-terminal domain have proven to be enormous hurdles to overcome.

It is my hope that my thesis work will provide stepping stones for other researchers in the UGT field to build upon and further advance our understanding of UGT protein-protein interactions and their functional role as homo/heterodimer complexes. To truly comprehend the nature of these proteins we must be able to visualize the physical structure of the UGTs in order to understand the architecture of the dimeric complexes. Unfortunately, crystallization of the UGT proteins has continued to elude researchers. Through use of structure prediction programs and homology modeling analysis, we hope that some inspiration might be gained in order to design truncated UGT constructs or chimeras that may be more amenable to crystallographic analysis. It is our hope that by elucidating the complex structure and topology of these detoxifying enzymes, we can begin to understand the molecular mechanisms of their catalytic function, binding affinity, and substrate specificity, which someday could be implemented for rational drug design.

REFERENCES

Barré L, Magdalou J, Netter P, Fournel-Gigleux S, Ouzzine M. The stop transfer sequence of the human UDP-glucuronosyltransferase 1A determines localization to the endoplasmic reticulum by both static retention and retrieval mechanisms. FEBS J. 2005 Feb;272(4):1063-71.

Carulli N, Ponz de Leon M, Mauro E, Manenti F, Ferrari A. Alteration of drug metabolism in Gilbert's syndrome. Gut. 1976 Aug;17(8):581-7.

Coffman BL, Kearney WR, Goldsmith S, Knosp BM, Tephly TR. Opioids bind to the amino acids 84 to 118 of UDP-glucuronosyltransferase UGT2B7. Mol Pharmacol. 2003 Feb;63(2):283-8.

Coutinho PM, Deleury E, Davies GJ, Henrissat B. An evolving hierarchical family classification for glycosyltransferases. J Mol Biol. 2003 Apr 25;328(2):307-17.

Desai AA, Innocenti F, Ratain MJ. UGT pharmacogenomics: implications for cancer risk and cancer therapeutics. Pharmacogenetics. 2003 Aug;13(8):517-23.

Douglas AP, Savage RL, Rawlins MD. Paracetamol (acetaminophen) kinetics in patients with Gilber's syndrome. Eur J Clin Pharmacol. 1978 May 31;13(3):209-12.

Fremont JJ, Wang RW, King CD. Coimmunoprecipitation of UDP-glucuronosyltransferase isoforms and cytochrome P450 3A4. Mol Pharmacol. 2005 Jan;67(1):260-2. Epub 2004 Oct 14.

Fujiwara R, Nakajima M, Yamanaka H, Katoh M, Yokoi T. Interactions between human UGT1A1, UGT1A4, and UGT1A6 affect their enzymatic activities. Drug Metab Dispos. 2007a Oct;35(10):1781-7. Epub 2007 Jul 9.

Fujiwara R, Nakajima M, Yamanaka H, Nakamura A, Katoh M, Ikushiro S, Sakaki T, Yokoi T. Effects of coexpression of UGT1A9 on enzymatic activities of human UGT1A isoforms. Drug Metab Dispos. 2007 May;35(5):747-57. Epub 2007b Feb 9.

Ghosh SS, Lu Y, Lee SW, Wang X, Guha C, Roy-Chowdhury J, Roy-Chowdhury N. Role of cysteine residues in the function of human UDP glucuronosyltransferase isoform 1A1 (UGT1A1). Biochem J. 2005 Dec 15;392(Pt 3):685-92.

Ghosh SS, Sappal BS, Kalpana GV, Lee SW, Chowdhury JR, Chowdhury NR. Homodimerization of human bilirubin-uridine-diphosphoglucuronate glucuronosyltransferase-1 (UGT1A1) and its functional implications. J Biol Chem. 2001 Nov 9;276(45):42108-15. Epub 2001 Aug 23.

Gschaidmeier H, Bock KW. Radiation inactivation analysis of microsomal UDP-glucuronosyltransferases catalysing mono- and diglucuronide formation of 3,6-dihydroxybenzo(a)pyrene and 3,6-dihydroxychrysene. Biochem Pharmacol. 1994 Oct 18;48(8):1545-9.

Guillemette C. Pharmacogenomics of human UDP-glucuronosyltransferase enzymes. Pharmacogenomics J. 2003;3(3):136-58. Review.

Ikushiro S, Sahara M, Emi Y, Yabusaki Y, Iyanagi T. Functional co-expression of xenobiotic metabolizing enzymes, rat cytochrome P450 1A1 and UDP-glucuronosyltransferase 1A6, in yeast microsomes. Biochim Biophys Acta. 2004 May 3;1672(2):86-92.

Ishii Y, Miyoshi A, Watanabe R, Tsuruda K, Tsuda M, Yamaguchi-Nagamatsu Y, Yoshisue K, Tanaka M, Maji D, Ohgiya S, Oguri K. Simultaneous expression of guinea pig UDP-glucuronosyltransferase 2B21 and 2B22 in COS-7 cells enhances UDP-glucuronosyltransferase 2B21-catalyzed morphine-6-glucuronide formation. Mol Pharmacol. 2001 Nov;60(5):1040-8.

Ishii Y, Takeda S, Yamada H, Oguri K. Functional protein-protein interaction of drug metabolizing enzymes. Front Biosci. 2005 Jan 1;10:887-95.

Ishii Y, Iwanaga M, Nishimura Y, Takeda S, Ikushiro S, Nagata K, Yamazoe Y, Mackenzie PI, Yamada H. Protein-protein interactions between rat hepatic cytochromes P450 (P450s) and UDP-glucuronosyltransferases (UGTs): evidence for the functionally active UGT in P450-UGT complex. Drug Metab Pharmacokinet. 2007 Oct;22(5):367-76.

Ito M, Yamamoto K, Maruo Y, Sato H, Fujiyama Y, Bamba T. Effect of a conserved mutation in uridine diphosphate glucuronosyltransferase 1A1 and 1A6 on glucuronidation of a metabolite of flutamide. Eur J Clin Pharmacol. 2002 Apr;58(1):11-4. Epub 2002 Feb 16.

Iyer L, King CD, Whitington PF, Green MD, Roy SK, Tephly TR, Coffman BL, Ratain MJ. Genetic predisposition to the metabolism of irinotecan (CPT-11). Role of uridine diphosphate glucuronosyltransferase isoform 1A1 in the glucuronidation of its active metabolite (SN-38) in human liver microsomes. J Clin Invest. 1998 Feb 15;101(4):847-54.

Li C, Wu Q. Adaptive evolution of multiple-variable exons and structural diversity of drug-metabolizing enzymes. BMC Evol Biol. 2007 May 2;7:69.

Locuson CW, Tracy TS. arative modelling of the human UDP-glucuronosyltransferases: insights into structure and mechanism. Xenobiotica. 2007 Feb;37(2):155-68.

Kawato Y, Aonuma M, Hirota Y, Kuga H, Sato K. Intracellular roles of SN-38, a metabolite of the camptothecin derivative CPT-11, in the antitumor effect of CPT-11. Cancer Res. 1991 Aug 15;51(16):4187-91.

Koiwai O, Aono S, Adachi Y, Kamisako T, Yasui Y, Nishizawa M, Sato H. Crigler-Najjar syndrome type II is inherited both as a dominant and as a recessive trait. Hum Mol Genet. 1996 May;5(5):645-7.

Kubota T, Lewis BC, Elliot DJ, Mackenzie PI, Miners JO. Critical roles of residues 36 and 40 in the phenol and tertiary amine aglycone substrate selectivities of UDP-glucuronosyltransferases 1A3 and 1A4. Mol Pharmacol. 2007 Oct;72(4):1054-62. Epub 2007 Jul 17.

Kurkela M, Garcia-Horsman JA, Luukkanen L, Morsky S, Taskinen J, Baumann M, Kostiainen R, Hirvonen J, Finel M. Expression and characterization of recombinant human UDP-glucuronosyltransferases (UGTs). UGT1A9 is more resistant to detergent inhibition than other UGTs and was purified as an active dimeric enzyme. J Biol Chem. 2003 Feb 7;278(6):3536-44. Epub 2002 Nov 14

Kurkela M, Hirvonen J, Kostiainen R, Finel M. The interactions between the N-terminal and C-terminal domains of the human UDP-glucuronosyltransferases are partly isoform-specific, and may involve both monomers. Biochem Pharmacol. 2004 Dec 15;68(12):2443-50.

Kurkela M, Patana AS, Mackenzie PI, Court MH, Tate CG, Hirvonen J, Goldman A, Finel M. Interactions with other human UDP-glucuronosyltransferases attenuate the consequences of the Y485D mutation on the activity and substrate affinity of UGT1A6. Pharmacogenet Genomics. 2007 Feb;17(2):115-26

Lévesque E, Girard H, Journault K, Lépine J, Guillemette C. ulation of the UGT1A1 bilirubin-conjugating pathway: role of a new splicing event at the UGT1A locus. Hepatology. 2007 Jan;45(1):128-38.

Li D, Fournel-Gigleux S, Barré L, Mulliert G, Netter P, Magdalou J, Ouzzine M. Identification of Aspartic Acid and Histidine Residues Mediating the Reaction Mechanism and the Substrate Specificity of the Human UDP-glucuronosyltransferases 1A. J Biol Chem. 2007 Dec 14;282(50):36514-24. Epub 2007 Oct 23.

Mackenzie PI. Expression of chimeric cDNAs in cell culture defines a region of UDP glucuronosyltransferase involved in substrate selection. J Biol Chem. 1990 Feb 25;265(6):3432-5.

Mackenzie PI, Owens IS, Burchell B, Bock KW, Bairoch A, Belanger A, Fournel-Gigleux S, Green M, Hum DW, Iyanagi T, Lancet D, Louisot P, Magdalou J, Chowdhury

JR, Ritter JK, Schachter H, Tephly TR, Tipton KF, Nebert DW. The UDP glycosyltransferase gene superfamily: recommended nomenclature update based on evolutionary divergence. Pharmacogenetics. 1997 Aug;7(4):255-69. Review.

Matern H, Matern S, Gerok W. Isolation and characterization of rat liver microsomal UDP-glucuronosyltransferase activity toward chenodeoxycholic acid and testosterone as a single form of enzyme. J Biol Chem. 1982 Jul 10;257(13):7422-9.

Matsui M, Nagai F. Genetic deficiency of androsterone UDP-glucuronosyltransferase activity in Wistar rats is due to the loss of enzyme protein. Biochem J. 1986 Feb 15;234(1):139-44.

Meech R, Mackenzie PI. UDP-glucuronosyltransferase, the role of the amino terminus in dimerization. J Biol Chem. 1997 Oct 24;272(43):26913-7.

Miley MJ, Zielinska AK, Keenan JE, Bratton SM, Radominska-Pandya A, Redinbo MR. Crystal structure of the cofactor-binding domain of the human phase II drug-metabolism enzyme UDP-glucuronosyltransferase 2B7. J Mol Biol. 2007 Jun 1;369(2):498-511. Epub 2007 Mar 30.

Nagar S, Remmel RP. Uridine diphosphoglucuronosyltransferase pharmacogenetics and cancer. Oncogene. 2006 Mar 13;25(11):1659-72. Review.

Nagar S, Zalatoris JJ, Blanchard RL. Human UGT1A6 pharmacogenetics: identification of a novel SNP, characterization of allele frequencies and functional analysis of recombinant allozymes in human liver tissue and in cultured cells. Pharmacogenetics. 2004 Aug;14(8):487-99.

Offen W, Martinez-Fleites C, Yang M, Kiat-Lim E, Davis BG, Tarling CA, Ford CM, Bowles DJ, Davies GJ. Structure of a flavonoid glucosyltransferase reveals the basis for plant natural product modification. EMBO J. 2006 Mar 22;25(6):1396-405. Epub 2006 Feb 16.

Ouzzine M, Antonio L, Burchell B, Netter P, Fournel-Gigleux S, Magdalou J. Importance of histidine residues for the function of the human liver UDP-glucuronosyltransferase UGT1A6: evidence for the catalytic role of histidine 370. Mol Pharmacol. 2000 Dec;58(6):1609-15

Patana AS, Kurkela M, Goldman A, Finel M. The human UDP-glucuronosyltransferase: identification of key residues within the nucleotide-sugar binding site. Mol Pharmacol. 2007 Sep;72(3):604-11. Epub 2007 Jun 19.

Peters WH, Jansen PL, Nauta H. The molecular weights of UDP-glucuronyltransferase determined with radiation-inactivation analysis. A molecular model of bilirubin UDP-glucuronyltransferase. J Biol Chem. 1984 Oct 10;259(19):11701-5.

Radominska-Pandya A, Czernik PJ, Little JM, Battaglia E, Mackenzie PI. Structural and functional studies of UDP-glucuronosyltransferases. Drug Metab Rev. 1999 Nov;31(4):817-99. Review.

Ross J, Li Y, Lim E, Bowles DJ. Higher plant glycosyltransferases. Genome Biol. 2001;2(2):REVIEWS3004. Epub 2001 Feb 7. Review.

Senay C, Ouzzine M, Battaglia E, Pless D, Cano V, Burchell B, Radominska A, Magdalou J, Fournel-Gigleux S. Arginine 52 and histidine 54 located in a conserved amino-terminal hydrophobic region (LX2-R52-G-H54-X3-V-L) are important amino acids for the functional and structural integrity of the human liver UDP-glucuronosyltransferase UGT1*6. Mol Pharmacol. 1997 Mar;51(3):406-13.

Senay C, Jedlitschky G, Terrier N, Burchell B, Magdalou J, Fournel-Gigleux S. The importance of cysteine 126 in the human liver UDP-glucuronosyltransferase UGT1A6. Biochim Biophys Acta. 2002 May 20;1597(1):90-6.

Shao H, He X, Achnine L, Blount JW, Dixon RA, Wang X. Crystal structures of a multifunctional triterpene/flavonoid glycosyltransferase from Medicago truncatula. Plant Cell. 2005 Nov;17(11):3141-54. Epub 2005 Oct 7.

Sorich MJ, Smith PA, Miners JO, Mackenzie PI, McKinnon RA. Recent advances in the in silico modelling of UDP glucuronosyltransferase substrates. Curr Drug Metab. 2008 Jan;9(1):60-9.

Takeda S, Ishii Y, Mackenzie PI, Nagata K, Yamazoe Y, Oguri K, Yamada H. Modulation of UDP-glucuronosyltransferase 2B7 function by cytochrome P450s in vitro: differential effects of CYP1A2, CYP2C9 and CYP3A4. Biol Pharm Bull. 2005 Oct;28(10):2026-7.

Taura KI, Yamada H, Hagino Y, Ishii Y, Mori MA, Oguri K. Interaction between cytochrome P450 and other drug-metabolizing enzymes: evidence for an association of CYP1A1 with microsomal epoxide hydrolase and UDP-glucuronosyltransferase. Biochem Biophys Res Commun. 2000 Jul 14;273(3):1048-52.

Wasserman E, Myara A, Lokiec F, Goldwasser F, Trivin F, Mahjoubi M, Misset JL, Cvitkovic E. Severe CPT-11 toxicity in patients with Gilbert's syndrome: two case reports. Ann Oncol. 1997 Oct;8(10):1049-51.

Xiong Y, Patana AS, Miley MJ, Zielinska AK, Bratton SM, Miller GP, Goldman A, Finel M, Redinbo MR, Radominska-Pandya A. The First Aspartic Acid of the DQxD Motif for Human UDP-Glucuronosyltransferase 1A10 Interacts with UDP-Glucuronic Acid During Catalysis. Drug Metab Dispos. 2008 Mar;36(3):517-22.